ANNUAL REVIEWS

Annual Review of Vision Science

Feature Detection by Retinal Ganglion Cells

Daniel Kerschensteiner

John F. Hardesty, MD, Department of Ophthalmology and Visual Sciences; Department of Neuroscience; Department of Biomedical Engineering; and Hope Center for Neurological Disorders, Washington University School of Medicine, Saint Louis, Missouri, USA; email: kerschensteinerd@wustl.edu

Keywords

receptive field, direction selectivity, object motion, looming, orientation selectivity, luminance contrast

Abstract

Retinal circuits transform the pixel representation of photoreceptors into the feature representations of ganglion cells, whose axons transmit these representations to the brain. Functional, morphological, and transcriptomic surveys have identified more than 40 retinal ganglion cell (RGC) types in mice. RGCs extract features of varying complexity; some simply signal local differences in brightness (i.e., luminance contrast), whereas others detect specific motion trajectories. To understand the retina, we need to know how retinal circuits give rise to the diverse RGC feature representations. A catalog of the RGC feature set, in turn, is fundamental to understanding visual processing in the brain. Anterograde tracing indicates that RGCs innervate more than 50 areas in the mouse brain. Current maps connecting RGC types to brain areas are rudimentary, as is our understanding of how retinal signals are transformed downstream to guide behavior. In this article, I review the feature selectivities of mouse RGCs, how they arise, and how they are utilized downstream. Not only is knowledge of the behavioral purpose of RGC signals critical for understanding the retinal contributions to vision; it can also guide us to the most relevant areas of visual feature space.

1. INTRODUCTION

Light traverses the circuitry of the retina before the outer segments of photoreceptors absorb it. The rods and two types of mouse cones differ in absolute and spectral sensitivities but uniformly reduce glutamate release in response to light (Masland 2001, Wässle 2004). This synaptic signal is picked up by second-order bipolar cells, which transmit information from the outer plexiform layer (OPL) to the inner plexiform layer (IPL) (Euler et al. 2014) (**Figure 1a**). In the IPL, bipolar cell axons innervate amacrine cells and RGCs, the retina's output neurons (Demb & Singer 2015, Diamond 2017).

One of the retina's most striking features is its neuronal diversity (**Figure 1b**). The mouse retina contains three types of photoreceptors (one rod, two cones); one horizontal cell type, which provides feedback to photoreceptors; 15 bipolar cell types; 63 amacrine cell types; and more than 40 RGC types (Baden et al. 2016, Bae et al. 2018, Helmstaedter et al. 2013, Rheaume et al. 2018,
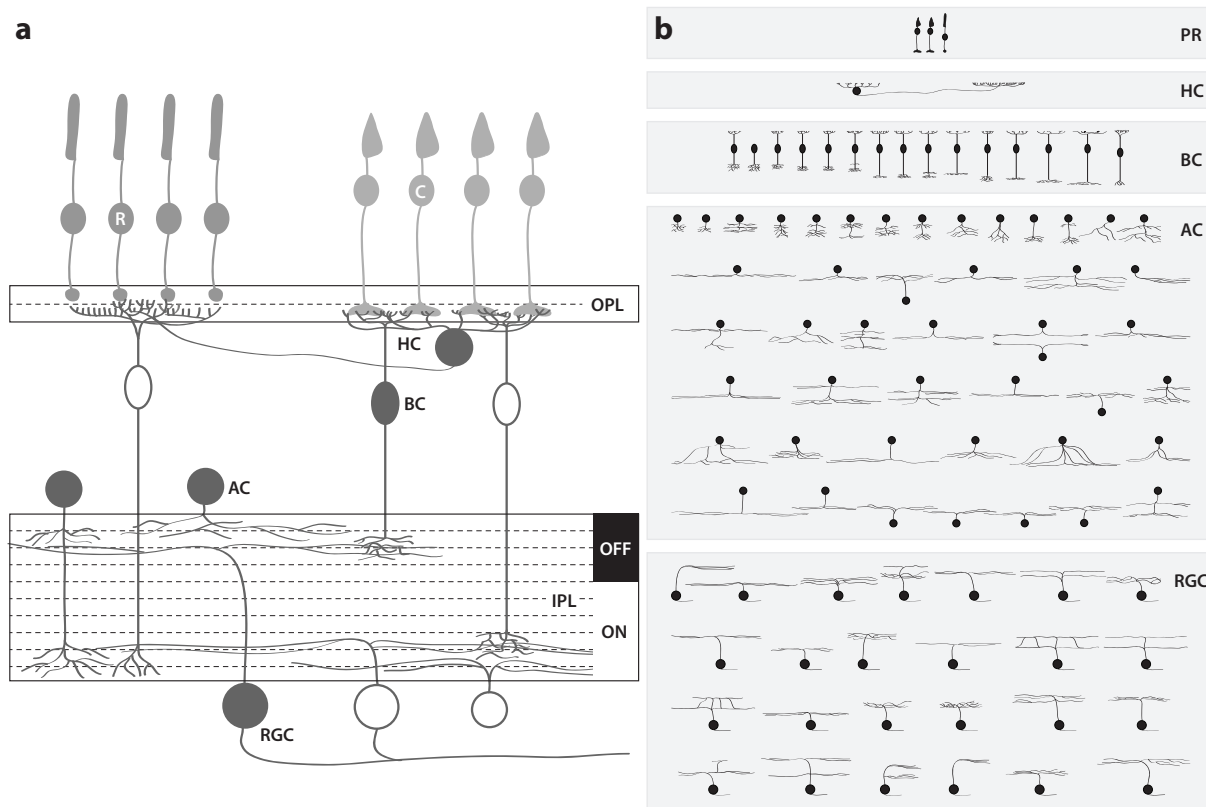

Figure 1

Retinal circuit architecture and neuron complement. (*a*) Simplified schematic of the retina. Rod (R) and cone (C) photoreceptors (PRs) in the outer retina translate changes in photon flux into changes in glutamate release onto bipolar cell (BC) dendrites and horizontal cell (HC) axons (rods) and dendrites (cones) in the outer plexiform layer (OPL). ON bipolar cells (open somas) invert the sign of the PR response, depolarize to light, and stratify their axons in the inner three-fifths of the inner plexiform layer (IPL). OFF bipolar cells (filled somas) depolarize to light decrements and stratify their axons in the outer two-fifths of the IPL. Bipolar cells synapse onto amacrine cells (ACs), which make up a diverse class of retinal interneurons, and retinal ganglion cells (RGCs), the eye's output neurons. (*b*) A catalog of the diverse cell types within the five main neuron classes. The mouse retina contains three types of PRs (two cones, one rod), one HC type, 15 BC types, 63 AC types, and more than 40 RGC types (subsets of the latter two are shown in the figure).
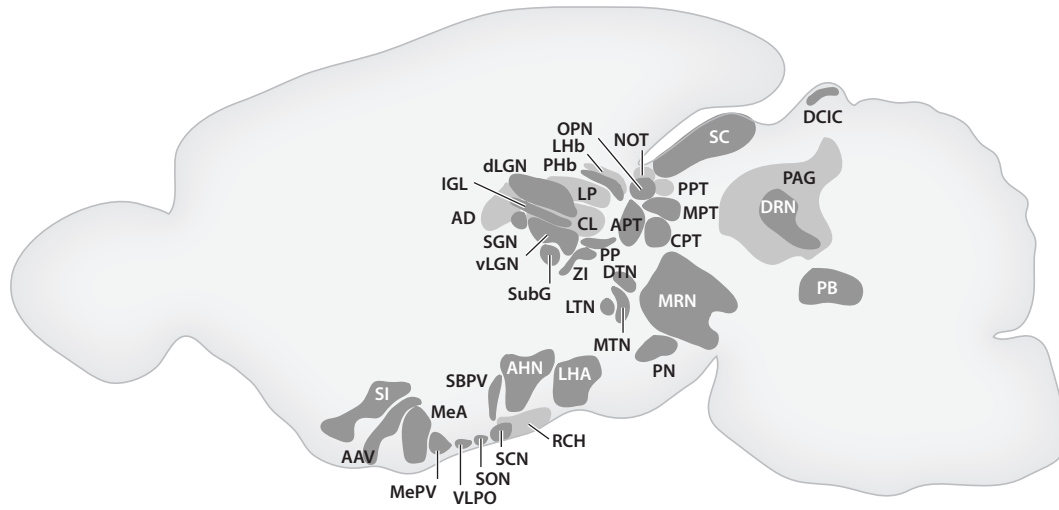
Figure 2

Retinorecipient brain areas. As illustrated, diverse brain areas receive RGC input. Abbreviations: AAV, anterior amygdaloid area, ventral; AD, anterodorsal thalamic nucleus; AHN, anterior hypothalamic area; APT, anterior pretectal nucleus; CL, centrolateral thalamic nucleus; CPT, commissural pretectal nucleus; DCIC, dorsal cortex of the inferior colliculus; dLGN, dorsolateral geniculate nucleus of the thalamus; DRN, dorsal raphe nucleus; DTN, dorsal terminal nucleus; IGL, intergeniculate leaflet; LHA, lateral hypothalamic area; LHb, lateral habenula; LHN, lateral hypothalamic area; LP, lateral posterior nucleus of the thalamus; LTN, lateral terminal nucleus; MeA, medial amygdala, anterior; MePV, medial amygdala, posteroventral; MPT, medial pretectal nucleus; MRN, midbrain reticular nucleus; MTN, medial terminal nucleus; NOT, nucleus of the optic tract; OPN, olivary pretectal nucleus; PAG, periaqueductal gray; PB, parabrachial nucleus; PHb, perihabenular nucleus; PN, paranigral nucleus; PP, peripeduncular nucleus; PPT, posterior pretectal nucleus; RCH, retrochiasmatic area; RGC, retinal ganglion cell; SGN, suprageniculate nucleus; SBPV, subparaventricular zone; SC, superior colliculus; SCN, suprachiasmatic nucleus; SI, substantia innominate; SON, supraoptic nucleus; SubG, subgeniculate nucleus; vLGN, ventrolateral geniculate nucleus; VLPO, ventrolateral preoptic area; ZI, zona incerta.

Shekhar et al. 2016, Tran et al. 2019, Yan et al. 2020). The assembly of diverse neurons into specific circuits is aided by the laminar architecture of the retina (Sanes & Zipursky 2010). The OPL and the IPL are divided into sublayers. Rods form synapses with their partners (horizontal cell axons and rod bipolar cells) in the outer OPL, whereas cones contact their partners (horizontal cell dendrites and cone bipolar cells) in the inner OPL. The IPL has 10 morphologically distinct sublaminae (Sanes & Zipursky 2010). In the inner six, rod and cone bipolar cells that depolarize to light increments (i.e., ON bipolar cells) stratify their axons, whereas the outer four are innervated by cone bipolar cells activated by light decrements (i.e., OFF bipolar cells). RGCs stratify their dendrites in cell type–specific patterns in the IPL to recruit excitatory and inhibitory input from unique combinations of bipolar and amacrine cells. These patterns of synaptic input combine with cell-intrinsic mechanisms to shape the feature preferences of RGCs.

RGCs innervate more than 50 areas of the mouse brain (Martersteck et al. 2017, Morin & Studholme 2014) (**Figure 2**). The dorsolateral geniculate nucleus (dLGN) of the thalamus passes information to the visual cortex and supports conscious visual perception (Kerschensteiner & Guido 2017, Liang & Chen 2020). The superior colliculus (SC) combines retinal signals with other sensory inputs to identify salient features and events in the environment, direct attention, and guide approach toward attractive stimuli and escape from threats (Cang et al. 2018, Dean et al. 1989, Krauzlis et al. 2013). In addition to these major retinorecipient targets innervated by most RGCs (Ellis et al. 2016, Román Rosón et al. 2019), a large number of brain areas receive type-restricted RGC input to mediate a wide range of behaviors and influences of light on physiology.

2. MOTION

Motion is one of the most common visual features that we experience. There are two primary sources of visual motion: movements of the observer (i.e., self-motion) and movements of objects in the observed world (i.e., object motion) (Frost 2010). In the retina, movements of the observer and objects cause global and local image motion, respectively. Motion-processing circuits in the retina either explicitly distinguish these forms of motion (e.g., object motion–sensitive circuits) or prefer local or global motion while selectively encoding other motion parameters [e.g., direction-selective (DS) circuits]. Finally, some retinal circuits respond strongly to objects approaching the observer (i.e., looming detection circuits) and initiate defensive responses to avoid collisions and evade predators.

2.1. Direction Selectivity

DS responses pervade the visual system. They help animals infer self-motion from optic flow and track moving objects. Motion direction is computed at multiple stages of the visual system, starting in the retina.

2.1.1. Direction-selective circuits and retinal ganglion cell types. DS RGCs were first discovered in rabbits (Barlow & Hill 1963, Barlow & Levick 1965, Barlow et al. 1964). The mouse retina dedicates approximately one-fifth of its output to signaling motion direction. The respective ganglion cells fall into two categories: ON DS RGCs, which respond to light increments, and ON-OFF DS RGCs, which respond to light increments and decrements (**Figure 3a,b**). The presynaptic circuits of ON and ON-OFF DS RGCs overlap and compute motion direction by shared mechanisms, while unique mechanisms differentiate the speed and contrast preferences of ON and ON-OFF DS RGCs to match their behavioral functions (Mauss et al. 2017, Reinhard et al. 2020, Wei 2018).

At the core of retinal DS circuits, starburst amacrine cells (SACs) provide asymmetric inhibition to DS RGCs (ON SACs to ON DS RGCs and ON and OFF SACs to ON-OFF DS RGCs) (Briggman et al. 2011, Fried et al. 2002, Wei et al. 2011, Yonehara et al. 2011). SACs have radially symmetric dendrite arbors that receive input in their center and send output from their periphery (Briggman et al. 2011, Ding et al. 2016, Famiglietti 1991, Vlasits et al. 2016). Each primary SAC dendrite with its daughter branches functions as an independent motion sensor, preferring motion from the soma to the dendrite tips (Euler et al. 2002, Koren et al. 2017, Poleg-Polsky et al. 2018). This centrifugal motion preference arises from the passive membrane properties of SAC dendrites, their voltage-gated conductances, distributions of excitatory and inhibitory inputs, the dependence of excitatory input kinetics on distance from the soma, and SAC–SAC inhibition (Ding et al. 2016, Fransen & Borghuis 2017, Greene et al. 2016, Hausselt et al. 2007, Kim et al. 2014, Lee & Zhou 2006, Vlasits et al. 2016). Asymmetric connections of SACs with DS RGCs convert the SAC dendrites' centrifugal motion preferences into DS inhibition (Briggman et al. 2011); SAC dendrites pointing in the nasal direction form GABAergic synapses with DS RGCs that prefer temporal motion, whereas SAC dendrites pointing in the temporal direction form GABAergic synapses with nasal motion–preferring DS RGCs (Briggman et al. 2011). When SACs are silenced or killed, DS RGCs respond to motion in all directions (Pei et al. 2015, Vlasits et al. 2014, Yoshida et al. 2001), and increases and decreases in the SAC dendrites' retinal coverage sharpen and broaden DS RGC tuning, respectively (Morrie & Feller 2018, Soto et al. 2019). Thus, the subcellular computations of SAC dendrites and their asymmetric inhibitory connections determine the feature-selective output of DS RGCs.
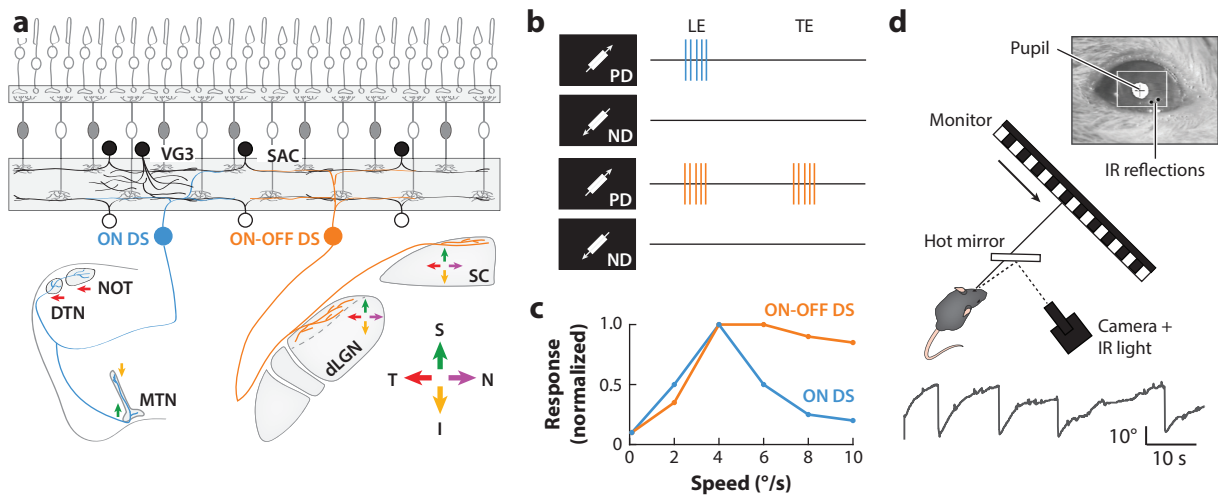
Figure 3

Direction-selective (DS) retinal ganglion cell (RGC) types, pathways, and functions. (*a*) ON and ON-OFF DS RGCs receive directionally selective inhibition from starburst amacrine cells (SACs). ON DS RGCs also receive input from VGLUT3-expressing (VG3) amacrine cells. ON DS RGCs preferentially innervate nuclei of the accessory optic system (AOS). Superior (S) and inferior (I) motion–preferring ON DS RGCs target the ventral and dorsal medial terminal nucleus (MTN), respectively. Temporal (T) [and potentially nasal (N)] motion–preferring ON DS RGCs target the nucleus of the optic tract (NOT) and dorsal terminal nucleus (DTN). ON-OFF DS RGCs of all direction preferences innervate the dorsolateral geniculate nucleus (dLGN) shell and the superior colliculus (SC). (*b*) Schematic of ON and ON-OFF DS RGC responses to bright bars moving in their preferred direction (PD) and opposite (i.e., null) direction (ND). ON DS RGCs respond to the leading edge (LE) of the stimulus only, whereas ON-OFF DS RGCs respond to the LE and the trailing edge (TE). (*c*) Responses of ON DS RGCs decline sharply with increasing stimulus speed, whereas ON-OFF DS RGCs signal motion direction over a wide range of speed. Tuning curves in this plot are estimated from Dhande et al. (2013). (*d*) Measurements of the optokinetic reflex driven by ON DS RGCs in head-fixed mice. Eye movements are measured by the differences in the position of the pupil relative to the reflections of an infrared (IR) light source. Panel *d* adapted with permission from Shen et al. (2020).

SACs are dual-transmitter neurons that release acetylcholine in addition to GABA (Lee et al. 2010). Cholinergic SAC–DS RGC connectivity is symmetric and supplements the excitatory drive from bipolar cells, particularly at low contrasts, to stabilize feature selectivity across lighting conditions (Lee et al. 2010, Pearson & Kerschensteiner 2015, Sethuramanujam et al. 2016, Yao et al. 2018).

In addition to GABAergic and cholinergic SAC input, ON-OFF DS RGCs receive glutamatergic input from bipolar cells. Two-photon calcium and glutamate imaging initially suggested that bipolar cell signals are not directionally tuned (Chen et al. 2014, Franke et al. 2017, Park et al. 2014, Yonehara et al. 2013). However, a recent study indicated that glutamate release from some boutons of type 2 (OFF) and type 7 (ON) bipolar cell axons, which synapse onto ON-OFF DS RGCs, may be DS (Matsumoto et al. 2020). This bouton-specific tuning relies on cholinergic and GABAergic modulation of bipolar cell axons by SACs (Matsumoto et al. 2020).

There are four ON-OFF DS RGC types in the mouse retina; they differ in their direction preferences (retinal direction: superior, inferior, nasal, and temporal) and gene expression and are labeled in different transgenic mouse lines (Bae et al. 2018, Elstrott et al. 2008, Fiscella et al. 2015, Huberman et al. 2009, Kay et al. 2011, Rivlin-Etzion et al. 2011, Sabbah et al. 2017, Tran et al. 2019, Trenholm et al. 2013). One of the four, the superior motion–preferring ON-OFF DS RGC, has asymmetric dendrite arbors that form gap junctions with same-type neighbors (Trenholm et al. 2013, 2014). This electrical coupling provides an anticipatory drive that counters the lag

between movement of stimuli and ganglion cell activation, bringing their positions into register (i.e., lag normalization) (Trenholm et al. 2013, 2014). Gap-junctional coupling also broadens the direction preferences of superior motion–preferring ON-OFF DS RGCs in dim light, favoring motion detection over directional precision (Yao et al. 2018). The behavioral significance of these adjustments and their restriction to a single ON-OFF DS RGC type remains to be determined.

ON-OFF DS RGCs are indirectly inhibited by wide-field amacrine cells, attenuating responses to global motion. Therefore, ON-OFF DS RGCs preferentially signal object motion direction, which they encode stably across a wide range of stimulus speeds (Hoggarth et al. 2015, Weng et al. 2005).

ON DS RGCs receive input from ON SACs, four ON bipolar cell types (5i, 5o, 5t, and 7), and VGLUT3-expressing (VG3) amacrine cells (Krishnaswamy et al. 2015, Lee et al. 2014, Matsumoto et al. 2019). Two-photon glutamate imaging and electron microscopic reconstructions suggest that the ON bipolar cell and VG3 amacrine cell inputs are arranged asymmetrically across ON DS RGC dendrites such that motion in the preferred direction activates slower inputs before faster ones, causing both slow and fast inputs to add up (Matsumoto et al. 2019). In contrast, motion in the opposite (i.e., null) direction elicits temporally dispersed excitation. Effective summation of excitation depends on the speed of preferred-direction motion. Thus, asymmetric excitation contributes to the ON DS RGCs' preference for slow stimulus speeds (Dhande et al. 2013, Gauvain & Murphy 2015, Matsumoto et al. 2019) (**Figure 3c**).

Most studies have identified three ON DS RGC types that differ in their direction preferences (superior, inferior, and temporal), marker expression, and labeling in transgenic mouse lines (Dhande et al. 2013; Lilley et al. 2019; Martersteck et al. 2017; Yonehara et al. 2008, 2009). A recent study discovered a putative fourth, nasal motion–preferring ON DS RGC using large-scale two-photon calcium imaging (Sabbah et al. 2017). This study also revealed that the direction preferences of ON and ON-OFF DS RGCs vary across the retina to align with the optic flow fields generated by movements of mice forward and back and up and down (Sabbah et al. 2017).

In addition to ON and ON-OFF DS RGCs, DS responses have been reported for three RGC types with asymmetric dendrites (JAM-B, F-mini-ON, and F-mini-OFF RGCs) (Kim et al. 2008, Rousso et al. 2016). These RGC types are DS in specific stimulus conditions and robustly encode other visual features (Cooler & Schwartz 2020, Joesch & Meister 2016, Nath & Schwartz 2017). To what extent downstream pathways extract information about motion direction from JAM-B, F-mini-ON, and F-mini-OFF RGC inputs remains to be determined.

2.1.2. Downstream pathways and behavioral significance of retinal direction selectivity. DS RGCs differentially innervate three pathways (**Figure 3a**). ON-OFF DS RGC axons preferentially target the dLGN of the thalamus and the SC, whereas ON DS RGC axons preferentially target nuclei of the accessory optic system (AOS). Recent studies have begun to uncover how downstream pathways process DS RGC inputs to guide behavior (Rasmussen & Yonehara 2020, Reinhard et al. 2020).

The dLGN passes signals from the retina to the primary visual cortex (V1) to support visual perception. The mouse dLGN is divided into a dorsolateral core and a ventromedial shell (Kerschensteiner & Guido 2017). ON-OFF DS RGCs predominantly innervate the dLGN shell (horizontal motion–preferring DS RGCs innervate the shell exclusively and vertical motion–preferring ON-OFF DS RGCs preferentially), while other RGCs innervate the dLGN core (Cruz-Martín et al. 2014, Hong et al. 2018, Huberman et al. 2009, Kay et al. 2011, Rivlin-Etzion et al. 2011). High-resolution functional imaging revealed that dLGN neurons in the shell receive input from DS RGC axons with similar or near-opposite direction preferences (Liang et al. 2018). This could, in principle, explain the abundant DS and motion axis–selective responses among

dLGN shell neurons (Liang et al. 2018, Marshel et al. 2012, Piscopo et al. 2013). Interestingly, in mice without horizontal motion–preferring DS RGCs, dLGN neuron preferences shift to vertical motion, but some horizontally DS responses persist (Rasmussen et al. 2020). Thus, direction selectivity in dLGN is partly inherited from the retina and partly generated by other mechanisms (e.g., computed in the dLGN or inherited from V1 or SC).

The axons of dLGN shell neurons innervate layer 2/3 of V1, whereas dLGN core neurons target V1's layer 4, continuing the parallel pathways from the retina (Cruz-Martín et al. 2014). Consistent with the preference of ON-OFF DS RGCs for the dLGN shell, perturbations of retinal direction selectivity disrupt responses in layer 2/3 but not layer 4, which generates DS responses from untuned dLGN inputs (Hillier et al. 2017, Lien & Scanziani 2018, Rasmussen et al. 2020). The deficits in layer 2/3 primarily affect high-speed posterior motion created when mice run forward (Hillier et al. 2017, Rasmussen et al. 2020). The behavioral significance of this ON-OFF DS RGC-dependent signal to cortical processing and behavior remains to be explored.

The SC integrates multisensory information, directs attention and orienting behaviors, and guides the pursuit of prey and escape from predators (Cang et al. 2018, Ito & Feldheim 2018). Most (85–90%) RGCs innervate the superficial SC (sSC) (Ellis et al. 2016, Hofbauer & Dräger 1985), and ON-OFF DS RGC axons stratify at the top of this retinorecipient zone (Huberman et al. 2009, Kay et al. 2011, Kim et al. 2010, Rivlin-Etzion et al. 2011). Many neurons near the surface of the SC are DS (de Malmazet et al. 2018, Inayat et al. 2015, Ito et al. 2017, Shi et al. 2017). Unlike the dLGN and V1, SC direction selectivity depends entirely on DS retinal input (Shi et al. 2017). Narrow-field cells are a genetically and morphologically distinct group of DS sSC neurons that project to the parabigeminal nucleus and deeper layers of the SC (Gale & Murphy 2014, Reinhard et al. 2019). Narrow-field neuron silencing impairs the ability of mice to detect and pursue prey (Hoy et al. 2019). Whether this contribution of narrow-field cells relies on their direction selectivity and if predator evasion or other SC-dependent behaviors are driven or modulated by ON-OFF DS RGC input remain to be tested.

A recent two-photon imaging study revealed that direction preferences in the SC are distributed inhomogeneously across visual space (de Malmazet et al. 2018). Specifically, SC neurons in the visual field's binocular area prefer nasal motion, whereas SC neurons in the monocular region prefer temporal motion (de Malmazet et al. 2018). This arrangement is well suited to distinguish optic flow from translations and rotations and may thus guide approach and escape behaviors.

Mice frequently move their eyes to compensate for head movements (Meyer et al. 2018, 2020; Michaiel et al. 2020). Two reflexes control gaze-stabilizing eye movements: the optokinetic reflex and the vestibulo-ocular reflex. The optokinetic reflex is driven by retinal image slip and operates at head-motion speeds too slow to activate the vestibular system (Faulstich et al. 2004) (**Figure 3d**). The optokinetic reflex is mediated by the AOS, which encompasses the nucleus of the optic tract (NOT), the dorsal terminal nucleus (DTN), and the medial terminal nucleus (MTN) (Simpson 1984). ON DS RGCs dominate input to AOS nuclei (Dhande et al. 2013, Yonehara et al. 2009). Inferior and superior motion–preferring ON DS RGCs innervate the dorsal and ventral MTN, respectively, while nasal motion–preferring ON and ON-OFF DS RGCs innervate the NOT and DTN (Dhande et al. 2013; Kay et al. 2011; Yonehara et al. 2008, 2009) (**Figure 3a**). Several lines of evidence suggest that DS RGC inputs to AOS nuclei drive gaze-stabilizing eye movements. First, SAC ablation or silencing abolishes the optokinetic reflex (Yoshida et al. 2001). Second, mutations of *Frmd7*, a common genetic cause of congenital nystagmus in humans (Tarpey et al. 2006), eliminate horizontal direction selectivity in the retina and the horizontal optokinetic reflex in mice and humans (Yonehara et al. 2016). Third, mutations that affect the connectivity of ON DS RGCs with AOS nuclei disrupt gaze-stabilizing eye movements (Osterhout et al. 2015,

Sun et al. 2015). The preference of ON DS RGCs for slow motion matches the speed tuning of the optokinetic reflex and complements the vestibulo-ocular reflex.

2.2. Object Motion Sensitivity

Object motion draws animals' attention (Kingdom & Prins 2016, Sillar et al. 2016). To reliably detect moving objects, retinal circuits need to distinguish local motion in a scene from global image motion caused by head and eye movements.

2.2.1. Object motion–sensitive circuits and retinal ganglion cell types. RGCs that distinguish local and global motion [i.e., object motion–sensitive (OMS) RGCs] were first identified in salamanders and rabbits (Baccus et al. 2008, Olveczky et al. 2003). Recently, a group of small OMS RGCs was identified in mice (Jacoby & Schwartz 2017, Zhang et al. 2012) (**Figure 4***a*). Based on transgenic labeling, Zhang et al. (2012) named one cell W3B (or W3), whereas Jacoby & Schwartz (2017) named four cells, based on morphology and resemblance to a famous rabbit RGC (Levick 1967, van Wyk et al. 2006), high-definition 1 (HD1), high-definition 2 (HD2), ultrahigh-definition (UHD), and local edge detector (LED) RGCs. It appears that UHD RGCs correspond to W3 RGCs (Schwartz & Swygart 2020). The four OMS RGCs' dendrites stratify in the middle of the IPL, where they receive input from rectified transient ON and OFF bipolar cells (Borghuis et al. 2013, Franke et al. 2017). This allows OMS RGCs to respond to local motion in their receptive field center, independent of the contrast composition (i.e., bright versus dark elements) of the moving object (Jacoby & Schwartz 2017, Zhang et al. 2012). In addition, OMS RGCs receive strong inhibition from their receptive field surrounds. Because this surround inhibition, like center excitation, is driven by rectified subunits, OMS RGCs are suppressed by
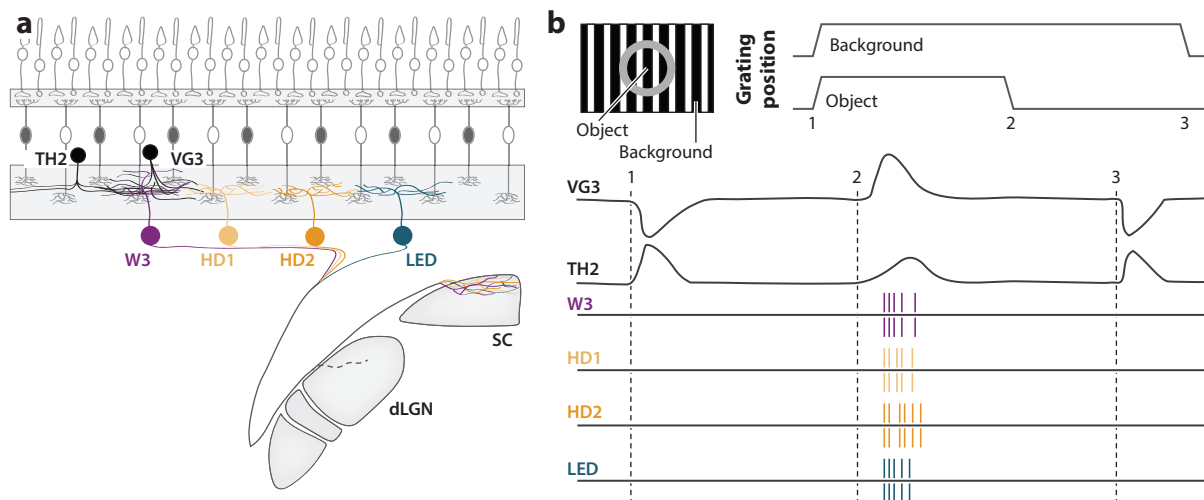

Figure 4

Object motion–sensitive (OMS) retinal ganglion cell (RGC) types, pathways, and functions. (*a*) Schematic of four small OMS RGCs identified in the mouse retina. W3 [or ultrahigh-definition (UHD)] RGCs receive excitatory input from VGLUT3-expressing (VG3) amacrine cells and inhibitory input from TH2 amacrine cells. OMS RGCs are underrepresented or absent from the dorsolateral geniculate nucleus (dLGN)-projecting set and strongly innervate the superior colliculus (SC). (*b*) VG3 amacrine cells distinguish local (2) and global (1) or surround (3) motion in their response polarity, whereas TH2 amacrine cells distinguish these stimuli in their response kinetics. All OMS RGCs respond strongly to isolated motion in their receptive field center, independent of the stimulus pattern, but are suppressed by simultaneous motion in the surround (i.e., global motion). Additional abbreviations: HD1, high-definition RGC type 1; HD2, high-definition RGC type 2; LED, local edge detector RGC.

global motion independent of the pattern of the shifting scene (Jacoby & Schwartz 2017, Zhang et al. 2012) (**Figure 4***b*). The four OMS RGC types prefer different motion speeds and delays between center and surround motion (Jacoby & Schwartz 2017), indicating that they may cooperate in signaling the speed of object motion relative to the observer.

Dissections of the composition and computations of W3 RGC circuits have provided interesting results. In addition to bipolar cells, W3 RGCs receive glutamatergic input from VG3 amacrine cells (Kim et al. 2015, Krishnaswamy et al. 2015, Lee et al. 2014). VG3 amacrine cells are themselves OMS and selectively amplify this feature in the W3 RGC response (Hsiang et al. 2017, Kim et al. 2015) (**Figure 4***b*). VG3 amacrine cells' dendrites are larger than those of bipolar cells but process inputs locally and, therefore, signal object motion with high spatial precision (Chen et al. 2017, Hsiang et al. 2017). The insertion of VG3 amacrine cells into the vertical pathway to W3 RGCs could delay excitation during motion in the receptive field center, allowing surround inhibition to cancel center excitation effectively during global image motion (Krishnaswamy et al. 2015) and/or enhance OMS responses by adding a layer of surround inhibition to the excitatory pathway (Kim & Kerschensteiner 2017, Kim et al. 2015).

W3 RGCs receive surround inhibition from TH2 amacrine cells (Brüggen et al. 2015, Kim & Kerschensteiner 2017, Knop et al. 2011), which respond to local and global motion but distinguish between these stimuli in their response kinetics (Kim & Kerschensteiner 2017) (**Figure 4***b*). Thus, global motion activates TH2 amacrine cells quickly, whereas local motion depolarizes them slowly. Slow depolarizations fail to elicit GABA release from TH2 amacrine cells, and differences in response kinetics are thus translated into global motion–selective inhibition of W3 RGCs (Kim & Kerschensteiner 2017). Thus, the OMS responses of W3 RGCs are shaped by the complementary actions of two amacrine cells. VG3 amacrine cells amplify responses to local motion, while TH2 amacrine cells suppress responses to global motion (Kim & Kerschensteiner 2017, Kim et al. 2015).

2.2.2. Downstream pathways and behavioral significance of retinal object motion sensitivity.
Transgenic labeling revealed that W3 (UHD) RGC axons target the upper layer of the retinorecipient sSC (Zhang et al. 2012) (**Figure 4***a*). Disynaptic tracing showed that HD1 and HD2 RGCs innervate sSC neurons that send signals to the parabigeminal nucleus and the lateral posterior (LP) nucleus of the thalamus (i.e., the mouse pulvinar) (Reinhard et al. 2019). The targets of OMS RGCs in the sSC include wide-field cells, a genetically and morphologically distinct neuron type that innervates the LP nucleus of the thalamus (Gale & Murphy 2014). As their name suggests, wide-field neurons have large dendrites and correspondingly large receptive fields. However, they prefer motion of small objects anywhere within their receptive fields (Gale & Murphy 2014). Besides OMS RGC input, there are two key ingredients to the OMS responses of wide-field cells. First, dendritic spikes propagate signals elicited by object motion anywhere within their large dendritic arbors to the soma (Gale & Murphy 2016). Second, inhibitory inputs from sSC horizontal cells suppress responses to movements of large objects (Gale & Murphy 2016). Intriguingly, wide-field neuron silencing selectively impairs the mouse's ability to detect prey without affecting its pursuit (Hoy et al. 2019).

Retrograde labeling studies suggest that OMS RGCs are underrepresented in the dLGN-projecting set, indicating that among the two major retinorecipient targets, OMS RGCs preferentially innervate the SC (Ellis et al. 2016, Román Rosón et al. 2019) (**Figure 4***a*).

2.3. Looming Detection

Among object trajectories, a collision course with the observer is most alarming. Approaching objects cast expanding shadows (i.e., looming) that elicit innate defensive responses in most animals,
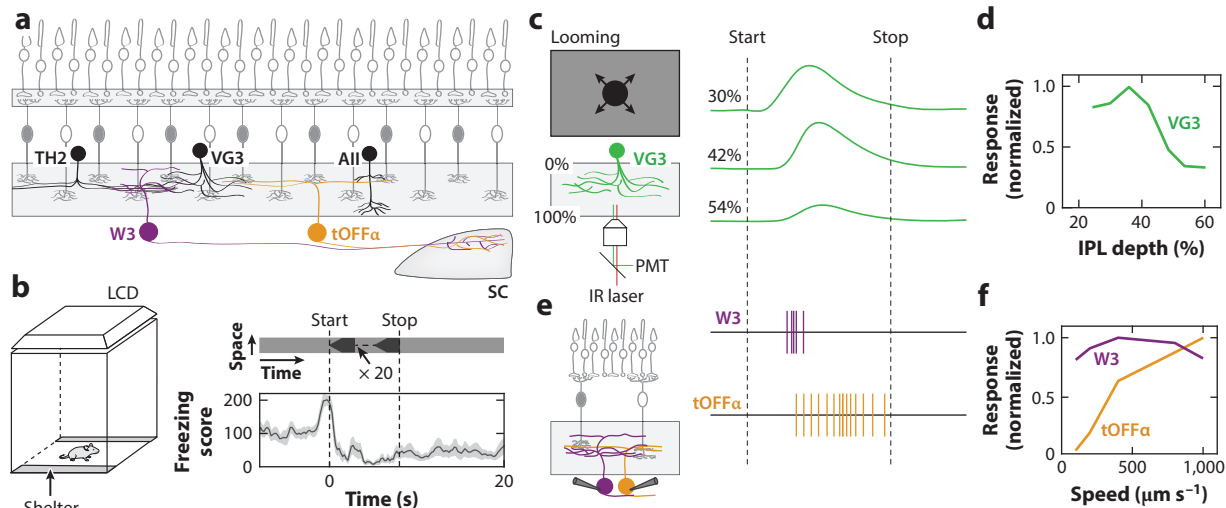
Figure 5

Looming detection and defensive behavior. (*a*) In looming detection circuits of the retina, VGLUT3-expressing (VG3) amacrine cells provide feature-selective excitatory input to W3 and tOFFα retinal ganglion cells (RGCs), which drive innate defensive responses through projections to the superior colliculus (SC). W3 RGCs combine this excitatory input with inhibition from TH2 amacrine cells, whereas tOFFα RGCs receive tonic inhibition from AII amacrine cells, which is relieved during looming. (*b*) Looming causes mice to flee to a virtual shelter and freeze (dashed lines indicate stimulus start and stop). (*c*) Two-photon calcium imaging of VG3 amacrine cell dendrites. (*d*) Looming responses are restricted to the proximal layers of the VG3 dendrite arbor. (*e,f*) By combining shared excitatory input with dissimilar inhibition, W3 and tOFFα RGCs encode the onset and speed of approach motion, respectively. Panels *b–f* adapted from Kim et al. (2020).

from insects to humans (Fotowat & Gabbiani 2011, Peek & Card 2016). Mice use vision to evade aerial predators (De Franceschi et al. 2016, Yilmaz & Meister 2013). Studies are beginning to elucidate the retinal circuits, RGC types, and downstream pathways that detect looming and drive innate defensive responses in mice.

2.3.1. Looming detection circuits and retinal ganglion cell types. Many RGCs respond to looming; fewer distinguish looming from related forms of motion (receding, white looming, etc.) (Münch et al. 2009, Reinhard et al. 2019). Knowing which retinal circuits drive innate defensive responses helps prioritize studies of looming processing. A recent study identified such a circuit in the mouse retina (Kim et al. 2020) (**Figure 5a**). At the core of this circuit, VG3 amacrine cells, which receive input from ON and OFF bipolar cells, respond strongly to looming and weakly to related forms of motion. This preference arises from the stimulus-specific timing of excitation and inhibition. During looming, transient excitation precedes sustained inhibition, whereas excitation and inhibition coincide in response to expanding bright stimuli (Kim et al. 2020). The looming preferences of VG3 amacrine cells are enhanced by dendritic processing. Thus, looming-sensitive calcium transients in the VG3 dendrite arbor's proximal layer are segregated from weaker responses to related forms of motion in the distal dendrite layer (Kim et al. 2020) (**Figure 5c,d**).

The proximal layer of the VG3 dendrite arbor provides glutamatergic input to two RGC types (W3 and tOFFα RGCs) that have been suggested to signal approaching aerial predators (Kim et al. 2015, 2020; Krishnaswamy et al. 2015; Lee et al. 2014; Münch et al. 2009; Zhang et al. 2012). W3 and tOFFα RGCs combine VG3 excitation with dissimilar inhibition to encode the onset (i.e., critical size) and speed of looming, respectively (**Figure 5e,f**). During looming, W3 RGCs, like VG3

amacrine cells, receive transient excitation followed by sustained inhibition, in part from TH2 amacrine cells (Kim & Kerschensteiner 2017, Kim et al. 2020). This input sequence restricts W3 RGC responses to the onset of looming (critical size is approximately 4.5°). For stimuli expanding at different speeds, W3 RGC excitation and inhibition covary, keeping response amplitudes constant. Thus, W3 RGCs encode the onset (critical size) of looming independent of its speed (Kim et al. 2020). In contrast, tOFFα RGCs receive tonic inhibition, in part from AII amacrine cells, which is relieved by looming (Kim et al. 2020, Münch et al. 2009). Because excitation and disinhibition diverge as a function of stimulus speed, tOFFα RGC responses encode the speed of looming (Kim et al. 2020, Münch et al. 2009). The divergent feature representations of W3 and tOFFα RGCs resemble response types observed in looming-sensitive neurons in the pigeon tectum (equivalent to the SC of mice), indicating a conserved strategy in assessing predatory approaches (Sun & Frost 1998).

2.3.2. Downstream pathways and behavioral significance of retinal looming detection.

Deletion of VG3 amacrine cells attenuates W3 and tOFFα RGCs' looming responses and diminishes defensive (flight and freeze) reactions to looming (Kim et al. 2020) (**Figure 5b**). W3 and tOFFα RGCs innervate the sSC (Huberman et al. 2008, Reinhard et al. 2019, Zhang et al. 2012), which mediates defensive responses to visual threats (Blanchard et al. 1981, Dean et al. 1989, Sahibzada et al. 1986, Wei et al. 2015). On average, neurons in the sSC are innervated by six RGCs (Chandrasekaran et al. 2007). How input from W3, tOFFα, and other RGC types is combined to shape looming responses in the sSC remains to be explored. Neurons in the sSC respond robustly to looming (Lee et al. 2020, Reinhard et al. 2019, Zhao et al. 2014a). They inherit feature preferences from the retina, while input from V1 amplifies looming responses and enhances behavioral reactions to visual threats (Liang et al. 2015, Wang & Burkhalter 2013, Zhao et al. 2014a).

The responses of mice to looming depend on the environment and stimulus parameters. If shelters are available, then mice run to safety and freeze, even if threats are presented between them and the shelter (Vale et al. 2017, Yilmaz & Meister 2013). Escape delays depend on the stimulus salience (i.e., contrast) (Evans et al. 2018). Mice quickly learn the positions of shelters and update their escape behavior when shelters are moved (Vale et al. 2017). The shelter direction is conveyed continuously to the SC from the retrosplenial cortex and combined with threat assessments from the retina (Vale et al. 2020). When no shelters are available, mice freeze in place in response to looming (Vale et al. 2017, Wei et al. 2015, Yilmaz & Meister 2013), a behavior that is also elicited by sweeping visual stimuli (De Franceschi et al. 2016).

Looming signals of sSC neurons propagate along three pathways to shape defensive responses. First, sSC signals percolate to deeper layers of the SC (dSC). Compared to the sSC, dSC neurons are more selective for looming and depend less on stimulus positions, encode the behavioral salience (e.g., contrast) of the stimulus, and adapt quickly to repeated presentations (Evans et al. 2018, Lee et al. 2020). Neurons in the dSC innervate the dorsal periaqueductal gray with weak and unreliable excitatory connections that act as a threshold for escape initiation (Evans et al. 2018). dSC neurons also innervate GABAergic neurons in the ventral tegmental area, which respond to looming and inhibit the central amygdala (CeA). Inhibition of the CeA via this pathway promotes escape (Zhou et al. 2019). Second, sSC neurons provide input to the LP either directly or via the SC's intermediate layers. In turn, LP neurons send signals to the lateral amygdala (LA) (Wei et al. 2015). Optogenetic silencing and activation of neurons in these pathways prevent and promote freezing, respectively (Shang et al. 2018, Wei et al. 2015, Zingg et al. 2017). Third, sSC neurons innervate the parabigeminal nucleus (PBGN), which passes signals to the CeA (Shang et al. 2015). Optogenetic manipulations in this pathway suggest that it regulates escape responses

to visual threats, although the evidence is somewhat mixed (Evans et al. 2018; Shang et al. 2015, 2018; Zingg et al. 2017).

The sSC neurons that project to LP versus PBGN pathways receive input from overlapping but distinct RGC types (Reinhard et al. 2019). In addition, axon collaterals of one SC-projecting RGC type innervate GABAergic neurons in the dorsal raphe nucleus (DRN); these neurons inhibit their serotonergic DRN neighbors to promote escapes (Huang et al. 2017). In addition to understanding how different RGC types and different downstream pathways cooperate to initiate and guide defensive responses, determining where and how environmental factors and internal states intersect with visual signals to adapt behavioral responses to the animal's needs is an interesting area for future investigation (Evans et al. 2019).

3. ORIENTATION SELECTIVITY

Preferences for the orientation of static or moving stimuli (i.e., orientation selectivity) are prominent in the visual system, beginning in the retina. Different excitatory and inhibitory mechanisms give rise to orientation-selective (OS) responses of RGCs. Similar to DS RGCs, the contributions of OS RGCs to responses downstream are complex and target specific; their behavioral significance remains obscure.

3.1. Orientation-Selective Circuits and Retinal Ganglion Cell Types

OS RGCs were first identified in pigeons (Maturana & Frenk 1963) and rabbits (Levick 1967), where circuit mechanisms have been studied in some detail (Antinucci & Hindges 2018). More recently, robust OS responses were recorded in the mouse retina (Baden et al. 2016, Pearson & Kerschensteiner 2015, Zhao et al. 2013). Four morphologically and functionally distinct OS RGCs have been identified (Nath & Schwartz 2016, 2017) (**Figure 6a**). Two OS RGCs prefer light increments (ON OS RGCs), and two prefer light decrements (OFF OS RGCs). In each category, one OS RGC prefers horizontal and the other vertical stimulus orientations (Nath & Schwartz 2016, 2017).

The excitation of ON OS RGCs is tuned to their preferred stimulus orientation, and their inhibition is orthogonally tuned (**Figure 6b**). ON OS RGCs receive excitatory input from bipolar cells. Horizontal ON OS RGCs have horizontally elongated dendrite arbors and receive more bipolar cell input for stimuli aligned with their dendritic orientation (Nath & Schwartz 2016). In contrast, vertical ON OS RGCs have symmetric dendrite arbors, raising questions about their excitation tuning mechanisms. Because bipolar cells do not have oriented dendrites, one may speculate that presynaptic inhibition confers orientation selectivity to the output of some bipolar cell axons, similar to recent observations in DS circuits (Matsumoto et al. 2020). Orientation-tuned bipolar cell output has been observed in zebrafish but remains to be explored in the mouse retina (Johnston et al. 2019). Inhibition of vertical and horizontal ON OS RGCs is provided by OS GABAergic amacrine cells (Bloomfield 1994, Murphy-Baum & Taylor 2015, Nath & Schwartz 2016).

OFF OS RGCs combine orientation-tuned excitation and untuned inhibition (Nath & Schwartz 2017) (**Figure 6b**). Intriguingly, rather than glutamatergic input from bipolar cells, gap-junctional input from OS amacrine cells with asymmetric dendrites drives OFF OS RGC responses (Nath & Schwartz 2017). Thus, OS amacrine cells are critical for the feature selectivity of ON (synaptic inhibition) and OFF (gap junctions) OS RGC responses. The identity of OS amacrine cells and how dendritic orientations and computations shape their feature preferences remain to be uncovered.
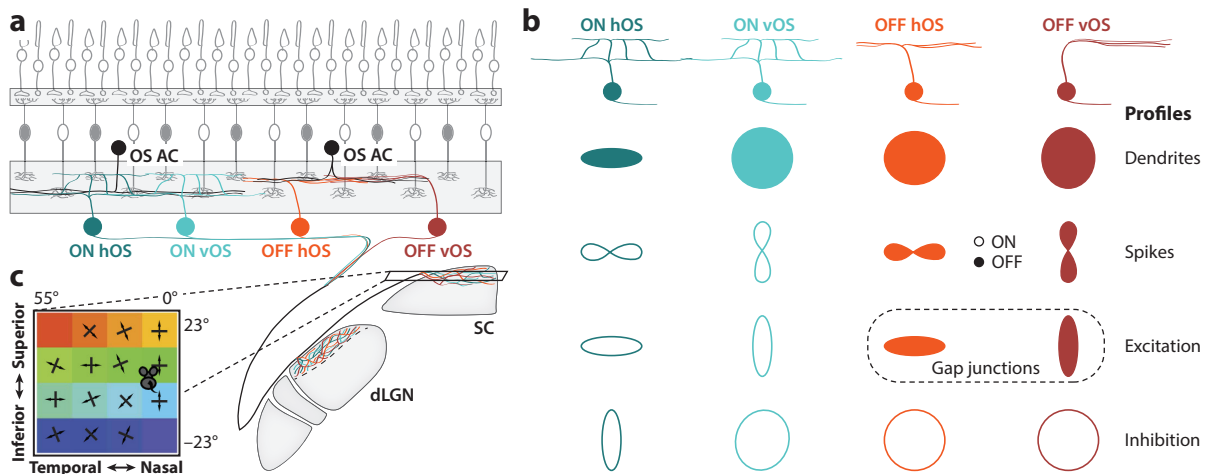
Figure 6

Orientation-selective (OS) retinal ganglion cell (RGC) types, pathways, and functions. (*a*) Four OS RGCs have been identified in mice; they respond to light increments (ON) or decrements (OFF) and one of two cardinal stimulus orientations [horizontal (hOS) and vertical (vOS)]. (*b*) Spatial profiles of dendrite, spike, excitatory, and inhibitory receptive fields of the four OS RGCs. The OS input to OFF OS RGCs is provided by gap junctions, likely with OS amacrine cells (ACs). Panel adapted with permission from Antinucci & Hindges (2018). (*c*) OS RGCs project to the dorsolateral geniculate nucleus (dLGN) shell and the superior colliculus (SC). Functional imaging of the sSC revealed that the orientation preferences of neurons are arranged concentrically around the center of the visual field. Panel adapted from Ahmadlou & Heimel (2015) (CC BY 4.0).

3.2. Downstream Pathways and Behavioral Significance of Retinal Orientation Selectivity

The vertical OFF OS RGC, also known as the JAM-B RGC, innervates the dLGN shell and the upper layer of the sSC (Kim et al. 2008, Nath & Schwartz 2017) (**Figure 6*c***). OS responses have been recorded in both targets (Marshel et al. 2012, Piscopo et al. 2013, Scholl et al. 2013, Wang et al. 2010, Zhao et al. 2013).

In the dLGN, OS (or motion axis–selective) responses are restricted to the shell (Marshel et al. 2012, Piscopo et al. 2013) and are partially inherited from OS RGCs and partially constructed by combining input from DS RGCs with opposite direction preferences (Liang et al. 2018). Restriction to the shell suggests that OS signals from the retina and dLGN reach the superficial layers of V1 through a distinct channel, similar to DS signals (Cruz-Martín et al. 2014). The contribution of this channel to cortical processing and its behavioral purpose remains to be elucidated. Independently, V1 layer 4 neurons derive OS responses from untuned dLGN inputs, as originally proposed by Hubel & Wiesel (1962; see also Lien & Scanziani 2013).

Approximately 20% of sSC neurons are OS (de Malmazet et al. 2018, Wang et al. 2010). In vivo two-photon imaging revealed that the orientation preferences of sSC neurons are organized into columns (Ahmadlou & Heimel 2015, Feinberg & Meister 2015). Neurons within each column prefer the same stimulus orientation throughout the depth of the sSC. Surprisingly, adjacent columns not only differ in their orientation preferences, but also cover different areas of visual space (Ahmadlou & Heimel 2015, Feinberg & Meister 2015). Consequently, orientation preferences are distributed inhomogeneously across visual space with gaps in coverage (Ahmadlou & Heimel 2015, de Malmazet et al. 2018, Feinberg & Meister 2015). Intriguingly, sSC columns in the binocular part of the mouse visual field prefer horizontal stimulus orientations, whereas sSC columns in the monocular part are concentrically arranged in visual space (Ahmadlou & Heimel

2015, de Malmazet et al. 2018) (**Figure 6c**). The behavioral significance of this arrangement and its interactions with the independent direction selectivity maps of the SC remain to be uncovered.

4. LUMINANCE CONTRAST

Spatiotemporal variations in brightness (i.e., luminance contrast) are a fundamental feature of visual scenes and shape our perception of the world (Delorme et al. 2000, Kaplan 2008, Stone et al. 1990). Most RGCs, including those with higher-order feature selectivities, are activated by simple luminance contrast stimuli (e.g., flashing bright or dark spots). Yet, from rodents to primates, one RGC class is active in featureless environments and suppressed by contrast.

4.1. Contrast Detection

The orthodox view of RGC function is that their center-surround receptive fields extract local luminance contrast (Kuffler 1953). However, even among the more conventional mouse RGC types, recent studies have identified diverse receptive field architectures and synaptic mechanisms that differentiate contrast preferences to fit behavioral demands that remain to be fully understood.

4.1.1. Contrast detection circuits and retinal ganglion cell types.
This section reviews three groups of contrast-encoding mouse RGCs: α RGCs, Pix$_{ON}$ RGCs, and F RGCs (**Figure 7a**). When targeting large cell bodies in the ganglion cell layer of the mouse retina, one consistently records three RGC types: one with sustained ON responses, one with sustained OFF responses, and one with transient OFF responses (Margolis & Detwiler 2007, Murphy & Rieke 2006, Pang et al. 2003). Based on morphological similarities to cat RGCs, these cells are called α RGCs (Boycott & Wässle 1974, Pang et al. 2003, Sun et al. 2002). Sustained ONα (sONα) and sustained OFFα (sOFFα) RGCs form a paramorphic pair (i.e., ON and OFF versions of a morphological type), possibly homologous to α (-like) RGC pairs in other rodents, cats, nonhuman primates, and humans (Boycott & Wässle 1974, Dacey & Petersen 1992, Peichl et al. 1987, Soto et al. 2020, Vitek et al. 1985).

Despite their paramorphy, sONα and sOFFα differ functionally beyond their preference for ON versus OFF stimuli. sONα and sOFFα RGCs exemplify two canonical arrangements of excitatory and inhibitory receptive fields (**Figure 7a**). sONα RGCs receive excitation from ON bipolar cells and inhibition from amacrine cells driven by the same bipolar cells (i.e., ON amacrine cells) (Morgan et al. 2011, Park et al. 2018, Schwartz et al. 2012). In this feedforward circuit, sONα RGCs' firing to temporal contrast is driven by excitation (Murphy & Rieke 2006). Type 6 bipolar cells account for approximately 70% of the excitatory input to sONα RGCs (Morgan et al. 2011, Schwartz et al. 2012, Tien et al. 2017). Tonic glutamate release from type 6 bipolar cells contributes to the high firing rates of sONα RGCs at the mean light level in an environment and their exquisite sensitivity to small fluctuations around the mean (i.e., high contrast sensitivity) (Sabbah et al. 2018, Schwartz et al. 2012, Zaghloul et al. 2003). Interestingly, sONα RGCs can substitute B6 cells with a type-specific complement of other bipolar cells to preserve their high contrast sensitivity and linear response functions when B6 cells are ablated during development (Tien et al. 2017).

In contrast, sOFFα RGCs receive excitation from OFF bipolar cells—including a unique dendriteless type—and inhibition from ON amacrine cells (Della Santina et al. 2016, Murphy & Rieke 2006, Pang et al. 2003). In this push–pull circuit, the firing of sOFFα RGCs to temporal contrast is driven by the coincidence of excitation and disinhibition (Murphy & Rieke 2006).

In addition to differences in temporal contrast processing, sONα and sOFFα RGCs integrate spatial contrast differently. The nonlinear subunits of sONα RGC receptive fields allow them to
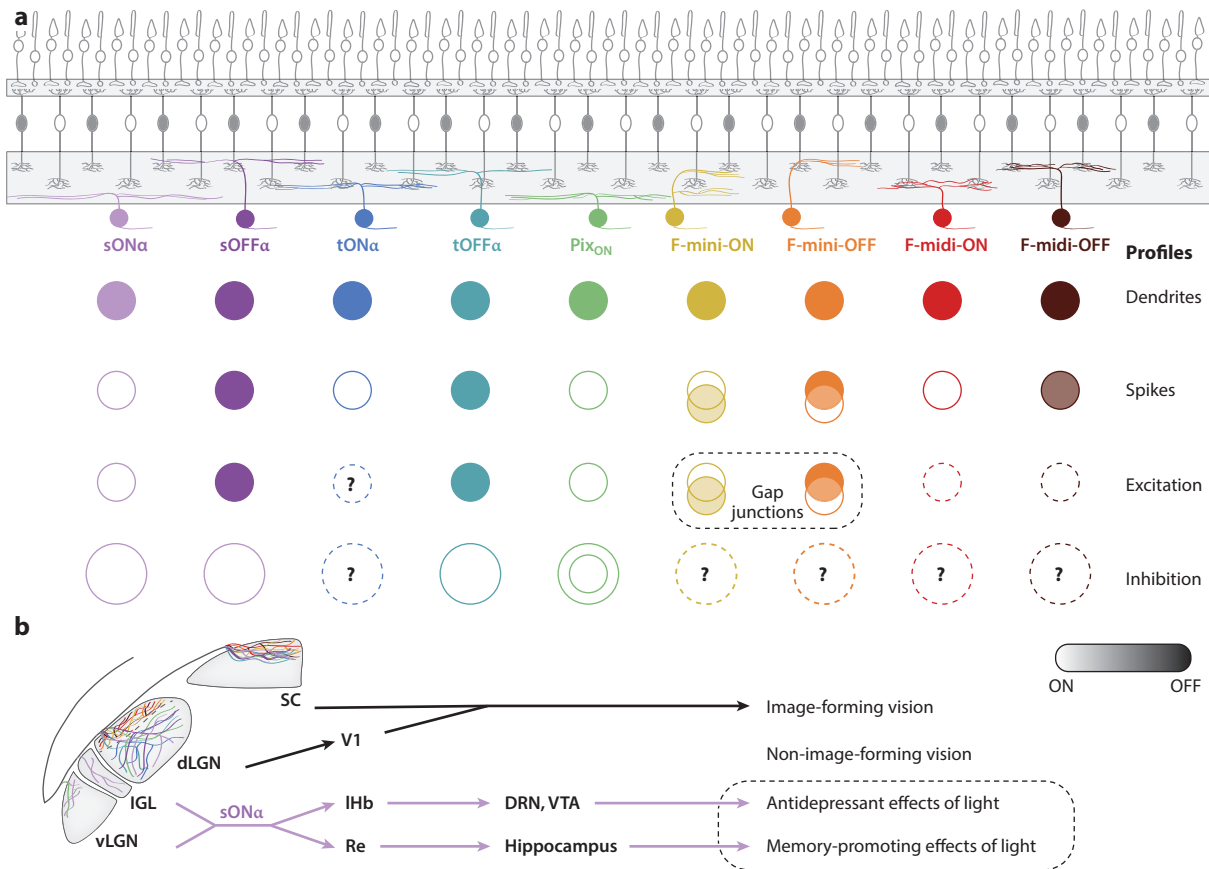
Figure 7

Contrast-encoding α, Pix$_{ON}$, and F retinal ganglion cells (RGCs), pathways, and functions. (*a*) Schematic of four α RGCs (sONα, sOFFα, tONα, tOFFα), the Pix$_{ON}$ RGC, and four F RGCs (F-mini-ON, F-mini-OFF, F-midi-ON, F-midi-OFF) and the spatial profiles of their dendrites and spike, excitatory, and inhibitory receptive fields. (*b*) α and Pix$_{ON}$ RGCs project to the dorsolateral geniculate nucleus (dLGN) core, whereas F RGCs project to the dLGN shell. Projections to the dLGN and superior colliculus (SC) mediate image-forming functions of vision. In addition, sONα RGCs densely innervate the ventrolateral geniculate nucleus (vLGN) and intergeniculate leaflet (IGL) to mediate non-image-forming functions. Additional abbreviations: 1Hb, lateral habenula; DRN, dorsal raphe nucleus; Re, nucleus reuniens; V1, primary visual cortex; VTA, ventral tegmental area.

respond to luminance-invariant changes in stimulus patterns (i.e., nonlinear spatial integration), whereas sOFFα RGCs sum stimulus intensity across their receptive fields and respond only if the result changes (i.e., linear spatial integration) (Krieger et al. 2017, Schwartz et al. 2012). In addition to extending response functions to higher spatial frequencies (i.e., finer spatial detail), nonlinear interactions of bipolar cells, which comprise the receptive field subunits, sensitize sONα RGCs to motion (Kuo et al. 2016). In dim light, the spatial integration of sONα RGCs becomes linear, as the membrane potential of the bipolar cells depolarizes to a linear input–output range (Grimes et al. 2014). This switch to linear integration may average out noise from quantal fluctuations in photon absorption and preserve contrast sensitivity at the expense of fine spatial detail in dim light (Grimes et al. 2014).

Finally, sONα but not sOFFα RGCs encode luminance (Schmidt et al. 2014, Sonoda et al. 2018). The luminance encoding of sONα RGCs depends on their expression of the photopigment

melanopsin—sONα RGCs are, therefore, also known as M4 intrinsically photosensitive RGCs (ipRGCs) (Ecker et al. 2010). Melanopsin mediates only small photocurrents in sONα RGCs, but second messengers close potassium channels to increase sONα RGC excitability and firing rates in a light-dependent manner (Ecker et al. 2010, Jiang et al. 2018, Schmidt et al. 2014, Sonoda et al. 2018). It has been suggested that bipolar cells also contribute to the luminance encoding of sONα RGCs (Sabbah et al. 2018).

Transient OFFα (tOFFα) RGCs combine OFF excitation with ON inhibition (i.e., push–pull circuit), and their firing to temporal contrast relies on coincident excitation and disinhibition (Murphy & Rieke 2006, Pang et al. 2003) (**Figure 7a**). As discussed in Section 2.3, VG3 amacrine cells contribute to the excitation of tOFFα RGCs, and AII amacrine cells contribute to their tonic inhibition (Kim et al. 2020, Krishnaswamy et al. 2015, Lee et al. 2014, Münch et al. 2009). tOFFα RGCs integrate spatial information nonlinearly and are highly sensitive to motion, particularly approach motion (Kim et al. 2020, Krieger et al. 2017, Münch et al. 2009). In addition, tOFFα RGCs receive gap-junctional input, which increases their sensitivity to dim light flashes (Murphy & Rieke 2011).

Recent studies identified a putative paramorphic partner of transient tOFFα RGCs. tONα RGCs are labeled with the other α RGCs in *Kcgn4-Cre* transgenic mice; express the group-specific markers SMI32 and SPP1; cluster with the other α RGCs in transcriptomic analyses; and, like the other α RGCs, have narrow action potentials (Krieger et al. 2017, Tran et al. 2019). tONα RGCs integrate spatial information nonlinearly. The stimulus preferences of tONα RGCs and underlying circuit mechanisms remain to be studied in more detail.

In primates, midget RGCs mediate high-acuity vision. The simple preferences of midget RGCs, particularly in the fovea, resemble photoreceptor pixel representations (Sinha et al. 2017). A recent study identified a pixel-encoder RGC type (Pix$_{ON}$ RGCs) with noncanonical receptive fields in mice (Johnson et al. 2018) (**Figure 7a**). Pix$_{ON}$ RGCs receive only excitatory input (from ON bipolar cells) for stimuli overlaying their dendrites and only inhibitory input (from ON amacrine cells) for stimuli outside of their dendrite arbors (Johnson et al. 2018). Excitatory inputs to Pix$_{ON}$ RGCs integrate spatial information linearly, and, because of tonic excitation and high baseline firing rates, Pix$_{ON}$ RGCs signal increases and decreases in stimulus intensity approximately linearly (Johnson et al. 2018). The exclusion of inhibition from the receptive field center increases the gain of excitation-to-spike conversion. The truly lateral inhibition from the donut-shaped inhibitory receptive fields is provided by spiking GABAergic amacrine cells and is temporally matched to excitation, simplifying the contrast encoding of Pix$_{ON}$ RGCs and enhancing the representation of edges in a scene (Johnson et al. 2018).

An analysis of transcription factor profiles revealed that approximately 20% of RGCs express the forkhead/winged-helix domain protein FOXP2 (i.e., F RGCs) (Rousso et al. 2016). The F RGC family has four members comprising two paramorphic pairs named for their arbor size and contrast preferences, F-midi-ON and F-midi-OFF and F-mini-ON and F-mini-OFF (Rousso et al. 2016) (**Figure 7a**). The four F RGCs coexpress unique combinations of FOXP1 and BRN3a-c with FOXP2, suggesting that a combinatorial transcription factor code drives their differentiation (Rousso et al. 2016). F-midi-ON cells respond exclusively to light increments, F-midi-OFF cells respond more robustly to light decrements, and both F-midi-ON and F-midi-OFF cells prefer small stimuli (Rousso et al. 2016). Other stimulus preferences and the underlying circuit mechanisms remain to be uncovered.

F-mini-ON and F-mini-OFF RGCs are the second and third most abundant RGC types in the mouse retina, respectively, and account for 13% of all RGCs (Rousso et al. 2016). Despite differences in their dendritic stratification, both F-mini-ON (bistratified) and F-mini-OFF

(monostratified) RGCs respond to light increments and decrements (Cooler & Schwartz 2020). Intriguingly, the ON and OFF receptive fields of F-mini-ON RGCs are consistently offset, with OFF fields offset 30–40 μm ventrally from ON fields (Cooler & Schwartz 2020). Rather than glutamate release from OFF bipolar cells, gap-junctional coupling to F-mini-OFF RGCs delivers OFF excitation to F-mini-ON RGCs and vice versa (Cooler & Schwartz 2020). On average, four F-mini-OFF RGCs are coupled to each F-mini-ON RGC, and approximately four F-mini-ON RGCs are coupled to each F-mini-OFF RGC. In conjunction with dendritic asymmetries, this unexpected consummation of their paramorphic pairing accounts for the offset between the ON and OFF receptive field of F-mini-ON and F-mini-OFF RGCs, which modeling suggests increases the precision of edge detection in the retina (Cooler & Schwartz 2020).

4.1.2. Downstream pathways and behavioral significance of retinal contrast detection. Although projection patterns remain to be mapped comprehensively and cell type specifically, transgenic labeling and retrograde tracing revealed that α RGCs, Pix$_{ON}$ RGCs, and F RGCs target the dLGN (Ecker et al. 2010, Ellis et al. 2016, Huberman et al. 2008, Johnson et al. 2018, Martersteck et al. 2017, Román Rosón et al. 2019, Rompani et al. 2017, Rousso et al. 2016) (**Figure 7b**). α RGCs and Pix$_{ON}$ RGCs innervate the dLGN core, and F RGCs innervate the dLGN shell, indicating that they provide input to parallel pathways from the retina to V1 (Cruz-Martín et al. 2014, Ecker et al. 2010, Huberman et al. 2008, Johnson et al. 2018, Martersteck et al. 2017, Rompani et al. 2017, Rousso et al. 2016).

The convergence of RGC axons onto thalamocortical (TC) projection neurons in the dLGN has been analyzed extensively (Liang & Chen 2020). Recent anatomical and functional evidence indicates that 10 or more RGCs converge onto each TC neuron, but a few dominate its responses (Hammer et al. 2015, Litvina & Chen 2017, Morgan et al. 2016, Rompani et al. 2017). Different modes of functional convergence can be distinguished. Whereas some TC neurons combine input from a single or functionally similar RGC type(s) (i.e., relay mode), others combine input from RGCs with different feature preferences (i.e., combination mode) (Liang et al. 2018, Rompani et al. 2017). α RGCs and Pix$_{ON}$ RGCs are overrepresented in the dLGN-projecting set and contribute to relay-mode and combination-mode convergence, which preserves and transforms, respectively, the RGCs' responses on the way to V1 (Piscopo et al. 2013, Román Rosón et al. 2019, Rompani et al. 2017, Suresh et al. 2016). TC neurons of the dLGN core project to layer 4 of V1. Precise spatial offsets of approximately 80 converging ON and OFF TC neurons generate OS responses in V1 layer 4 neurons, and spatial offsets combine with temporal mismatches (i.e., transient-sustained, sustained-transient) of ON and OFF TC neurons to generate DS responses (Lien & Scanziani 2013, 2018; Liu et al. 2010).

A recent study found that sONα RGCs determine the perceptual threshold for dim light detection in mice, likely through signals propagating along the retino-geniculo-cortical pathway (Smeds et al. 2019).

Axon collaterals of α RGCs, Pix$_{ON}$ RGCs, and F RGCs innervate the sSC (Ecker et al. 2010, Ellis et al. 2016, Hong et al. 2011, Huberman et al. 2009, Johnson et al. 2018, Martersteck et al. 2017, Rousso et al. 2016) (**Figure 7b**). Functional evidence indicates that approximately six RGCs converge onto each sSC neuron (Chandrasekaran et al. 2007). Unlike TC neurons (Grubb & Thompson 2003), most sSC neurons combine inputs from ON and OFF responsive RGCs (Wang et al. 2010). Recently, Reinhard et al. (2019) analyzed the RGC complements that provide input via the sSC to the PBGN and LP. They found that sOFFα, tOFFα, tONα, Pix$_{ON}$, F-mini-ON, and F-midi-ON RGCs distribute input evenly between both pathways. In contrast, sONα RGCs send signals preferentially to the PBGN, F-mini-OFF RGCs send signals preferentially to the

LP, and F-midi-OFF RGCs send signals to neither (Reinhard et al. 2019). These distinct RGC complements' contributions to feature representations along these pathways and behavior remain to be uncovered.

Recently, sONα RGCs were found to dominate input to two pathways through the ventrolateral geniculate nucleus (vLGN) and intergeniculate leaflet (IGL), which, together with the dLGN, make up the LGN complex (Monavarfeshani et al. 2017) (**Figure 7b**). First, sONα RGCs innervate GABAergic neurons in the vLGN and IGL that project to the lateral habenula (LHb) and mediate antidepressant effects of light (Huang et al. 2019). Second, sONα RGCs innervate CaMKIIα neurons in the vLGN and IGL, which provide a mixture of excitation and inhibition to the nucleus reuniens (Re) to promote spatial memory formation (Huang et al. 2021). Antidepressant and memory-promoting effects are thought to rely on luminance rather than contrast signals. How parallel pathways through the LGN complex extract different information from the sONα RGC inputs (the dLGN extracting contrast information and the vLGN and IGL extracting luminance information) is a fundamental open question.

4.2. Suppressed-by-Contrast Signals

All of the RGCs discussed above fire action potentials to signal positive contrast features (ON), negative contrast features (OFF), or both (ON-OFF). However, one conserved RGC class is active in featureless environments and silenced by contrast.

4.2.1. Suppressed-by-contrast circuits and retinal ganglion cell types.

Suppressed-by-contrast (SbC) RGCs were first discovered in rabbits and cats (Levick 1967, Rodieck 1967) and later identified in nonhuman primates (de Monasterio 1978). Because they prefer featureless environments, SbC RGCs have also been called uniformity detectors (Levick 1967, Sivyer & Vaney 2010, Sivyer et al. 2010). Recently, two groups characterized SbC RGCs with different suppression kinetics in mice (Jacoby et al. 2015, Tien et al. 2015) (**Figure 8a,b**). Transient SbC (tSbC) RGCs stop firing for approximately 0.5 s after light increments or decrements (Tien et al. 2015), whereas sustained SbC (sSbC) RGCs are silenced for the duration of light steps (up to 20 s) (Jacoby et al. 2015). tSbC RGCs have also been described as delayed ON RGCs because their firing rates can rebound above baseline after light increments transiently suppress them (Jacoby & Schwartz 2018, Mani & Schwartz 2017). Both tSbC and sSbC RGCs have bistratified
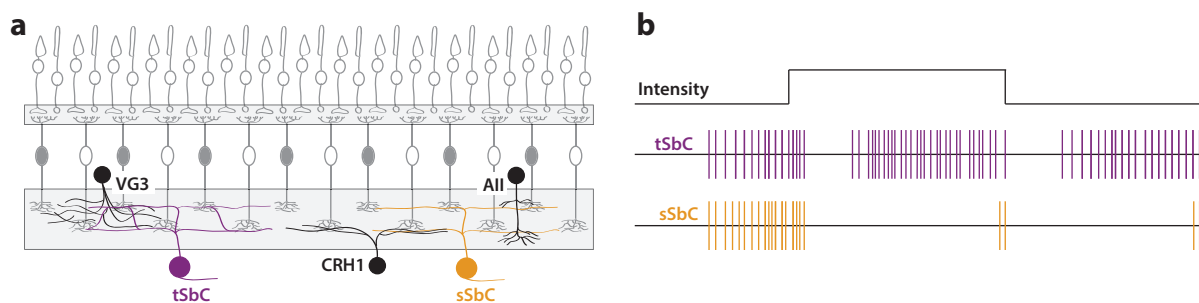

Figure 8

Suppressed-by-contrast RGC types. (*a*) Schematic illustration of tSbC and sSbC RGCs and the presynaptic amacrine cell types that shape the suppressive contrast encoding. (*b*) Schematic of transient and sustained spike suppression light increments and decrements in tSbC and sSbC RGCs, respectively. Abbreviations: AII, amacrine cell; CRH1, corticotropin-releasing hormone-expressing amacrine cell type 1; RGC, retinal ganglion cell; sSbC, sustained suppressed-by-contrast; tSbC, transient suppressed-by-contrast; VG3, VGLUT3-expressing amacrine cell.

dendrites but receive glutamatergic input only from ON bipolar cells (Jacoby et al. 2015, Tien et al. 2015). ON excitation is weak and overwhelmed by ON inhibition, whereas suppression of tonic excitation coincides with inhibition at light OFF (Jacoby et al. 2015, Tien et al. 2015). The arbors of tSbC RGCs have frequent recursions in which dendrites from the OFF layer dive back to the ON layer and ON dendrites ascent to the OFF layer far from the soma (Ivanova et al. 2013, Tien et al. 2015, Zhu et al. 2014). Recursive dendrite arbors are also a hallmark of SbC RGCs in rabbits (Sivyer & Vaney 2010).

Inhibition kinetics differentiate the suppressive responses of tSbC and sSbC RGCs. tSbC RGCs receive transient, predominantly glycinergic inhibition at light ON and OFF (Tien et al. 2015). Optogenetic and anatomical circuit mapping identified VG3 amacrine cells as a source of tSbC RGC inhibition (Lee et al. 2016, Tien et al. 2016). This, in turn, identified VG3 amacrine cells as dual transmitter neurons, which use their two transmitters (glutamate and glycine) in a target-specific manner (Lee et al. 2016, Tien et al. 2016). Interestingly, the transient VG3 amacrine cells preferentially synapse onto the ascending and descending processes of tSbC dendrites, providing a functional explanation for this conserved morphological feature (Tien et al. 2016). Type-specific cell deletion showed that VG3 amacrine cells silence tSbC RGCs in response to small OFF stimuli (Tien et al. 2016). The amacrine cells that inhibit tSbC RGCs in response to ON and large OFF stimuli remain to be identified. In contrast, sSbC RGCs receive sustained predominantly GABAergic inhibition at light ON and OFF (Jacoby et al. 2015). Paired recordings and type-specific cell ablation demonstrated that CRH-1 amacrine cells are the source of sustained ON inhibition to sSbC RGCs (Jacoby et al. 2015). The amacrine cells that inhibit sSbC RGCs in response to OFF stimuli remain to be identified. Thus, tSbC and sSbC RGCs illustrate how specific amacrine cell combinations shape the feature representations of the retinal output. The modularity of interneuron circuits in the retina may be replicated in other parts of the nervous system.

4.2.2. Downstream pathways and behavioral significance of retinal suppressed-by-contrast signals.

The projection patterns of tSbC RGCs and sSbC RGCs remain to be analyzed in detail, but recent retrograde labeling experiments indicated that SbC-responsive cells abound among the dLGN-projecting RGCs (Román Rosón et al. 2019). SbC responses have also been recorded in the dLGN and V1 of mice and nonhuman primates (Niell & Stryker 2010, Piscopo et al. 2013, Zeater et al. 2015), suggesting that tSbC and sSbC RGC signals may propagate along dedicated pathways from the retina to the cortex. In addition, SbC responses could arise independently at subsequent stages of the retino-geniculo-cortical pathway, analogous to OS and DS responses (Niell 2013). SbC RGC inputs also converge with conventional RGC inputs in the dLGN (Liang et al. 2018). The function of SbC signals, which have also been recorded in the SC, remains mysterious (Ito et al. 2017, Masland & Martin 2007). Current hypotheses range from contrast gain control of conventional signals to detection of self-generated visual stimuli (e.g., eye movements and blinks) (Masland & Martin 2007, Tailby et al. 2007, Tien et al. 2015).

4.3. Luminance Encoding

Ambient light levels influence a wide range of physiological processes and behaviors (i.e., non-image-forming vision). The persistence of these influences (e.g., circadian photoentrainment and suppression of melatonin) in patients and mice without rods and cones, and the loss of these influences in enucleated mice and *Math5* mutants, which lack signals from the eye to the brain, suggested the existence of another photoreceptive neuron in the retina (Brzezinski et al. 2005, Czeisler et al. 1995, Ebihara & Tsuji 1980, Freedman et al. 1999, Lucas et al. 1999, Wee et al. 2002, Zaidi et al. 2007).
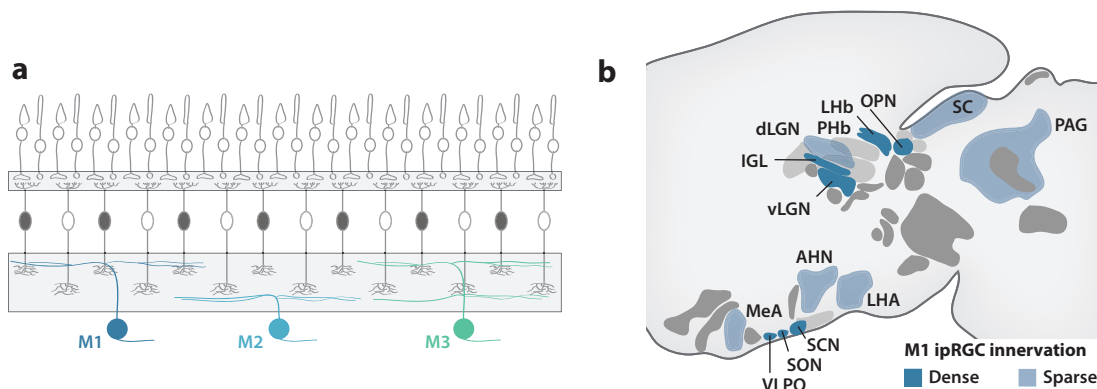
Figure 9

Melanopsin-expressing RGC types and pathways. (*a*) Schematic illustration of M1–M3 ipRGCs. (*b*) M1 ipRGCs send luminance signals to a wide range of brain areas that mediate image-forming and non-image-forming functions. Abbreviations: AHN, anterior hypothalamic area; dLGN, dorsolateral geniculate nucleus; IGL, intergeniculate leaflet; ipRGC, intrinsically photosensitive RGC; LHA, lateral hypothalamic area; LHb, lateral habenula; MeA, medial amygdala, anterior; OPN, olivary pretectal nucleus; PAG, periaqueductal gray; PHb, perihabenular nucleus; RGC, retinal ganglion cell; SC, superior colliculus; SCN, suprachiasmatic nucleus; SON, supraoptic nucleus; vLGN, ventrolateral geniculate nucleus; VLPO, ventrolateral preoptic area.

4.3.1. Luminance-encoding circuits and retinal ganglion cell types. Through retrograde tracing from the suprachiasmatic nucleus (SCN), the source of circadian rhythms and the site of their photoentrainment, Berson et al. (2002) discovered RGCs that remained light sensitive when pharmacologically or physically removed from the retina. Hattar et al. (2002) demonstrated that these ipRGCs express melanopsin, a photopigment previously identified in the retina (Provencio et al. 1998, 2000), and project to brain areas involved in non-image-forming vision. Since then, several melanopsin-expressing (M) ipRGC types have been distinguished in mice, and their contributions to physiology and behavior are being deciphered. The ipRGCs have been reviewed comprehensively elsewhere (Aranda & Schmidt 2020, Do 2019, Do & Yau 2010, Lazzerini Ospri et al. 2017, Van Gelder & Buhr 2016). In this section, I highlight recent advances in our understanding of ipRGC diversity and the downstream pathways through which they shape physiology and behavior.

The count of ipRGC types is up to six (M1–M6) (**Figure 9a**). The M1 ipRGCs initially identified by Berson et al. (2002) have the largest intrinsic photocurrents and signal changes in average luminance, with little response to transient or local fluctuations in light intensity (i.e., contrast) (Ecker et al. 2010, Zhao et al. 2014b). By comparison, M2–M6 ipRGCs have small intrinsic photocurrents. Driven by synaptic inputs, the spike trains of M2–M6 ipRGCs encode contrast (Ecker et al. 2010, Quattrochi et al. 2018, Zhao et al. 2014b). In addition, the average firing rates of M2–M4 ipRGCs signal average luminance (Ecker et al. 2010, Zhao et al. 2014b). To what extent this luminance signal reflects sustained excitatory synaptic inputs, intrinsic photocurrents, and melanopsin's influences on excitability remains to be determined (Ecker et al. 2010, Sabbah et al. 2018, Sonoda et al. 2018, Zhao et al. 2014b). In M4 ipRGCs (also known as sONα RGCs), second-messenger signals from melanopsin close potassium channels, increasing input resistance and the impact of synaptic excitation (Sonoda et al. 2018). Thus, increases in luminance raise the contrast sensitivity of M4 ipRGCs, highlighting the importance of understanding the interactions of intrinsic and synaptic signals in ipRGCs (Sonoda et al. 2018). Luminance encoding of M5 ipRGC (also known as Pix_{ON} RGCs) has not been explored (Johnson et al. 2018, Stabio et al. 2017), and M6 ipRGCs appear not to signal luminance (Levine & Schwartz 2020).

The dendrites of M1–M6 ipRGCs stratify in different patterns. M1 dendrites stratify in the IPL's OFF sublamina; M2, M4, and M5 dendrites stratify in the ON sublamina; and M3 and M6 dendrites are bistratified, targeting the ON and OFF sublamina. Despite differences in stratification, the dendrites of all ipRGC types receive glutamatergic input exclusively from ON bipolar cells (Ecker et al. 2010, Quattrochi et al. 2018, Zhao et al. 2014b). M1 dendrites recruit ON bipolar cell inputs from axons passing through the IPL's OFF layer (Dumitrescu et al. 2009, Hoshi et al. 2009). The vast majority (approximately 95%) of en-passant synapses are formed by type 6 bipolar cells and differ ultrastructurally from their terminal synapses (Sabbah et al. 2018). The purpose of this arrangement and functional consequences of the en-passant synapse ultrastructure remain to be uncovered.

Luminance varies by $>10^9$ from moonless nights to sunny days (Rieke & Rudd 2009). Encoding this vast brightness range with a single neuron type could result in poor luminance resolution. However, recent studies revealed that M1 ipRGCs divide the light intensity range among themselves to encode luminance accurately as a population (Milner & Do 2017) and identified mechanisms underlying this population coding (Emanuel et al. 2017, Lee et al. 2019). Milner & Do (2017) discovered that most M1 ipRGCs have nonmonotonic intensity-response functions, in which firing rates rise from darkness to a preferred-luminance peak and then decline as lights get brighter (Milner & Do 2017). Sodium channel inactivation from increasing depolarizations accounts for the bright-light decline (Milner & Do 2017). The biophysical properties of M1 ipRGCs determine the setpoint of this depolarization block, and the differences among them distribute intensity encoding across the population (Emanuel et al. 2017). Rod-driven synaptic inputs extend the luminance encoding of M1 ipRGCs to dim light levels. Lee et al. (2019) discovered that a subset of M1 ipRGCs receive no rod input and that the strengths of rod-driven M1 ipRGC responses covary with their dendritic complexity. Thus, morphological, input, and biophysical variation of M1 ipRGCs support robust population encoding of ambient light levels. This gain in luminance resolution comes at the cost of spatial resolution.

4.3.2. Downstream pathways and behavioral significance of retinal luminance signals.
M1 ipRGCs send luminance signals to numerous brain areas involved in non-image-forming vision (Hattar et al. 2002, 2006) (**Figure 9b**). M1 ipRGCs were discovered through their projections to the SCN (Berson et al. 2002). When M1 ipRGCs are ablated, photoentrainment is lost, and circadian rhythms run free (Göz et al. 2008, Güler et al. 2008, Hatori et al. 2008). M1 ipRGCs also provide input to the shell of the olivary pretectal nucleus (OPN) (Hattar et al. 2002, 2006). SCN-projecting and OPN-projecting M1 ipRGCs differ in their expression of the transcription factor Brn3b. SCN-projecting M1 ipRGCs are BRN3b-negative, whereas OPN-projecting M1 ipRGCs are BRN3b-positive (Chen et al. 2011). An intersectional cell ablation strategy revealed that the BRN3b-positive M1 ipRGCs are required for normal pupillary light responses (mediated by the OPN) but dispensable for circadian photoentrainment, which relies on BRN3b-negative M1 ipRGCs (Chen et al. 2011).

M1 ipRGCs exhibit further diversity in their synaptic output. Most M1 ipRGCs release glutamate and the neuropeptide pituitary adenylyl cyclase–activating polypeptide (PCAP) (Engelund et al. 2010, Hannibal et al. 2002). PCAP plays a modulatory role in circadian photoentrainment (Beaulé et al. 2009; Colwell et al. 2004; Kawaguchi et al. 2003, 2010) and supports sustained pupil constriction in response to light (Keenan et al. 2016). Intriguingly, Sonoda et al. (2020) discovered a subset of M1 ipRGCs that releases GABA to dampen the sensitivity of circadian photoentrainment and pupil constriction in response to light. This may explain the discrepancy between the high light sensitivity of M1 ipRGCs and the low light sensitivity of the behaviors they mediate (Sonoda et al. 2020).

Mice are nocturnal rodents that forage at night and sleep in the day. In addition to circadian rhythms in sleep–wake cycles, light pulses early in the night promote sleep acutely (Borbély 1978, Lupi et al. 2008). Different M1 ipRGCs and brain areas mediate the circadian and acute light effects on sleep. BRN3b-negative M1 ipRGC projections to the SCN entrain circadian sleep–wake cycles, whereas BRN3b-positive M1 ipRGC projections to the ventrolateral preoptic nucleus regulate sleep acutely (Rupp et al. 2019).

Projections of BRN3b-negative M1 ipRGCs to the SCN have also been shown to mediate the detrimental effects of shortened (3.5 h–3.5 h) light–dark cycles on spatial learning independent of circadian rhythms, whereas projections of BRN3b-negative M1 ipRGCs to the perihabenular nucleus of the thalamus mediate adverse effects on mood (Fernandez et al. 2018, LeGates et al. 2012). Interestingly, 2–3-h bright-light pulses have been shown to improve spatial learning and increase resilience to adverse stimuli in mice on a normal (12 h–12 h) light–dark cycle. These memory- and mood-enhancing effects of light were shown to be mediated M4 ipRGC (also known as sONα) signals propagating via the IGL and vLGN to the Re and the LHb, respectively (Huang et al. 2019, 2021).

5. REGIONAL SPECIALIZATION AND COLOR PROCESSING

In many species, RGCs are unevenly distributed across the retina. The dendrites of most RGCs maintain constant overlap with same-type neighbors. Therefore, dendritic and receptive field sizes scale as the inverse of RGC density (Masland 2001, Wässle 2004). Areas of high density and small receptive field size are referred to as acute zones (Baden et al. 2020). When looking at the overall RGC density, no acute zones are apparent in the mouse retina (Dräger & Olsen 1981, Jeon et al. 1998). However, Bleckert et al. (2014) discovered that sONα and sOFFα RGCs are packed more densely in the temporal retina, which covers the binocular visual field in mice. Acute zones in the binocular field (i.e., area centralis) are near-universal signs of functional binocular vision (Cartmill 1974, Pettigrew 1986). Therefore, the cell type–specific area centralis suggests that sONα and sOFFα RGCs play an important role in binocular vision of mice.

Additional inhomogeneities in RGC type distributions have been reported for W3 RGCs (enriched in the ventral retina), F RGCs except for F-midi-ON (enriched in the ventral retina), posterior motion–preferring ON-OFF DS RGCs (enriched in the temporal retina), Pix$_{ON}$ RGCs (or M5 ipRGCs, enriched in the nasal retina), and GABAergic M1 ipRGCs (enriched in the dorsotemporal retina) (El-Danaf & Huberman 2019, Rousso et al. 2016, Sonoda et al. 2020, Zhang et al. 2012). In cases where these apparent inhomogeneities were detected by transgenic labeling, independent confirmation is needed. In all cases, the impact of inhomogeneous feature representations on downstream processing and their behavioral purpose remain to be discovered.

Color processing varies along the dorsoventral axis of the mouse retina. Mice have two types of cone photoreceptors: true S-cones, which express only the short-wavelength-sensitive (S-) opsin, and mixed M/S-cones, which coexpress S- and middle-wavelength-sensitive (M-) opsins (Applebury et al. 2000, Haverkamp et al. 2005, Nadal-Nicolás et al. 2020, Ng et al. 2001, Wang et al. 2011). True S-cones are abundant in the ventral retina, where they account for up to 30% of all cones, but are sparse in the dorsal retina (Nadal-Nicolás et al. 2020). Furthermore, mixed M/S-cones express predominantly S-opsin in the ventral and M-opsin in the dorsal retina (Applebury et al. 2000, Haverkamp et al. 2005, Nadal-Nicolás et al. 2020, Ng et al. 2001, Wang et al. 2011). This asymmetry matches the spectral compositions of the upper (sky-dominated) and lower (ground-dominated) visual fields viewed by the ventral and dorsal retina, respectively (Baden et al. 2013).

A dedicated S-cone bipolar cell type (i.e., type 9) has been identified in mice (Breuninger et al. 2011, Haverkamp et al. 2005) and recently shown to be enriched in the ventral retina (Nadal-Nicolás et al. 2020). Blue–yellow opponent RGC types that utilize input from S-cone bipolar cells have been identified in several species (Chichilnisky & Baylor 1999, Dacey & Lee 1994, Sher & DeVries 2012). However, in mice, no single RGC type appears to be dedicated to color-opponent signaling. Instead, color opponency is restricted to the ventral retina and distributed across RGC types (Szatko et al. 2020). In primates, color-opponency relies on circuit comparisons of different cones through type-specific wiring. In mice, the majority of color-opponent RGCs rely on one of two regionally restricted mechanisms. First, in the opsin transition zone around the horizon, RGCs, by chance and position, can have different M- and S-opsin weights in their receptive field center versus surround (Chang et al. 2013). Second, in the ventral retina, some RGCs compare S-opsin-dominant cone input in their center to middle-wavelength-sensitive rod signals in their surround (Joesch & Meister 2016, Szatko et al. 2020). Consistent with these regional mechanisms, color-opponent responses in the dLGN are restricted to the dorsal visual field, and mice can only distinguish chromatic stimuli above the horizon (Denman et al. 2017, 2018).

6. SUMMARY

Recent years have seen tremendous progress in the cataloging of RGCs. Anatomical, functional, and transcriptomic surveys agree that there are more than 40 RGC types in mice (Baden et al. 2016, Bae et al. 2018, Rheaume et al. 2018, Tran et al. 2019). The feature selectivities and circuit mechanisms of only a minority of these cells have been studied in detail, and therefore, much work remains. Beyond filling in these gaps, challenges remain in trying to understand how individual RGCs encode multiple features (i.e., multiplexing), as in sONα RGCs signaling luminance and contrast; how features are encoded in the activity of RGC populations; and how they are extracted from naturalistic stimuli (Turner et al. 2019).

By comparison to our knowledge of RGC types and the circuit mechanisms that underlie their feature preferences, our understanding of the downstream pathways and behavioral significance of RGC signals remains rudimentary. Many of the relevant paragraphs of this review might have ended in "Here be dragons." I hope that more researchers will venture into these scarcely explored territories; trace the projection patterns of more RGC types; and elucidate how their signals are demultiplexed, transformed, and combined with other sensory inputs and information about internal states to guide behavior. This is critical for understanding the retina's diverse contributions to vision and will also anchor investigations of retinal processing.

DISCLOSURE STATEMENT

The author is not aware of any affiliations, memberships, funding, or financial holdings that might be perceived as affecting the objectivity of this review.

ACKNOWLEDGMENTS

LITERATURE CITED

Ahmadlou M, Heimel JA. 2015. Preference for concentric orientations in the mouse superior colliculus. *Nat. Commun.* 6:6773

Antinucci P, Hindges R. 2018. Orientation-selective retinal circuits in vertebrates. *Front. Neural Circuits* 12:11

Applebury ML, Antoch MP, Baxter LC, Chun LL, Falk JD, et al. 2000. The murine cone photoreceptor: a single cone type expresses both S and M opsins with retinal spatial patterning. *Neuron* 27(3):513–23

Aranda ML, Schmidt TM. 2020. Diversity of intrinsically photosensitive retinal ganglion cells: circuits and functions. *Cell. Mol. Life Sci.* 78(3):889–907

Baccus SA, Olveczky BP, Manu M, Meister M. 2008. A retinal circuit that computes object motion. *J. Neurosci.* 28(27):6807–17

Baden T, Berens P, Franke K, Román Rosón M, Bethge M, Euler T. 2016. The functional diversity of retinal ganglion cells in the mouse. *Nature* 529(7586):345–50

Baden T, Euler T, Berens P. 2020. Understanding the retinal basis of vision across species. *Nat. Rev. Neurosci.* 21(1):5–20

Baden T, Schubert T, Chang L, Wei T, Zaichuk M, et al. 2013. A tale of two retinal domains: near-optimal sampling of achromatic contrasts in natural scenes through asymmetric photoreceptor distribution. *Neuron* 80(5):1206–17

Bae JA, Mu S, Kim JS, Turner NL, Tartavull I, et al. 2018. Digital museum of retinal ganglion cells with dense anatomy and physiology. *Cell* 173(5):1293–306.e19

Barlow HB, Hill RM. 1963. Selective sensitivity to direction of movement in ganglion cells of the rabbit retina. *Science* 139(3553):412–14

Barlow HB, Hill RM, Levick WR. 1964. Retinal ganglion cells responding selectively to direction and speed of image motion in the rabbit. *J. Physiol.* 173:377–407

Barlow HB, Levick WR. 1965. The mechanism of directionally selective units in rabbit's retina. *J. Physiol.* 178(3):477–504

Beaulé C, Mitchell JW, Lindberg PT, Damadzic R, Eiden LE, Gillette MU. 2009. Temporally restricted role of retinal PACAP: integration of the phase-advancing light signal to the SCN. *J. Biol. Rhythms* 24(2):126–34

Berson DM, Dunn FA, Takao M. 2002. Phototransduction by retinal ganglion cells that set the circadian clock. *Science* 295(5557):1070–73

Blanchard DC, Williams G, Lee EMC, Blanchard RJ. 1981. Taming of wild *Rattus norvegicus* by lesions of the mesencephalic central gray. *Physiol. Psychol.* 9(2):157–63

Bleckert A, Schwartz GW, Turner MH, Rieke F, Wong ROL. 2014. Visual space is represented by nonmatching topographies of distinct mouse retinal ganglion cell types. *Curr. Biol.* 24(3):310–15

Bloomfield SA. 1994. Orientation-sensitive amacrine and ganglion cells in the rabbit retina. *J. Neurophysiol.* 71(5):1672–91

Borbély AA. 1978. Effects of light on sleep and activity rhythms. *Prog. Neurobiol.* 10(1):1–31

Borghuis BG, Marvin JS, Looger LL, Demb JB. 2013. Two-photon imaging of nonlinear glutamate release dynamics at bipolar cell synapses in the mouse retina. *J. Neurosci.* 33(27):10972–85

Boycott BB, Wässle H. 1974. The morphological types of ganglion cells of the domestic cat's retina. *J. Physiol.* 240(2):397–419

Breuninger T, Puller C, Haverkamp S, Euler T. 2011. Chromatic bipolar cell pathways in the mouse retina. *J. Neurosci.* 31(17):6504–17

Briggman KL, Helmstaedter M, Denk W. 2011. Wiring specificity in the direction-selectivity circuit of the retina. *Nature* 471(7337):183–88

Brüggen B, Meyer A, Boven F, Weiler R, Dedek K. 2015. Type 2 wide-field amacrine cells in TH::GFP mice show a homogenous synapse distribution and contact small ganglion cells. *Eur. J. Neurosci.* 41(6):734–47

Brzezinski JA, Brown NL, Tanikawa A, Bush RA, Sieving PA, et al. 2005. Loss of circadian photoentrainment and abnormal retinal electrophysiology in Math5 mutant mice. *Investig. Ophthalmol. Vis. Sci.* 46(7):2540–51

Cang J, Savier E, Barchini J, Liu X. 2018. Visual function, organization, and development of the mouse superior colliculus. *Annu. Rev. Vis. Sci.* 4:239–62

Cartmill M. 1974. Rethinking primate origins. *Science* 184(4135):436–43

Chandrasekaran AR, Shah RD, Crair MC. 2007. Developmental homeostasis of mouse retinocollicular synapses. *J. Neurosci.* 27(7):1746–55

Chang L, Breuninger T, Euler T. 2013. Chromatic coding from cone-type unselective circuits in the mouse retina. *Neuron* 77(3):559–71

Chen M, Lee S, Park SJH, Looger LL, Zhou ZJ. 2014. Receptive field properties of bipolar cell axon terminals in direction-selective sublaminas of the mouse retina. *J. Neurophysiol.* 112(8):1950–62

Chen M, Lee S, Zhou ZJ. 2017. Local synaptic integration enables ON-OFF asymmetric and layer-specific visual information processing in vGluT3 amacrine cell dendrites. *PNAS* 114(43):11518–23

Chen S-K, Badea TC, Hattar S. 2011. Photoentrainment and pupillary light reflex are mediated by distinct populations of ipRGCs. *Nature* 476(7358):92–95

Chichilnisky EJ, Baylor DA. 1999. Receptive-field microstructure of blue-yellow ganglion cells in primate retina. *Nat. Neurosci.* 2(10):889–93

Colwell CS, Michel S, Itri J, Rodriguez W, Tam J, et al. 2004. Selective deficits in the circadian light response in mice lacking PACAP. *Am. J. Physiol. Regul. Integr. Comp. Physiol.* 287(5):R1194–201

Cooler S, Schwartz GW. 2020. An offset ON-OFF receptive field is created by gap junctions between distinct types of retinal ganglion cells. *Nat. Neurosci.* 24:105–15

Cruz-Martín A, El-Danaf RN, Osakada F, Sriram B, Dhande OS, et al. 2014. A dedicated circuit links direction-selective retinal ganglion cells to the primary visual cortex. *Nature* 507(7492):358–61

Czeisler CA, Shanahan TL, Klerman EB, Martens H, Brotman DJ, et al. 1995. Suppression of melatonin secretion in some blind patients by exposure to bright light. *N. Engl. J. Med.* 332(1):6–11

Dacey DM, Lee BB. 1994. The "blue-on" opponent pathway in primate retina originates from a distinct bistratified ganglion cell type. *Nature* 367(6465):731–35

Dacey DM, Petersen MR. 1992. Dendritic field size and morphology of midget and parasol ganglion cells of the human retina. *PNAS* 89(20):9666–70

De Franceschi G, Vivattanasarn T, Saleem AB, Solomon SG. 2016. Vision guides selection of freeze or flight defense strategies in mice. *Curr. Biol.* 26(16):2150–54

de Malmazet D, Kühn NK, Farrow K. 2018. Retinotopic separation of nasal and temporal motion selectivity in the mouse superior colliculus. *Curr. Biol.* 28(18):2961–69.e4

de Monasterio FM. 1978. Properties of ganglion cells with atypical receptive-field organization in retina of macaques. *J. Neurophysiol.* 41(6):1435–49

Dean P, Redgrave P, Westby GW. 1989. Event or emergency? Two response systems in the mammalian superior colliculus. *Trends Neurosci.* 12(4):137–47

Della Santina L, Kuo SP, Yoshimatsu T, Okawa H, Suzuki SC, et al. 2016. Glutamatergic monopolar interneurons provide a novel pathway of excitation in the mouse retina. *Curr. Biol.* 26(15):2070–77

Delorme A, Richard G, Fabre-Thorpe M. 2000. Ultra-rapid categorisation of natural scenes does not rely on colour cues: a study in monkeys and humans. *Vis. Res.* 40(16):2187–200

Demb JB, Singer JH. 2015. Functional circuitry of the retina. *Annu. Rev. Vis. Sci.* 1:263–89

Denman DJ, Luviano JA, Ollerenshaw DR, Cross S, Williams D, et al. 2018. Mouse color and wavelength-specific luminance contrast sensitivity are non-uniform across visual space. *eLife* 7:e31209

Denman DJ, Siegle JH, Koch C, Reid RC, Blanche TJ. 2017. Spatial organization of chromatic pathways in the mouse dorsal lateral geniculate nucleus. *J. Neurosci.* 37(5):1102–16

Dhande OS, Estevez ME, Quattrochi LE, El-Danaf RN, Nguyen PL, et al. 2013. Genetic dissection of retinal inputs to brainstem nuclei controlling image stabilization. *J. Neurosci.* 33(45):17797–813

Diamond JS. 2017. Inhibitory interneurons in the retina: types, circuitry, and function. *Annu. Rev. Vis. Sci.* 3:1–24

Ding H, Smith RG, Poleg-Polsky A, Diamond JS, Briggman KL. 2016. Species-specific wiring for direction selectivity in the mammalian retina. *Nature* 535(7610):105–10

Do MTH. 2019. Melanopsin and the intrinsically photosensitive retinal ganglion cells: biophysics to behavior. *Neuron* 104(2):205–26

Do MTH, Yau K-W. 2010. Intrinsically photosensitive retinal ganglion cells. *Physiol. Rev.* 90(4):1547–81

Dräger UC, Olsen JF. 1981. Ganglion cell distribution in the retina of the mouse. *Investig. Ophthalmol. Vis. Sci.* 20(3):285–93

Dumitrescu ON, Pucci FG, Wong KY, Berson DM. 2009. Ectopic retinal ON bipolar cell synapses in the OFF inner plexiform layer: contacts with dopaminergic amacrine cells and melanopsin ganglion cells. *J. Comp. Neurol.* 517(2):226–44

Ebihara S, Tsuji K. 1980. Entrainment of the circadian activity rhythm to the light cycle: effective light intensity for a Zeitgeber in the retinal degenerate C3H mouse and the normal C57BL mouse. *Physiol. Behav.* 24(3):523–27

Ecker JL, Dumitrescu ON, Wong KY, Alam NM, Chen S-K, et al. 2010. Melanopsin-expressing retinal ganglion-cell photoreceptors: cellular diversity and role in pattern vision. *Neuron* 67(1):49–60

El-Danaf RN, Huberman AD. 2019. Sub-topographic maps for regionally enhanced analysis of visual space in the mouse retina. *J. Comp. Neurol.* 527(1):259–69

Ellis EM, Gauvain G, Sivyer B, Murphy GJ. 2016. Shared and distinct retinal input to the mouse superior colliculus and dorsal lateral geniculate nucleus. *J. Neurophysiol.* 116(2):602–10

Elstrott J, Anishchenko A, Greschner M, Sher A, Litke AM, et al. 2008. Direction selectivity in the retina is established independent of visual experience and cholinergic retinal waves. *Neuron* 58(4):499–506

Emanuel AJ, Kapur K, Do MTH. 2017. Biophysical variation within the M1 type of ganglion cell photoreceptor. *Cell Rep.* 21(4):1048–62

Engelund A, Fahrenkrug J, Harrison A, Hannibal J. 2010. Vesicular glutamate transporter 2 (VGLUT2) is co-stored with PACAP in projections from the rat melanopsin-containing retinal ganglion cells. *Cell Tissue Res.* 340(2):243–55

Euler T, Detwiler PB, Denk W. 2002. Directionally selective calcium signals in dendrites of starburst amacrine cells. *Nature* 418(6900):845–52

Euler T, Haverkamp S, Schubert T, Baden T. 2014. Retinal bipolar cells: elementary building blocks of vision. *Nat. Rev. Neurosci.* 15(8):507–19

Evans DA, Stempel AV, Vale R, Branco T. 2019. Cognitive control of escape behaviour. *Trends Cogn. Sci.* 23(4):334–48

Evans DA, Stempel AV, Vale R, Ruehle S, Lefler Y, Branco T. 2018. A synaptic threshold mechanism for computing escape decisions. *Nature* 558(7711):590–94

Famiglietti EV. 1991. Synaptic organization of starburst amacrine cells in rabbit retina: analysis of serial thin sections by electron microscopy and graphic reconstruction. *J. Comp. Neurol.* 309(1):40–70

Faulstich BM, Onori KA, du Lac S. 2004. Comparison of plasticity and development of mouse optokinetic and vestibulo-ocular reflexes suggests differential gain control mechanisms. *Vis. Res.* 44(28):3419–27

Feinberg EH, Meister M. 2015. Orientation columns in the mouse superior colliculus. *Nature* 519(7542):229–32

Fernandez DC, Fogerson PM, Lazzerini Ospri L, Thomsen MB, Layne RM, et al. 2018. Light affects mood and learning through distinct retina-brain pathways. *Cell* 175(1):71–84.e18

Fiscella M, Franke F, Farrow K, Müller J, Roska B, et al. 2015. Visual coding with a population of direction-selective neurons. *J. Neurophysiol.* 114(4):2485–99

Fotowat H, Gabbiani F. 2011. Collision detection as a model for sensory-motor integration. *Annu. Rev. Neurosci.* 34:1–19

Franke K, Berens P, Schubert T, Bethge M, Euler T, Baden T. 2017. Inhibition decorrelates visual feature representations in the inner retina. *Nature* 542(7642):439–44

Fransen JW, Borghuis BG. 2017. Temporally diverse excitation generates direction-selective responses in ON- and OFF-type retinal starburst amacrine cells. *Cell Rep.* 18(6):1356–65

Freedman MS, Lucas RJ, Soni B, von Schantz M, Muñoz M, et al. 1999. Regulation of mammalian circadian behavior by non-rod, non-cone, ocular photoreceptors. *Science* 284(5413):502–4

Fried SI, Münch TA, Werblin FS. 2002. Mechanisms and circuitry underlying directional selectivity in the retina. *Nature* 420(6914):411–14

Frost BJ. 2010. A taxonomy of different forms of visual motion detection and their underlying neural mechanisms. *Brain Behav. Evol.* 75(3):218–35

Gale SD, Murphy GJ. 2014. Distinct representation and distribution of visual information by specific cell types in mouse superficial superior colliculus. *J. Neurosci.* 34(40):13458–71

Gale SD, Murphy GJ. 2016. Active dendritic properties and local inhibitory input enable selectivity for object motion in mouse superior colliculus neurons. *J. Neurosci.* 36(35):9111–23

Gauvain G, Murphy GJ. 2015. Projection-specific characteristics of retinal input to the brain. *J. Neurosci.* 35(16):6575–83

Göz D, Studholme K, Lappi DA, Rollag MD, Provencio I, Morin LP. 2008. Targeted destruction of pho-
tosensitive retinal ganglion cells with a saporin conjugate alters the effects of light on mouse circadian
rhythms. *PLOS ONE* 3(9):e3153

Greene MJ, Kim JS, Seung HS, EyeWirers. 2016. Analogous convergence of sustained and transient inputs in
parallel On and Off pathways for retinal motion computation. *Cell Rep.* 14(8):1892–900

Grimes WN, Schwartz GW, Rieke F. 2014. The synaptic and circuit mechanisms underlying a change in
spatial encoding in the retina. *Neuron* 82(2):460–73

Grubb MS, Thompson ID. 2003. Quantitative characterization of visual response properties in the mouse
dorsal lateral geniculate nucleus. *J. Neurophysiol.* 90(6):3594–607

Güler AD, Ecker JL, Lall GS, Haq S, Altimus CM, et al. 2008. Melanopsin cells are the principal conduits for
rod-cone input to non-image-forming vision. *Nature* 453(7191):102–5

Hammer S, Monavarfeshani A, Lemon T, Su J, Fox MA. 2015. Multiple retinal axons converge onto relay
cells in the adult mouse thalamus. *Cell Rep.* 12(10):1575–83

Hannibal J, Hindersson P, Knudsen SM, Georg B, Fahrenkrug J. 2002. The photopigment melanopsin is
exclusively present in pituitary adenylate cyclase-activating polypeptide-containing retinal ganglion cells
of the retinohypothalamic tract. *J. Neurosci.* 22(1):RC191

Hatori M, Le H, Vollmers C, Keding SR, Tanaka N, et al. 2008. Inducible ablation of melanopsin-expressing
retinal ganglion cells reveals their central role in non-image forming visual responses. *PLOS ONE*
3(6):e2451

Hattar S, Kumar M, Park A, Tong P, Tung J, et al. 2006. Central projections of melanopsin-expressing retinal
ganglion cells in the mouse. *J. Comp. Neurol.* 497(3):326–49

Hattar S, Liao HW, Takao M, Berson DM, Yau KW. 2002. Melanopsin-containing retinal ganglion cells:
architecture, projections, and intrinsic photosensitivity. *Science* 295(5557):1065–70

Hausselt SE, Euler T, Detwiler PB, Denk W. 2007. A dendrite-autonomous mechanism for direction
selectivity in retinal starburst amacrine cells. *PLOS Biol.* 5(7):e185

Haverkamp S, Wässle H, Duebel J, Kuner T, Augustine GJ, et al. 2005. The primordial, blue-cone color
system of the mouse retina. *J. Neurosci.* 25(22):5438–45

Helmstaedter M, Briggman KL, Turaga SC, Jain V, Seung HS, Denk W. 2013. Connectomic reconstruction
of the inner plexiform layer in the mouse retina. *Nature* 500(7461):168–74

Hillier D, Fiscella M, Drinnenberg A, Trenholm S, Rompani SB, et al. 2017. Causal evidence for retina-
dependent and -independent visual motion computations in mouse cortex. *Nat. Neurosci.* 20:960–68

Hofbauer A, Dräger UC. 1985. Depth segregation of retinal ganglion cells projecting to mouse superior
colliculus. *J. Comp. Neurol.* 234(4):465–74

Hoggarth A, McLaughlin AJ, Ronellenfitch K, Trenholm S, Vasandani R, et al. 2015. Specific wiring of distinct
amacrine cells in the directionally selective retinal circuit permits independent coding of direction and
size. *Neuron* 86(1):276–91

Hong YK, Burr EF, Sanes JR, Chen C. 2018. Heterogeneity of retinogeniculate axon arbors. *Eur. J. Neurosci.*
49(7):948–56

Hong YK, Kim I-J, Sanes JR. 2011. Stereotyped axonal arbors of retinal ganglion cell subsets in the mouse
superior colliculus. *J. Comp. Neurol.* 519(9):1691–711

Hoshi H, Liu W-L, Massey SC, Mills SL. 2009. ON inputs to the OFF layer: bipolar cells that break the
stratification rules of the retina. *J. Neurosci.* 29(28):8875–83

Hoy JL, Bishop HI, Niell CM. 2019. Defined cell types in superior colliculus make distinct contributions to
prey capture behavior in the mouse. *Curr. Biol.* 29(23):4130–38.e5

Hsiang J-C, Johnson KP, Madisen L, Zeng H, Kerschensteiner D. 2017. Local processing in neurites of
VGluT3-expressing amacrine cells differentially organizes visual information. *eLife* 6:e31307

Huang L, Xi Y, Peng Y, Yang Y, Huang X, et al. 2019. A visual circuit related to habenula underlies the
antidepressive effects of light therapy. *Neuron* 102(1):128–42.e8

Huang L, Yuan T, Tan M, Xi Y, Hu Y, et al. 2017. A retinoraphe projection regulates serotonergic activity and
looming-evoked defensive behaviour. *Nat. Commun.* 8:14908

Huang X, Huang P, Huang L, Hu Z, Liu X, et al. 2021. A visual circuit related to the nucleus reuniens for the
spatial-memory-promoting effects of light treatment. *Neuron* 109(2):347–62.e7

Hubel DH, Wiesel TN. 1962. Receptive fields, binocular interaction and functional architecture in the cat's visual cortex. *J. Physiol.* 160:106–54

Huberman AD, Manu M, Koch SM, Susman MW, Lutz AB, et al. 2008. Architecture and activity-mediated refinement of axonal projections from a mosaic of genetically identified retinal ganglion cells. *Neuron* 59(3):425–38

Huberman AD, Wei W, Elstrott J, Stafford BK, Feller MB, Barres BA. 2009. Genetic identification of an On-Off direction-selective retinal ganglion cell subtype reveals a layer-specific subcortical map of posterior motion. *Neuron* 62(3):327–34

Inayat S, Barchini J, Chen H, Feng L, Liu X, Cang J. 2015. Neurons in the most superficial lamina of the mouse superior colliculus are highly selective for stimulus direction. *J. Neurosci.* 35(20):7992–8003

Ito S, Feldheim DA. 2018. The mouse superior colliculus: an emerging model for studying circuit formation and function. *Front. Neural Circuits* 12:10

Ito S, Feldheim DA, Litke AM. 2017. Segregation of visual response properties in the mouse superior colliculus and their modulation during locomotion. *J. Neurosci.* 37(35):8428–43

Ivanova E, Lee P, Pan Z-H. 2013. Characterization of multiple bistratified retinal ganglion cells in a Purkinje cell protein 2-Cre transgenic mouse line. *J. Comp. Neurol.* 521(9):2165–80

Jacoby J, Schwartz GW. 2017. Three small-receptive-field ganglion cells in the mouse retina are distinctly tuned to size, speed, and object motion. *J. Neurosci.* 37(3):610–25

Jacoby J, Schwartz GW. 2018. Typology and circuitry of suppressed-by-contrast retinal ganglion cells. *Front. Cell. Neurosci.* 12:269

Jacoby J, Zhu Y, DeVries SH, Schwartz GW. 2015. An amacrine cell circuit for signaling steady illumination in the retina. *Cell Rep.* 13(12):2663–70

Jeon CJ, Strettoi E, Masland RH. 1998. The major cell populations of the mouse retina. *J. Neurosci.* 18(21):8936–46

Jiang Z, Yue WWS, Chen L, Sheng Y, Yau K-W. 2018. Cyclic-nucleotide- and HCN-channel-mediated phototransduction in intrinsically photosensitive retinal ganglion cells. *Cell* 175(3):652–64.e12

Joesch M, Meister M. 2016. A neuronal circuit for colour vision based on rod-cone opponency. *Nature* 532(7598):236–39

Johnson KP, Zhao L, Kerschensteiner D. 2018. A pixel-encoder retinal ganglion cell with spatially offset excitatory and inhibitory receptive fields. *Cell Rep.* 22(6):1462–72

Johnston J, Seibel S-H, Darnet LSA, Renninger S, Orger M, Lagnado L. 2019. A retinal circuit generating a dynamic predictive code for oriented features. *Neuron* 102(6):1211–22.e3

Kaplan E. 2008. Luminance sensitivity and contrast detection. In *The Senses: A Comprehensive Reference*, Vol. 2, ed. RH Masland, TD Albright, P Dallos, D Oertel, S Firestein, et al., pp. 29–43. Amsterdam: Elsevier

Kawaguchi C, Isojima Y, Shintani N, Hatanaka M, Guo X, et al. 2010. PACAP-deficient mice exhibit light parameter-dependent abnormalities on nonvisual photoreception and early activity onset. *PLOS ONE* 5(2):e9286

Kawaguchi C, Tanaka K, Isojima Y, Shintani N, Hashimoto H, et al. 2003. Changes in light-induced phase shift of circadian rhythm in mice lacking PACAP. *Biochem. Biophys. Res. Commun.* 310(1):169–75

Kay JN, De la Huerta I, Kim I-J, Zhang Y, Yamagata M, et al. 2011. Retinal ganglion cells with distinct directional preferences differ in molecular identity, structure, and central projections. *J. Neurosci.* 31(21):7753–62

Keenan WT, Rupp AC, Ross RA, Somasundaram P, Hiriyanna S, et al. 2016. A visual circuit uses complementary mechanisms to support transient and sustained pupil constriction. *eLife* 5:e15392

Kerschensteiner D, Guido W. 2017. Organization of the dorsal lateral geniculate nucleus in the mouse. *Vis. Neurosci.* 34:E008

Kim I-J, Zhang Y, Meister M, Sanes JR. 2010. Laminar restriction of retinal ganglion cell dendrites and axons: subtype-specific developmental patterns revealed with transgenic markers. *J. Neurosci.* 30(4):1452–62

Kim I-J, Zhang Y, Yamagata M, Meister M, Sanes JR. 2008. Molecular identification of a retinal cell type that responds to upward motion. *Nature* 452(7186):478–82

Kim JS, Greene MJ, Zlateski A, Lee K, Richardson M, et al. 2014. Space-time wiring specificity supports direction selectivity in the retina. *Nature* 509(7500):331–36

Kim T, Kerschensteiner D. 2017. Inhibitory control of feature selectivity in an object motion sensitive circuit of the retina. *Cell Rep*. 19(7):1343–50

Kim T, Shen N, Hsiang J-C, Johnson KP, Kerschensteiner D. 2020. Dendritic and parallel processing of visual threats in the retina control defensive responses. *Sci. Adv.* 6(47):eabc9920

Kim T, Soto F, Kerschensteiner D. 2015. An excitatory amacrine cell detects object motion and provides feature-selective input to ganglion cells in the mouse retina. *eLife* 4:e08025

Kingdom FAA, Prins N. 2016. *Psychophysics: A Practical Introduction*. Cambridge, MA: Academic

Knop GC, Feigenspan A, Weiler R, Dedek K. 2011. Inputs underlying the ON-OFF light responses of type 2 wide-field amacrine cells in TH::GFP mice. *J. Neurosci.* 31(13):4780–91

Koren D, Grove JCR, Wei W. 2017. Cross-compartmental modulation of dendritic signals for retinal direction selectivity. *Neuron* 95(4):914–27.e4

Krauzlis RJ, Lovejoy LP, Zénon A. 2013. Superior colliculus and visual spatial attention. *Annu. Rev. Neurosci.* 36:165–82

Krieger B, Qiao M, Rousso DL, Sanes JR, Meister M. 2017. Four alpha ganglion cell types in mouse retina: function, structure, and molecular signatures. *PLOS ONE* 12(7):e0180091

Krishnaswamy A, Yamagata M, Duan X, Hong YK, Sanes JR. 2015. Sidekick 2 directs formation of a retinal circuit that detects differential motion. *Nature* 524(7566):466–70

Kuffler SW. 1953. Discharge patterns and functional organization of mammalian retina. *J. Neurophysiol.* 16(1):37–68

Kuo SP, Schwartz GW, Rieke F. 2016. Nonlinear spatiotemporal integration by electrical and chemical synapses in the retina. *Neuron* 90(2):320–32

Lazzerini Ospri L, Prusky G, Hattar S. 2017. Mood, the circadian system, and melanopsin retinal ganglion cells. *Annu. Rev. Neurosci.* 40:539–56

Lee KH, Tran A, Turan Z, Meister M. 2020. The sifting of visual information in the superior colliculus. *eLife* 9:e50678

Lee S, Chen L, Chen M, Ye M, Seal RP, Zhou ZJ. 2014. An unconventional glutamatergic circuit in the retina formed by vGluT3 amacrine cells. *Neuron* 84(4):708–15

Lee S, Kim K, Zhou ZJ. 2010. Role of ACh-GABA cotransmission in detecting image motion and motion direction. *Neuron* 68(6):1159–72

Lee S, Zhang Y, Chen M, Zhou ZJ. 2016. Segregated glycine-glutamate co-transmission from vGluT3 amacrine cells to contrast-suppressed and contrast-enhanced retinal circuits. *Neuron* 90(1):27–34

Lee S, Zhou ZJ. 2006. The synaptic mechanism of direction selectivity in distal processes of starburst amacrine cells. *Neuron* 51(6):787–99

Lee SK, Sonoda T, Schmidt TM. 2019. M1 intrinsically photosensitive retinal ganglion cells integrate rod and melanopsin inputs to signal in low light. *Cell Rep*. 29(11):3349–55.e2

LeGates TA, Altimus CM, Wang H, Lee H-K, Yang S, et al. 2012. Aberrant light directly impairs mood and learning through melanopsin-expressing neurons. *Nature* 491(7425):594–98

Levick WR. 1967. Receptive fields and trigger features of ganglion cells in the visual streak of the rabbits retina. *J. Physiol.* 188(3):285–307

Levine JN, Schwartz GW. 2020. The olivary pretectal nucleus receives visual input of high spatial resolution. bioRxiv 2020.06.23.168054. **https://doi.org/10.1101/2020.06.23.168054**

Liang F, Xiong XR, Zingg B, Ji X-Y, Zhang LI, Tao HW. 2015. Sensory cortical control of a visually induced arrest behavior via corticotectal projections. *Neuron* 86(3):755–67

Liang L, Chen C. 2020. Organization, function, and development of the mouse retinogeniculate synapse. *Annu. Rev. Vis. Sci.* 6:261–85

Liang L, Fratzl A, Goldey G, Ramesh RN, Sugden AU, et al. 2018. A fine-scale functional logic to convergence from retina to thalamus. *Cell* 173(6):1343–55.e24

Lien AD, Scanziani M. 2013. Tuned thalamic excitation is amplified by visual cortical circuits. *Nat. Neurosci.* 16(9):1315–23

Lien AD, Scanziani M. 2018. Cortical direction selectivity emerges at convergence of thalamic synapses. *Nature* 558(7708):80–86

Lilley BN, Sabbah S, Hunyara JL, Gribble KD, Al-Khindi T, et al. 2019. Genetic access to neurons in the accessory optic system reveals a role for Sema6A in midbrain circuitry mediating motion perception. *J. Comp. Neurol.* 527(1):282–96

Litvina EY, Chen C. 2017. Functional convergence at the retinogeniculate synapse. *Neuron* 96(2):330–38.e5

Liu B-H, Li P, Sun YJ, Li Y-T, Zhang LI, Tao HW. 2010. Intervening inhibition underlies simple-cell receptive field structure in visual cortex. *Nat. Neurosci.* 13(1):89–96

Lucas RJ, Freedman MS, Muñoz M, Garcia-Fernández JM, Foster RG. 1999. Regulation of the mammalian pineal by non-rod, non-cone, ocular photoreceptors. *Science* 284(5413):505–7

Lupi D, Oster H, Thompson S, Foster RG. 2008. The acute light-induction of sleep is mediated by OPN4-based photoreception. *Nat. Neurosci.* 11(9):1068–73

Mani A, Schwartz GW. 2017. Circuit mechanisms of a retinal ganglion cell with stimulus-dependent response latency and activation beyond its dendrites. *Curr. Biol.* 27(4):471–82

Margolis DJ, Detwiler PB. 2007. Different mechanisms generate maintained activity in ON and OFF retinal ganglion cells. *J. Neurosci.* 27(22):5994–6005

Marshel JH, Kaye AP, Nauhaus I, Callaway EM. 2012. Anterior-posterior direction opponency in the superficial mouse lateral geniculate nucleus. *Neuron* 76(4):713–20

Martersteck EM, Hirokawa KE, Evarts M, Bernard A, Duan X, et al. 2017. Diverse central projection patterns of retinal ganglion cells. *Cell Rep.* 18(8):2058–72

Masland RH. 2001. The fundamental plan of the retina. *Nat. Neurosci.* 4(9):877–86

Masland RH, Martin PR. 2007. The unsolved mystery of vision. *Curr. Biol.* 17(15):R577–82

Matsumoto A, Agbariah W, Nolte SS, Andrawos R, Levi H, et al. 2020. Synapse-specific direction selectivity in retinal bipolar cell axon terminals. bioRxiv 2020.10.12.335810. **https://doi.org/10.1101/2020.10.12.335810**

Matsumoto A, Briggman KL, Yonehara K. 2019. Spatiotemporally asymmetric excitation supports mammalian retinal motion sensitivity. *Curr. Biol.* 29(19):3277–88.e5

Maturana HR, Frenk S. 1963. Directional movement and horizontal edge detectors in the pigeon retina. *Science* 142(3594):977–79

Mauss AS, Vlasits A, Borst A, Feller M. 2017. Visual circuits for direction selectivity. *Annu. Rev. Neurosci.* 40:211–30

Meyer AF, O'Keefe J, Poort J. 2020. Two distinct types of eye-head coupling in freely moving mice. *Curr. Biol.* 30(11):2116–30.e6

Meyer AF, Poort J, O'Keefe J, Sahani M, Linden JF. 2018. A head-mounted camera system integrates detailed behavioral monitoring with multichannel electrophysiology in freely moving mice. *Neuron* 100(1):46–60.e7

Michaiel AM, Abe ETT, Niell CM. 2020. Dynamics of gaze control during prey capture in freely moving mice. *eLife* 9:e57458

Milner ES, Do MTH. 2017. A population representation of absolute light intensity in the mammalian retina. *Cell* 171(4):865–76.e16

Monavarfeshani A, Sabbagh U, Fox MA. 2017. Not a one-trick pony: diverse connectivity and functions of the rodent lateral geniculate complex. *Vis. Neurosci.* 34:E012

Morgan JL, Berger DR, Wetzel AW, Lichtman JW. 2016. The fuzzy logic of network connectivity in mouse visual thalamus. *Cell* 165(1):192–206

Morgan JL, Soto F, Wong ROL, Kerschensteiner D. 2011. Development of cell type-specific connectivity patterns of converging excitatory axons in the retina. *Neuron* 71(6):1014–21

Morin LP, Studholme KM. 2014. Retinofugal projections in the mouse. *J. Comp. Neurol.* 522(16):3733–53

Morrie RD, Feller MB. 2018. A dense starburst plexus is critical for generating direction selectivity. *Curr. Biol.* 28(8):1204–12.e5

Münch TA, da Silveira RA, Siegert S, Viney TJ, Awatramani GB, Roska B. 2009. Approach sensitivity in the retina processed by a multifunctional neural circuit. *Nat. Neurosci.* 12(10):1308–16

Murphy GJ, Rieke F. 2006. Network variability limits stimulus-evoked spike timing precision in retinal ganglion cells. *Neuron* 52(3):511–24

Murphy GJ, Rieke F. 2011. Electrical synaptic input to ganglion cells underlies differences in the output and absolute sensitivity of parallel retinal circuits. *J. Neurosci.* 31(34):12218–28

Murphy-Baum BL, Taylor WR. 2015. The synaptic and morphological basis of orientation selectivity in a polyaxonal amacrine cell of the rabbit retina. *J. Neurosci.* 35(39):13336–50

Nadal-Nicolás FM, Kunze VP, Ball JM, Peng BT, Krishnan A, et al. 2020. True S-cones are concentrated in the ventral mouse retina and wired for color detection in the upper visual field. *eLife* 9:e56840

Nath A, Schwartz GW. 2016. Cardinal orientation selectivity is represented by two distinct ganglion cell types in mouse retina. *J. Neurosci.* 36(11):3208–21

Nath A, Schwartz GW. 2017. Electrical synapses convey orientation selectivity in the mouse retina. *Nat. Commun.* 8:2025

Ng L, Hurley JB, Dierks B, Srinivas M, Saltó C, et al. 2001. A thyroid hormone receptor that is required for the development of green cone photoreceptors. *Nat. Genet.* 27(1):94–98

Niell CM. 2013. Vision: more than expected in the early visual system. *Curr. Biol.* 23(16):R681–84

Niell CM, Stryker MP. 2010. Modulation of visual responses by behavioral state in mouse visual cortex. *Neuron* 65(4):472–79

Olveczky BP, Baccus SA, Meister M. 2003. Segregation of object and background motion in the retina. *Nature* 423(6938):401–8

Osterhout JA, Stafford BK, Nguyen PL, Yoshihara Y, Huberman AD. 2015. Contactin-4 mediates axon-target specificity and functional development of the accessory optic system. *Neuron* 86(4):985–99

Pang J-J, Gao F, Wu SM. 2003. Light-evoked excitatory and inhibitory synaptic inputs to ON and OFF α ganglion cells in the mouse retina. *J. Neurosci.* 23(14):6063–73

Park SJH, Kim I-J, Looger LL, Demb JB, Borghuis BG. 2014. Excitatory synaptic inputs to mouse on-off direction-selective retinal ganglion cells lack direction tuning. *J. Neurosci.* 34(11):3976–81

Park SJH, Pottackal J, Ke J-B, Jun NY, Rahmani P, et al. 2018. Convergence and divergence of CRH amacrine cells in mouse retinal circuitry. *J. Neurosci.* 38(15):3753–66

Pearson JT, Kerschensteiner D. 2015. Ambient illumination switches contrast preference of specific retinal processing streams. *J. Neurophysiol.* 114(1):540–50

Peek MY, Card GM. 2016. Comparative approaches to escape. *Curr. Opin. Neurobiol.* 41:167–73

Pei Z, Chen Q, Koren D, Giammarinaro B, Acaron Ledesma H, Wei W. 2015. Conditional knock-out of vesicular GABA transporter gene from starburst amacrine cells reveals the contributions of multiple synaptic mechanisms underlying direction selectivity in the retina. *J. Neurosci.* 35(38):13219–32

Peichl L, Buhl EH, Boycott BB. 1987. Alpha ganglion cells in the rabbit retina. *J. Comp. Neurol.* 263(1):25–41

Pettigrew JD. 1986. Evolution of binocular vision. In *Visual Neuroscience*, ed. JD Pettigrew, KJ Sanderson, WR Levick, pp. 208–22. Cambridge, UK: Cambridge Univ. Press

Piscopo DM, El-Danaf RN, Huberman AD, Niell CM. 2013. Diverse visual features encoded in mouse lateral geniculate nucleus. *J. Neurosci.* 33(11):4642–56

Poleg-Polsky A, Ding H, Diamond JS. 2018. Functional compartmentalization within starburst amacrine cell dendrites in the retina. *Cell Rep.* 22(11):2898–908

Provencio I, Jiang G, De Grip WJ, Hayes WP, Rollag MD. 1998. Melanopsin: an opsin in melanophores, brain, and eye. *PNAS* 95(1):340–45

Provencio I, Rodriguez IR, Jiang G, Hayes WP, Moreira EF, Rollag MD. 2000. A novel human opsin in the inner retina. *J. Neurosci.* 20(2):600–5

Quattrochi LE, Stabio ME, Kim I, Ilardi MC, Fogerson PM, et al. 2018. The M6 cell: a small-field bistratified photosensitive retinal ganglion cell. *J. Comp. Neurol.* 527(1):297–311

Rasmussen R, Matsumoto A, Dahlstrup Sietam M, Yonehara K. 2020. A segregated cortical stream for retinal direction selectivity. *Nat. Commun.* 11:831

Rasmussen R, Yonehara K. 2020. Contributions of retinal direction selectivity to central visual processing. *Curr. Biol.* 30(15):R897–903

Reinhard K, Kühn NK, Farrow K. 2020. Direction selectivity in the retina and beyond. In *The Senses: A Comprehensive Reference*, ed. B Fritzsch, pp. 423–46. Amsterdam: Elsevier. 2nd ed.

Reinhard K, Li C, Do Q, Burke EG, Heynderickx S, Farrow K. 2019. A projection specific logic to sampling visual inputs in mouse superior colliculus. *eLife* 8:e50697

Rheaume BA, Jereen A, Bolisetty M, Sajid MS, Yang Y, et al. 2018. Single cell transcriptome profiling of retinal ganglion cells identifies cellular subtypes. *Nat. Commun.* 9:2759

Rieke F, Rudd ME. 2009. The challenges natural images pose for visual adaptation. *Neuron* 64(5):605–16

Rivlin-Etzion M, Zhou K, Wei W, Elstrott J, Nguyen PL, et al. 2011. Transgenic mice reveal unexpected diversity of on-off direction-selective retinal ganglion cell subtypes and brain structures involved in motion processing. *J. Neurosci.* 31(24):8760–69

Rodieck RW. 1967. Receptive fields in the cat retina: a new type. *Science* 157(3784):90–92

Román Rosón M, Bauer Y, Kotkat AH, Berens P, Euler T, Busse L. 2019. Mouse dLGN receives functional input from a diverse population of retinal ganglion cells with limited convergence. *Neuron* 102(2):462–76.e8

Rompani SB, Müllner FE, Wanner A, Zhang C, Roth CN, et al. 2017. Different modes of visual integration in the lateral geniculate nucleus revealed by single-cell-initiated transsynaptic tracing. *Neuron* 93(4):767–76.e6

Rousso DL, Qiao M, Kagan RD, Yamagata M, Palmiter RD, Sanes JR. 2016. Two pairs of ON and OFF retinal ganglion cells are defined by intersectional patterns of transcription factor expression. *Cell Rep.* 15(9):1930–44

Rupp AC, Ren M, Altimus CM, Fernandez DC, Richardson M, et al. 2019. Distinct ipRGC subpopulations mediate light's acute and circadian effects on body temperature and sleep. *eLife* 8:e44358

Sabbah S, Gemmer JA, Bhatia-Lin A, Manoff G, Castro G, et al. 2017. A retinal code for motion along the gravitational and body axes. *Nature* 546(7659):492–97

Sabbah S, Papendorp C, Koplas E, Beltoja M. 2018. Synaptic circuits for irradiance coding by intrinsically photosensitive retinal ganglion cells. bioRxiv 442954. **https://doi.org/10.1101/442954**

Sahibzada N, Dean P, Redgrave P. 1986. Movements resembling orientation or avoidance elicited by electrical stimulation of the superior colliculus in rats. *J. Neurosci.* 6(3):723–33

Sanes JR, Zipursky SL. 2010. Design principles of insect and vertebrate visual systems. *Neuron* 66(1):15–36

Schmidt TM, Alam NM, Chen S, Kofuji P, Li W, et al. 2014. A role for melanopsin in alpha retinal ganglion cells and contrast detection. *Neuron* 82(4):781–88

Scholl B, Tan AYY, Corey J, Priebe NJ. 2013. Emergence of orientation selectivity in the mammalian visual pathway. *J. Neurosci.* 33(26):10616–24

Schwartz GW, Okawa H, Dunn FA, Morgan JL, Kerschensteiner D, et al. 2012. The spatial structure of a nonlinear receptive field. *Nat. Neurosci.* 15(11):1572–80

Schwartz GW, Swygart D. 2020. Circuits for feature selectivity in the inner retina. In *The Senses: A Comprehensive Reference*, ed. B Fritzsch, pp. 275–92. Amsterdam: Elsevier. 2nd ed.

Sethuramanujam S, McLaughlin AJ, deRosenroll G, Hoggarth A, Schwab DJ, Awatramani GB. 2016. A central role for mixed acetylcholine/GABA transmission in direction coding in the retina. *Neuron* 90(6):1243–56

Shang C, Chen Z, Liu A, Li Y, Zhang J, et al. 2018. Divergent midbrain circuits orchestrate escape and freezing responses to looming stimuli in mice. *Nat. Commun.* 9:1232

Shang C, Liu Z, Chen Z, Shi Y, Wang Q, et al. 2015. A parvalbumin-positive excitatory visual pathway to trigger fear responses in mice. *Science* 348(6242):1472–77

Shekhar K, Lapan SW, Whitney IE, Tran NM, Macosko EZ, et al. 2016. Comprehensive classification of retinal bipolar neurons by single-cell transcriptomics. *Cell* 166(5):1308–23.e30

Shen N, Wang B, Soto F, Kerschensteiner D. 2020. Homeostatic plasticity shapes the retinal response to photoreceptor degeneration. *Curr. Biol.* 30(10):1916–26.e3

Sher A, DeVries SH. 2012. A non-canonical pathway for mammalian blue-green color vision. *Nat. Neurosci.* 15(7):952–53

Shi X, Barchini J, Ledesma HA, Koren D, Jin Y, et al. 2017. Retinal origin of direction selectivity in the superior colliculus. *Nat. Neurosci.* 20(4):550–58

Sillar KT, Picton LD, Heitler WJ. 2016. *The Neuroethology of Predation and Escape*. Hoboken, NJ: Wiley

Simpson JI. 1984. The accessory optic system. *Annu. Rev. Neurosci.* 7:13–41

Sinha R, Hoon M, Baudin J, Okawa H, Wong ROL, Rieke F. 2017. Cellular and circuit mechanisms shaping the perceptual properties of the primate fovea. *Cell* 168(3):413–26.e12

Sivyer B, Taylor WR, Vaney DI. 2010. Uniformity detector retinal ganglion cells fire complex spikes and receive only light-evoked inhibition. *PNAS* 107(12):5628–33

Sivyer B, Vaney DI. 2010. Dendritic morphology and tracer-coupling pattern of physiologically identified transient uniformity detector ganglion cells in rabbit retina. *Vis. Neurosci.* 27(5–6):159–70

Smeds L, Takeshita D, Turunen T, Tihonen J, Westö J, et al. 2019. Paradoxical rules of spike train decoding revealed at the sensitivity limit of vision. *Neuron* 104(3):576–87

Sonoda T, Lee SK, Birnbaumer L, Schmidt TM. 2018. Melanopsin phototransduction is repurposed by ipRGC subtypes to shape the function of distinct visual circuits. *Neuron* 99(4):754–67.e4

Sonoda T, Li JY, Hayes NW, Chan JC, Okabe Y, et al. 2020. A noncanonical inhibitory circuit dampens behavioral sensitivity to light. *Science* 368(6490):527–31

Soto F, Hsiang J-C, Rajagopal R, Piggott K, Harocopos GJ, et al. 2020. Efficient coding by midget and parasol ganglion cells in the human retina. *Neuron* 107(4):656–66.e5

Soto F, Tien N-W, Goel A, Zhao L, Ruzycki PA, Kerschensteiner D. 2019. AMIGO2 scales dendrite arbors in the retina. *Cell Rep*. 29(6):1568–78.e4

Stabio ME, Sabbah S, Quattrochi LE, Ilardi MC, Fogerson PM, et al. 2017. The M5 cell: a color-opponent intrinsically photosensitive retinal ganglion cell. *Neuron* 97(1):150–63.e4

Stone LS, Watson AB, Mulligan JB. 1990. Effect of contrast on the perceived direction of a moving plaid. *Vis. Res.* 30(7):1049–67

Sun H, Frost BJ. 1998. Computation of different optical variables of looming objects in pigeon nucleus rotundus neurons. *Nat. Neurosci.* 1(4):296–303

Sun LO, Brady CM, Cahill H, Al-Khindi T, Sakuta H, et al. 2015. Functional assembly of accessory optic system circuitry critical for compensatory eye movements. *Neuron* 86(4):971–84

Sun W, Li N, He S. 2002. Large-scale morphological survey of mouse retinal ganglion cells. *J. Comp. Neurol.* 451(2):115–26

Suresh V, Çiftçioğlu UM, Wang X, Lala BM, Ding KR, et al. 2016. Synaptic contributions to receptive field structure and response properties in the rodent lateral geniculate nucleus of the thalamus. *J. Neurosci.* 36(43):10949–63

Szatko KP, Korympidou MM, Ran Y, Berens P, Dalkara D, et al. 2020. Neural circuits in the mouse retina support color vision in the upper visual field. *Nat. Commun.* 11:3481

Tailby C, Solomon SG, Dhruv NT, Majaj NJ, Sokol SH, Lennie P. 2007. A new code for contrast in the primate visual pathway. *J. Neurosci.* 27(14):3904–9

Tarpey P, Thomas S, Sarvananthan N, Mallya U, Lisgo S, et al. 2006. Mutations in FRMD7, a newly identified member of the FERM family, cause X-linked idiopathic congenital nystagmus. *Nat. Genet.* 38(11):1242–44

Tien N-W, Kim T, Kerschensteiner D. 2016. Target-specific glycinergic transmission from VGluT3-expressing amacrine cells shapes suppressive contrast responses in the retina. *Cell Rep*. 15(7):1369–75

Tien N-W, Pearson JT, Heller CR, Demas J, Kerschensteiner D. 2015. Genetically identified suppressed-by-contrast retinal ganglion cells reliably signal self-generated visual stimuli. *J. Neurosci.* 35(30):10815–20

Tien N-W, Soto F, Kerschensteiner D. 2017. Homeostatic plasticity shapes cell-type-specific wiring in the retina. *Neuron* 94(3):656–65.e4

Tran NM, Shekhar K, Whitney IE, Jacobi A, Benhar I, et al. 2019. Single-cell profiles of retinal ganglion cells differing in resilience to injury reveal neuroprotective genes. *Neuron* 104(6):1039–55.e12

Trenholm S, McLaughlin AJ, Schwab DJ, Turner MH, Smith RG, et al. 2014. Nonlinear dendritic integration of electrical and chemical synaptic inputs drives fine-scale correlations. *Nat. Neurosci.* 17(12):1759–66

Trenholm S, Schwab DJ, Balasubramanian V, Awatramani GB. 2013. Lag normalization in an electrically coupled neural network. *Nat. Neurosci.* 16(2):154–56

Turner MH, Sanchez Giraldo LG, Schwartz O, Rieke F. 2019. Stimulus- and goal-oriented frameworks for understanding natural vision. *Nat. Neurosci.* 22(1):15–24

Vale R, Campagner D, Iordanidou P, Arocas OP, Tan YL, et al. 2020. A cortico-collicular circuit for accurate orientation to shelter during escape. bioRxiv 2020.05.26.117598. **https://doi.org/10.1101/2020.05.26.117598**

Vale R, Evans DA, Branco T. 2017. Rapid spatial learning controls instinctive defensive behavior in mice. *Curr. Biol.* 27(9):1342–49

Van Gelder RN, Buhr ED. 2016. Ocular photoreception for circadian rhythm entrainment in mammals. *Annu. Rev. Vis. Sci.* 2:153–69

van Wyk M, Rowland Taylor W, Vaney DI. 2006. Local edge detectors: a substrate for fine spatial vision at low temporal frequencies in rabbit retina. *J. Neurosci.* 26(51):13250–63

Vitek DJ, Schall JD, Leventhal AG. 1985. Morphology, central projections, and dendritic field orientation of retinal ganglion cells in the ferret. *J. Comp. Neurol.* 241(1):1–11

Vlasits AL, Bos R, Morrie RD, Fortuny C, Flannery JG, et al. 2014. Visual stimulation switches the polarity of excitatory input to starburst amacrine cells. *Neuron* 83(5):1172–84

Vlasits AL, Morrie RD, Tran-Van-Minh A, Bleckert A, Gainer CF, et al. 2016. A role for synaptic input distribution in a dendritic computation of motion direction in the retina. *Neuron* 89(6):1317–30

Wang L, Sarnaik R, Rangarajan K, Liu X, Cang J. 2010. Visual receptive field properties of neurons in the superficial superior colliculus of the mouse. *J. Neurosci.* 30(49):16573–84

Wang Q, Burkhalter A. 2013. Stream-related preferences of inputs to the superior colliculus from areas of dorsal and ventral streams of mouse visual cortex. *J. Neurosci.* 33(4):1696–705

Wang YV, Weick M, Demb JB. 2011. Spectral and temporal sensitivity of cone-mediated responses in mouse retinal ganglion cells. *J. Neurosci.* 31(21):7670–81

Wässle H. 2004. Parallel processing in the mammalian retina. *Nat. Rev. Neurosci.* 5(10):747–57

Wee R, Castrucci AM, Provencio I, Gan L, Van Gelder RN. 2002. Loss of photic entrainment and altered free-running circadian rhythms in math5−/− mice. *J. Neurosci.* 22(23):10427–33

Wei P, Liu N, Zhang Z, Liu X, Tang Y, et al. 2015. Processing of visually evoked innate fear by a non-canonical thalamic pathway. *Nat. Commun.* 6:6756

Wei W. 2018. Neural mechanisms of motion processing in the mammalian retina. *Annu. Rev. Vis. Sci.* 4:165–92

Wei W, Hamby AM, Zhou K, Feller MB. 2011. Development of asymmetric inhibition underlying direction selectivity in the retina. *Nature* 469(7330):402–6

Weng S, Sun W, He S. 2005. Identification of ON–OFF direction-selective ganglion cells in the mouse retina. *J. Physiol.* 562(3):915–23

Yan W, Laboulaye MA, Tran NM, Whitney IE, Benhar I, Sanes JR. 2020. Mouse retinal cell atlas: molecular identification of over sixty amacrine cell types. *J. Neurosci.* 40(27):5177–95

Yao X, Cafaro J, McLaughlin AJ, Postma FR, Paul DL, et al. 2018. Gap junctions contribute to differential light adaptation across direction-selective retinal ganglion cells. *Neuron* 100(1):216–28.e6

Yilmaz M, Meister M. 2013. Rapid innate defensive responses of mice to looming visual stimuli. *Curr. Biol.* 23(20):2011–15

Yonehara K, Balint K, Noda M, Nagel G, Bamberg E, Roska B. 2011. Spatially asymmetric reorganization of inhibition establishes a motion-sensitive circuit. *Nature* 469(7330):407–10

Yonehara K, Farrow K, Ghanem A, Hillier D, Balint K, et al. 2013. The first stage of cardinal direction selectivity is localized to the dendrites of retinal ganglion cells. *Neuron* 79(6):1078–85

Yonehara K, Fiscella M, Drinnenberg A, Esposti F, Trenholm S, et al. 2016. Congenital nystagmus gene FRMD7 is necessary for establishing a neuronal circuit asymmetry for direction selectivity. *Neuron* 89(1):177–93

Yonehara K, Ishikane H, Sakuta H, Shintani T, Nakamura-Yonehara K, et al. 2009. Identification of retinal ganglion cells and their projections involved in central transmission of information about upward and downward image motion. *PLOS ONE* 4(1):e4320

Yonehara K, Shintani T, Suzuki R, Sakuta H, Takeuchi Y, et al. 2008. Expression of SPIG1 reveals development of a retinal ganglion cell subtype projecting to the medial terminal nucleus in the mouse. *PLOS ONE* 3(2):e1533

Yoshida K, Watanabe D, Ishikane H, Tachibana M, Pastan I, Nakanishi S. 2001. A key role of starburst amacrine cells in originating retinal directional selectivity and optokinetic eye movement. *Neuron* 30(3):771–80

Zaghloul KA, Boahen K, Demb JB. 2003. Different circuits for ON and OFF retinal ganglion cells cause different contrast sensitivities. *J. Neurosci.* 23(7):2645–54

Zaidi FH, Hull JT, Peirson SN, Wulff K, Aeschbach D, et al. 2007. Short-wavelength light sensitivity of circadian, pupillary, and visual awareness in humans lacking an outer retina. *Curr. Biol.* 17(24):2122–28

Zeater N, Cheong SK, Solomon SG, Dreher B, Martin PR. 2015. Binocular visual responses in the primate lateral geniculate nucleus. *Curr. Biol.* 25(24):3190–95

Zhang Y, Kim I-J, Sanes JR, Meister M. 2012. The most numerous ganglion cell type of the mouse retina is a selective feature detector. *PNAS* 109(36):E2391–98

Zhao X, Chen H, Liu X, Cang J. 2013. Orientation-selective responses in the mouse lateral geniculate nucleus. *J. Neurosci.* 33(31):12751–63

Zhao X, Liu M, Cang J. 2014a. Visual cortex modulates the magnitude but not the selectivity of looming-evoked responses in the superior colliculus of awake mice. *Neuron* 84(1):202–13

Zhao X, Stafford BK, Godin AL, King WM, Wong KY. 2014b. Photoresponse diversity among the five types of intrinsically photosensitive retinal ganglion cells. *J. Physiol.* 592(7):1619–36

Zhou Z, Liu X, Chen S, Zhang Z, Liu Y, et al. 2019. A VTA GABAergic neural circuit mediates visually evoked innate defensive responses. *Neuron* 103(3):473–88.e6

Zhu Y, Xu J, Hauswirth WW, DeVries SH. 2014. Genetically targeted binary labeling of retinal neurons. *J. Neurosci.* 34(23):7845–61

Zingg B, Chou X-L, Zhang Z-G, Mesik L, Liang F, et al. 2017. AAV-mediated anterograde transsynaptic tagging: mapping corticocollicular input-defined neural pathways for defense behaviors. *Neuron* 93(1):33–47
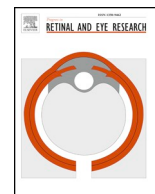
The dynamic receptive fields of retinal ganglion cells

Sophia Wienbar[1], Gregory W. Schwartz[*],[1]

Departments of Ophthalmology and Physiology, Feinberg School of Medicine, Northwestern University, United States

ABSTRACT

Retinal ganglion cells (RGCs) were one of the first classes of sensory neurons to be described in terms of a receptive field (RF). Over the last six decades, our understanding of the diversity of RGC types and the nuances of their response properties has grown exponentially. We will review the current understanding of RGC RFs mostly from studies in mammals, but including work from other vertebrates as well. We will argue for a new paradigm that embraces the fluidity of RGC RFs with an eye toward the neuroethology of vision. Specifically, we will focus on (1) different methods for measuring RGC RFs, (2) RF models, (3) feature selectivity and the distinction between fluid and stable RF properties, and (4) ideas about the future of understanding RGC RFs.

1. Introduction

The most outstanding feature in the present analysis is the flexibility and fluidity of the discharge patterns arising in each receptive field …. Stability […] disappears when one or more of several parameters, such as the adaptation level, stimulus intensity, and area of illumination, are changed singly or in combination. In the absence of a fixed pattern from the whole receptive field, it does not appear accurate enough to speak of "on, " "on-off" or "off" fibers in the cat's retina.

-Steven Kuffler (1953).

Remarkably, Steven Kuffler in the first description of receptive fields in a mammalian retina, already realized the fluidity of the concept of a receptive field (RF) (Kuffler, 1953). Sixty-five years later, we are still grappling with the difficulty of capturing concisely and completely how the visual world is encoded in the firing patterns of retinal ganglion cells (RGCs).

Another insight in Kuffler's 1953 paper that was decades ahead of its time was that a complete understanding of the visual code of the retina must capture how populations of RGCs signal together. The retina has emerged as one of the premier systems for the study of population codes (Meister, 1996; Shlens et al., 2008), but we will restrict our discussion here to the RF properties of individual RGCs, an enormous field on its own. The early history of RFs as a tool to characterize visual neurons has been reviewed elsewhere (Spillmann, 2014), and recent reviews have focused on RGC typology (Sanes and Masland, 2015) and principles of retinal computation (Gollisch and Meister, 2010). As our understanding of RGCs has improved, a set of studies over the last several years has brought new emphasis to the concept of RF fluidity. Fluidity of RGC computations with

light adaptation was the focus of another recent review (Rivlin-Etzion et al., 2018). We will discuss RGC RFs from this new perspective.

1.1. Conservation of RGC structure and function across species

While understanding the function of human RGCs is an important long-term goal of retinal research, we rely on animal models, so it is important to take stock of our current understanding of cross-species homology. Conscious visual perception in humans and non-human primates is dominated by the fovea, where the midget system with single cone resolution was a relatively recent evolutionary adaptation. In the peripheral retina, there are a wide variety of RGC types across many vertebrate species. Morphological similarity has been a key criterion for determining possible homologies between RGC types in different species, and compelling correspondence has been established from humans to non-human primates, to cats, and to rabbits (Goodchild et al., 1996; Rodieck, 1998; Sivyer et al., 2011). Studies have estimated similar RGC morphological diversity in primate (Dacey et al., 2003), cat (Boycott and Wassle, 1974; Isayama et al., 2000), rabbit (Rockhill et al., 2002), rat (Huxlin and Goodchild, 1997), and mouse (Kong et al., 2005; Sun et al., 2002; Völgyi et al., 2009). In several cases, functional parallels between species have also been established. Melanopsin expressing RGCs serve non-image forming visual functions in a set of pathways conserved across human (Provencio et al., 2000), non-human primate (Dacey et al., 2005), rat (Hannibal et al., 2014), mouse (Hattar et al., 2002), and chick (Bailey and Cassone, 2005). A functionally similar RGC type in rabbit, mouse, and non-human primates has been hypothesized to play a role in smooth pursuit eye movements (Puller

et al., 2015). Orientation selectivity (OS) is conserved in rabbit, mouse, and even teleost fish (Antinucci et al., 2016), and the OS computation in these different species may even involve morphologically homologous amacrine cells (Bloomfield, 1994; Hoshi and Mills, 2009; Nath and Schwartz, 2017; Wagner and Wagner, 1988).

This review will include results from many of these species, with an emphasis on mouse, where genetic tools have led to a recent explosion in new information about RGC types, circuits, and computations. Much of the data in this field comes from *ex vivo* preparations in which the retina is preserved in a light-responsive state outside of the animal. In rodents, the firing properties of RGCs measured *in vivo* in the optic nerve (Nobles et al., 2012) and *ex vivo* (Pang et al., 2003) are quite comparable. Several recent studies have also made direct links between RGC firing patterns measured *ex vivo* and responses in retino-recipient brain areas, like dorsal lateral geniculate nucleus (dLGN), measured *in vivo* (Piscopo et al., 2013; Román Rosón et al., 2018; Tikidji-Hamburyan et al., 2015).

Despite these encouraging signs suggesting that *ex vivo* preparations from a variety of animals share structural and functional motifs with the human retina, we should keep in mind the limitations that come from this set of model systems. RGC measurements from non-primates are likely to be poor comparisons for perceptual tasks involving the fovea that make up the majority of human psychophysics. The human peripheral retina – which contains the overwhelming majority of retinal area, diversity of RGC types, brain targets, and evolutionary history – is largely homologous to the retina of other species. Much work in visual neuroscience places emphasis on the fovea due to the fac t that humans have many concious visual perceptions such as reading. It is important to remember, when thinking about the diversity of RGC types and functions, that most of the circuitry linking photoreception to behavior lies outside the perceptual pipeline from retina to thalamus to cortex.

1.2. Defining a receptive field

The visual world is multi-dimensional and contains a wide variety of features. As the sole visual input to the brain, RGCs represent the behaviorally relevant complexity of the visual world in their spike trains. Unlike the pixel representation of a visual scene captured by the photoreceptors, RGCs transmit highly processed visual information about motion, shape, color, size, contrast, etc. The mammalian retina contains ∼100 different types of interneurons that process visual signals into ∼40 parallel channels defined by each RGC type (Baden et al., 2016; Bae et al., 2018; Masland, 2012; Sanes and Masland, 2015). The most general definition of a RGC RF would be a complete understanding of the stimulus to response relationship – the map between spatiotemporal patterns of light and RGC spikes.

Given the complexity of retinal circuits, a concise definition of the RF of a RGC includes simplifying assumptions and is necessarily incomplete. The central simplifying assumption in defining a receptive field is that it represents a static entity. We know that there are numerous sites of adaptation throughout the retina (Baccus and Meister, 2002; Rieke and Rudd, 2009), so any static RF represents, at best, a snapshot of the system in a particular steady state. Section 4 will probe this assumption in detail, exploring which aspects of RFs change with stimulus conditions and which are invariant.

Even for a static RF representation, there are tradeoffs associated with additional simplifying assumptions. In Section 3, we will examine a range of RF models from the simplest center-surround difference-of-Gaussians to substantially more detailed models. Models of RFs, of course are based on data, so before examining the models, we will discuss the various methods that have been employed to measure RGC RFs (Fig. 1) and the different kinds of data they provide.

2. Methods for measuring RGC receptive fields

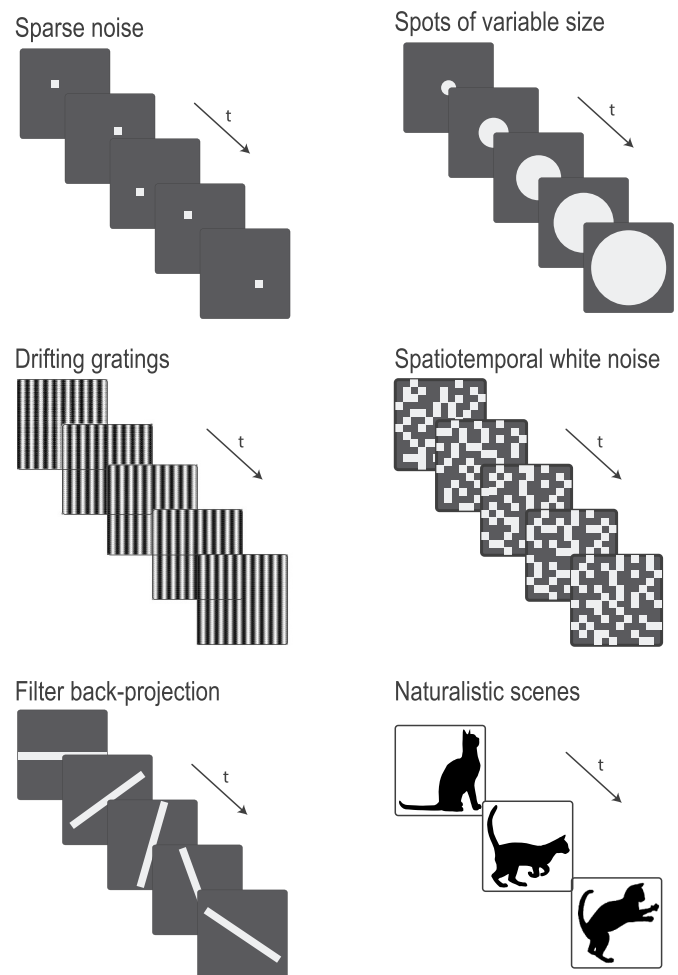The first-order classification of a RGC RF is generally made on the

Fig. 1. Stimuli used for measuring RGC RFs.

basis of the polarity of its light response. RGCs are classified as ON, OFF, or ON-OFF based on whether their firing rate increases at the onset of a light stimulus, the offset of the stimulus, or both (Sanes and Masland, 2015). A lesser-known fourth class of RGCs is the suppressed-by-contrast (SbC) RGCs, which decrease their steady firing at both light onset and offset (Jacoby et al., 2015; Levick, 1967; Mastronarde, 1983; Sivyer et al., 2011, 2010; Tien et al., 2015; Troy et al., 1989). After polarity, RF size is emphasized in RGC classification because the size of the RF has been associated with perceptual acuity (Dowling, 1967; Peichl and Wassle, 1979). The kinetics of RGC light responses (i.e. transient verses sustained) is another aspect of their RFs that has helped researchers distinguish between RGC types and describe their different functions (Baden et al., 2016; Caldwell and Daw, 1978; Lee, 1996; Levick, 1967; Silveira et al., 2004). We will see that other aspects of RGC responses (e.g. contrast sensitivity, spatial frequency sensitivity) and selectivity for specific features (e.g. direction of motion or orientation) are less commonly included in typical RFs, but they are vital in appreciating and predicting the full range of RGC light responses.

Methods for measuring RGC RFs have typically focused on the three aspects of light responses mentioned above: polarity, size, and kinetics. Not all methods are appropriate for all three properties, and we will emphasize how the RF one measures depends on methodology (Peichl and Wassle, 1979). There are also tradeoffs in experimental speed, parallelization, and precision (see Table 1).

2.1. Sparse noise

The measurement of RGC RFs in mammals began with Kuffler's

Table 1
Properties of receptive field measurement methods.

Method	ON-OFF separable	Spatial resolution	Kinetic information	Dataset Size requirements	Parallelizable	Data on subunits	Other considerations
Sparse Noise	Yes	Can be high but scales experiment time	Yes	Medium	Only for a few cells	No	Spatial RF depends on spot size and intensity
Spots of Variable Size	Yes	Low	Yes	Low	No	No	Center size conflated with surround strength
Drifting Gratings	No	Low to Medium	Limited	Low to Medium	Yes	Size but not location	Response to motion may differ from static RF
Spatiotemporal White Noise	No with STA; Yes with more complex analyses	Dependent on checker size	Limited	High	Yes	Yes, with recent analysis tools	Spatial resolution conflated with surround strength
Filter Back-Projection	Yes	Low to Medium	Yes	Medium	Yes, but experiment time scales with map area	No	Projection artifacts
Naturalistic Scenes	Yes	Medium	Yes	Very high	Yes	Yes in theory, but not shown experimentally	Computationally demanding, and optimal solution is not guaranteed

1953 characterization of cat RGCs. He employed a method now known as "sparse noise" (Brown et al., 2000; Jones et al., 1987; Reid et al., 1997). A small exploratory spot of light is randomly placed over the visual world and the response of the neuron is recorded (Daw, 1968; Kuffler, 1953; Rodieck and Stone, 1965). The spatial extent of the receptive field is defined as the region in which the spot elicits a response. A key advantage of the sparse noise method is that the distribution of responses is easily interpreted into the RF. The method also enables the experimenter to probe the polarity of the RGC, even allowing for the simultaneous measurement of separate ON and OFF RFs for ON-OFF cells. Sparse noise offers information about response kinetics only if each presentation of the exploratory spot is sufficiently long in duration, increasing the time of the experiment. Disadvantages of the sparse noise method include that it takes many repetitions and spatial locations to generate a robust RF, that it is not easily parallelizable (i.e. only one or possibly several cells can be measured at a time), and that the estimate of RF size is dependent on the size and intensity of the exploratory spot (Field and Chichilnisky, 2007; Kuffler, 1953).

2.2. Spots of various sizes

One method that naturally follows from sparse noise is using spots of various sizes (Enroth-Cugell and Lennie, 1975; Partridge and Brown, 1970; Peichl and Wassle, 1979; Sakmann and Creutzfeldt, 1969; Wiesel, 1960). Spots of different diameters are presented at a fixed location, and the smallest spot size that generates the maximal response is designated as having measured the size of the center of the RF. This method is highly interpretable and can rapidly offer information about polarity, size, and kinetics. The major disadvantage of this method is that it assumes circular symmetry, estimating the size but not the shape of the RF. Fine spatial structure and orientation selectivity cannot be measured by the spots-of-various-size method. Since the spots must be aligned to the RF center for the measurement to be valid, it is not robust to alignment errors, and it is not parallelizable at all; only one RGC can be measured at a time. Additionally, this method conflates the strength of suppression in the RF surround with the size of the center (Fig. 2).

2.3. Drifting gratings

Enroth-Cugel and Robson developed an alternative method for measuring RFs involving drifting gratings (Enroth-Cugell and Robson, 1966). A sinusoidal drifting grating represents a single spatial frequency. The authors measured contrast sensitivity at different spatial frequencies of the grating. They then used the inverse Fourier transform to convert their measurements from the frequency domain to the spatial domain, thus estimating a spatial RF. This method was revolutionary at the time, and it allowed for rapid measurement of the spatial RF with a stimulus to which most RGCs respond robustly. The drifting gratings method is also suitable for measuring many RFs simultaneously, making it useful for large-scale multi-electrode array recordings or calcium imaging studies (Borghuis et al., 2011; DeVries, 1999). Another advantage of this method that has led to its adoption in cortex is that, when gratings are presented at different orientations, it provides measurements of orientation and direction selectivity (De Valois et al., 1982). Despite these advantages, measuring a RGC RF using drifting gratings also has several disadvantages. Like the spots-of-various-size method, it does not resolve fine substructure within the RF center, and it conflates suppressive surround strength with center size. It also offers little information about response kinetics, since firing is controlled by the modulation frequency of the stimulus. Finally, while presenting a moving stimulus is useful to activate RGCs robustly, measuring a static spatial RF from a moving stimulus relies on the assumption that flashed images and moving objects are represented similarly in the retina. While this has been shown to be a reasonable assumption for certain RGCs in the regime of low contrast and low spatial frequency (Cooper et al., 2016), static and moving stimuli have also been shown to be
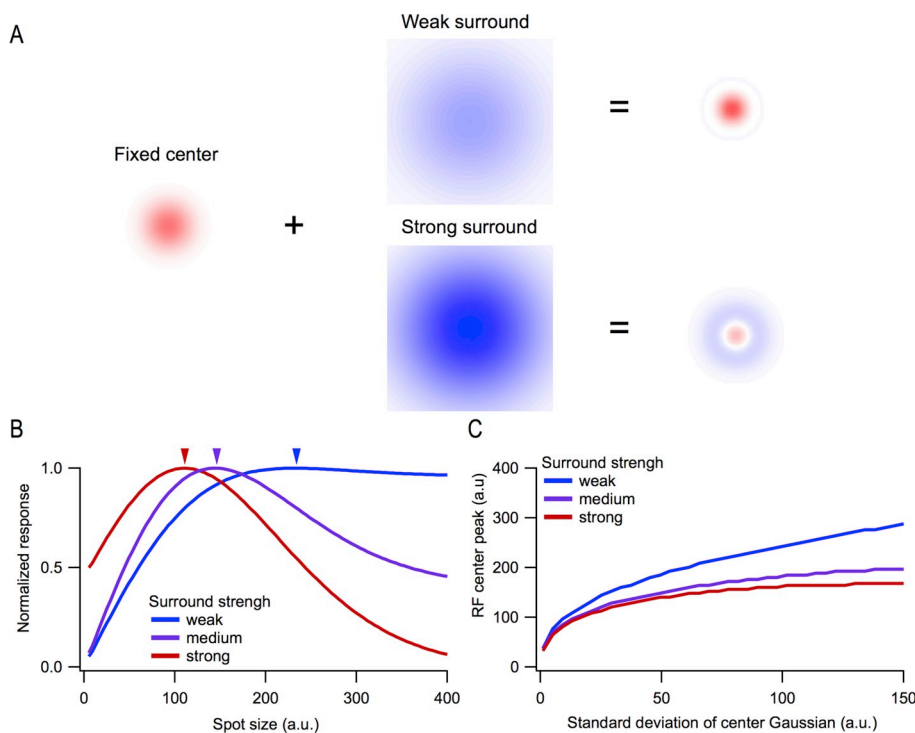
Fig. 2. Estimated RF center size can depend on surround strength. (**A**) Schematic of the sum of a fixed RF center with either a weak or a strong surround. (**B**) A model of normalized response (integral of RF) as a function of spot size for 3 different strengths of the surround. The RF center size is fixed. This is the response one would measure with the spots-of-varying-size technique. Arrowheads indicate the spot size giving the peak response, often used as a measure of the RF center size. (**C**) Relationship between the standard deviation of the RF center Gaussian and the estimated RF size from the peak response for 3 different surround strengths as in (**B**).

represented differently in many retinal circuits (Berry et al., 1999; Chen et al., 2013; Kim and Kerschensteiner, 2017; Kuo et al., 2016; Manookin et al., 2018; Schwartz et al., 2007; Vaney et al., 2012; Zhang et al., 2012).

2.4. Spatiotemporal white noise

Building on the linear systems approach of Enroth-Cugel and Robson, spatiotemporal white noise has become the most common stimulus employed to investigate RGC RFs (Brown et al., 2000; Chichilnisky, 2001; DeAngelis et al., 1995; Devries and Baylor, 1997; Field et al., 2010; Field and Chichilnisky, 2007; Gauthier et al., 2009; Reid et al., 1997; Yu and De Sa, 2003). In this method, a "checkerboard" with randomly flickering squares is presented to the retina and spike responses are recorded from RGCs. The straightforward method of spike-triggered-averaging (STA) – computing the mean stimulus sequence preceding a spike for each RGC – allows researchers to measure RFs from many cells in parallel. Using small checkers can reveal fine structure in spatial RFs, and response kinetics can be inferred from the mean temporal filter of the center pixels for each cell. These advantages have made spatiotemporal white noise the method of choice for most RGC RF mapping studies, and variations have been developed, including circular annuli (Fransen and Borghuis, 2017; Sakai and Naka, 1987), full field contrast flicker to investigate temporal responses in isolation (Fukada, 1971; Manookin et al., 2015), and random color checkboards to measure the contributions of individual cones (Field et al., 2010).

Despite the ubiquity of the spatiotemporal white noise STA approach, several important disadvantages limit interpretations of RFs measured by this method. One critical limitation of the standard STA approach is that it does not reveal separate ON and OFF RF components for ON-OFF cells. ON-OFF cells are classified as either ON or OFF based on which polarity dominates, and a perfectly balanced ON-OFF RF would cancel completely. This problem can be mitigated to some extent by more sophisticated analyses of the spike-triggered stimulus ensemble (Cantrell et al., 2010; Fairhall et al., 2006) – an issue we will return to below in our discussion of RF models.

Kinetic information is also limited in the spatiotemporal white noise

method. One can extract a temporal kernel from the RF center pixels, but the kernel predominantly represents information near the temporal frequency of the stimulus (i.e. the refresh rate of the checkerboard). The STA computation filters out both high and low temporal frequencies. This is a general problem in applying a linear analysis, like STA, to the nonlinear responses of RGCs, and we will explore the issue of nonlinearities in space and time in greater detail in the next section.

Finally, there is a tradeoff between the resolution of the stimulus (checker size) and the activation strength of different components of the RGC RF. Checkers that are very small compared to the RF center allow for fine resolution RF maps but create low total contrast across the RF center, so many cells respond weakly or not at all. The size vs. resolution tradeoff is even more problematic in the RF surround because its large integration area corresponds to extremely low contrast for small checkers. Thus, it is difficult to measure RF surrounds with spatiotemporal white noise, and estimates of center vs. surround strength are confounded by the choice of stimulus resolution (Fig. 3). The opposite problem occurs with excessive activation of a suppressive surround. Some RGC types are suppressed completely for wide-field stimuli and are, thus, silent for spatiotemporal white noise (Jacoby and Schwartz, 2017; Zhang et al., 2012).

2.5. Filter back-projection

A recently introduced method called filter back-projection (FBP) combines some of the advantages of sparse noise with the parallelizability of spatiotemporal white noise (Johnston et al., 2014). As opposed to randomly flashing spots, bars are flashed at different positions and at five or more orientations. The RF can then be computed using a method from X-ray scans called the inverse Radon transform (Radon, 1986). Like the related sparse noise method, FBP allows for the separate measurement of ON and OFF components of the RF, and the kinetics of RGC responses can be measured for sufficiently long stimulus durations. Unlike the classical sparse noise method, FBP is suitable for parallel measurements of RGC RFs on a multi-electrode array or by functional calcium imaging (although, unlike spatiotemporal white noise, experiment time scales with the total area being mapped). Because the stimuli are long bars, FBP is particularly useful for measuring orientation-
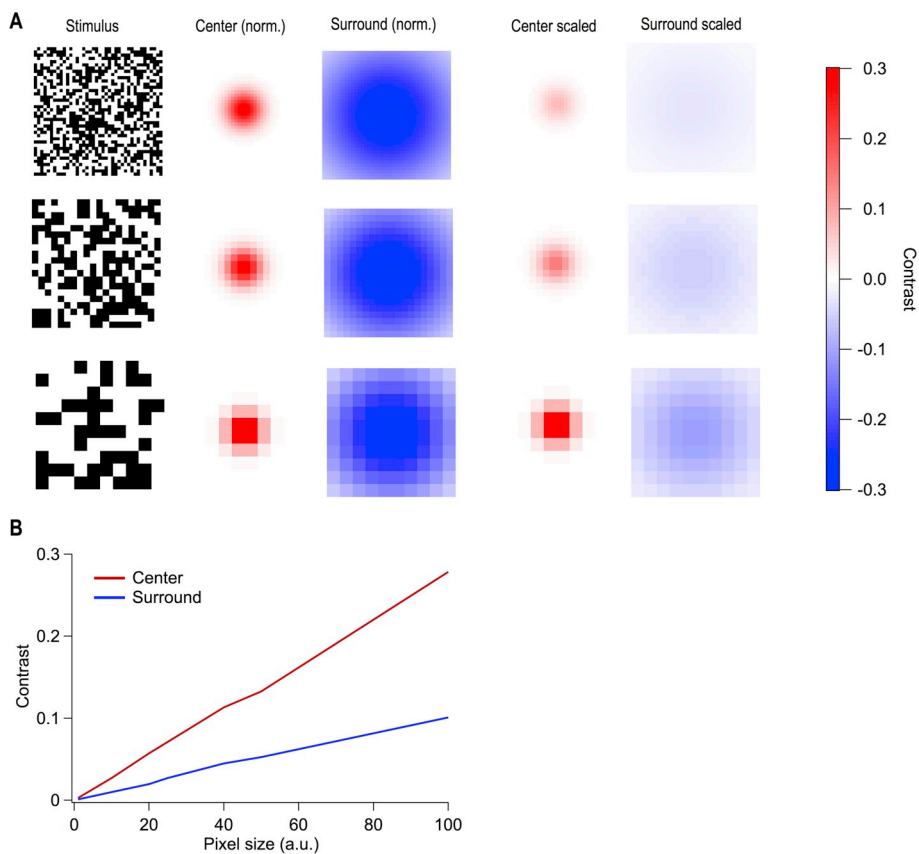
Fig. 3. Measurement of RF center and surround strength vary with the spatial resolution of a spatiotemporal white noise stimulus. (**A**) Example white noise stimuli at 3 spatial resolutions along with the RF center and RF surround sampled at each resolution. The final 2 columns show the RF center and surround measurements again, but scaled by their relative strength based on the contrast of the stimulus within the center and surround, respectively. Contrast scale corresponds to these last 2 columns. (**B**) The relationship between the pixel size of the white noise stimulus and the contrast elicited in the RF center and RF surround.

selective RFs. While it is generally more efficient than spatiotemporal white noise at measuring the basic shapes of RGC RFs, FBP is limited in its ability to resolve fine structure within the RF. Another disadvantage is that it is prone to projection artifacts, which appear as streaks in the spatial RF map.

2.6. Naturalistic stimuli

The natural visual world contains spatiotemporal correlations unlike pure Gaussian white noise (Eickenberg et al., 2012; Nirenberg et al., 2001; Pitkow and Meister, 2012). Therefore complex, naturalistic stimuli are used to investigate responses to more physiological stimuli that the visual sensory neurons might encounter in the wild (Kastner et al., 2015; Katz et al., 2016). These naturalistic stimuli have included natural temporal-chromatic movies with space removed (van Hateren et al., 2002), generated white-noise with long range spatiotemporal correlations (Pitkow and Meister, 2012), naturalistic motion stimuli (Leonardo and Meister, 2013), natural movie scenes (Haider et al., 2010; Nirenberg et al., 2001), even incorporating eye movements (Turner and Rieke, 2016). Using naturalistic stimuli invalidates the assumption of zero stimulus correlations that is required for linear STA-like analyses. Several analysis modifications have allowed researchers to adapt STA-like techniques to naturalistic stimuli. These include generalized linear models (Heitman et al., 2016), and removal of stimulus auto-correlation (Lesica et al., 2008). Most of these methods have had limited success, so theorists have devised a new set of tools to search for feature selectivity with stimuli of arbitrary statistics.

One such tool, called maximally informative dimensions (MID) involves an iterative search through stimulus space to find the dimensions that maximize the mutual information between the stimulus and the spike train (Sharpee et al., 2014). In theory, MID can find multiple selective dimensions in stimulus space given arbitrary natural stimuli. The disadvantages are that it requires a lot of data ($\sim 10^5$ spikes), and

the parameter space is non-convex, so there is no guarantee that a search algorithm will find the optimal solution. A variant of MID, called quadratic mutual information, has also been used to extract RGC filters from natural scenes (Katz et al., 2016). While the data requirements for this method are substantially less than for MID, it only revealed single spatiotemporal filters for each RGC that were not qualitatively different than the STA. Deep learning has also been employed in recent work to reveal aspects of retinal circuitry in the context of natural scenes (Maheswaranathan et al., 2018).

2.7. Closed loop experiments

All the RF measurement techniques we have discussed so far rely on recordings of spike responses from RGCs. Whole-cell recordings of synaptic currents in RGCs have also been measured and used to construct a class of RF models we will consider in the next section (Schwartz et al., 2012), but such recordings are much rarer and more labor intensive than spike recordings and do not scale to large numbers of simultaneously recorded cells. Additionally, the spiking output of RGCs is the signal ultimately sent to the brain, so a complete RF model should use spiking as the end point. One disadvantage of using spikes as the output measure is that nonlinearities associated with spike generation – including rectification at zero and saturation at high firing rates – can interfere with the experimenter's ability to measure underlying nonlinearities in the spatiotemporal RF filter.

The closed-loop, iso-response, method allows an experimenter to separate the output (spiking) nonlinearity from upstream nonlinearities using a RGC spike recording. In this method, an online algorithm measures the spike response to each stimulus presentation, and iteratively alters the stimulus to achieve a target response amplitude (Bölinger and Gollisch, 2012). For example, consider a target response of 10 spikes. If a spot of a certain size and contrast elicited 6 spikes, the spot could be made larger or the contrast increased on the next trial. If

making the spot larger reduced the response to 4 spikes, the algorithm would instead test a smaller spot. Thus, the algorithm can define the iso-response contour: the dimension in stimulus space that elicits the fixed response. In the early days, closed-loop experiments were often used to detect thresholds; for example Enroth-Cugel determined the minimum contrast necessary to elicit a detectable difference in firing (Enroth-Cugell and Robson, 1966). Even Kuffler's recordings of cat RGC RFs used a version of the closed loop technique (Kuffler, 1953). By maintaining a fixed response throughout the measurement, closed-loop experiments can thus reveal nonlinear RF mechanisms without interference from the output nonlinearity.

The usefulness of the closed-loop approach is related to the size of the stimulus space to be explored. Defining iso-response contours while varying one or two parameters of the stimulus is feasible, but measuring contours in three or higher dimensional stimulus space becomes experimentally unrealistic due to the exponential growth of the space. Thus, the closed-loop approach is a powerful tool to that can be applied as part of many of the different RF measurement methods described above. For example, an iso-response contour could map the spatial RF in a spots-of-variable-size type of experiment in which the experimenter also varied contrast. The resulting space would offer a measure of how much more contrast is required to make the cell fire for a non-optimal spot size.

3. Receptive field models

RGC RF models have progressed dramatically from the canonical concepts of center and surround to elaborate circuit models incorporating the many distinct cell types of the retina. The purposes for RF models have also progressed. What began as a fundamental and abstract field attempting links to human perception now lies at the frontier of translational systems neuroscience. Even with his uncanny insight, Kuffler could not have predicted that models of RGC RFs would one day be programmed into computers connected to electronic prosthetics to restore sight to the blind (Eiber et al., 2013; Ong and da Cruz, 2012; Weiland et al., 2005).

While the goals of RF modeling have changed, we will use three broad criteria as a common measuring stick: **predictive power**, **biological realism**, and **generalizability**. Not all RF models were designed with these goals in mind, and indeed no current model succeeds completely at all three, but they nonetheless provide useful comparisons.

Predictive power is the ability for a model to predict the response of a RGC to a particular set of visual stimuli.

Biological realism is the degree to which the components of the RF model correspond to known biological components of retinal circuits (i.e. cells, synapses, receptors, ion channels, signaling pathways). The models that are most successful in biological realism are not necessarily the most detailed. There is always a tradeoff between the simplifying assumptions in higher-level models and the explosion of free parameters in lower-level models.

Generalizability is a measure of the transfer of predictive power across stimuli. RF models are generally built from RGC responses to a small set of stimuli, thus they often fail to predict responses to stimuli outside this set. The set of possible visual stimuli is infinite, so of particular importance in considering generalizability will be naturalistic stimuli that attempt to capture aspects of the visual world for which RGCs evolved.

3.1. Difference of Gaussians

One of the most influential concepts in sensory neuroscience is the idea that RFs can be modeled as a difference of Gaussians (DoG). In the retina, the first DoG model of RGC RFs is attributed to Rodieck and Stone (1965). For a single polarity (ON or OFF) RGC, the spatial extent of the RF center is modeled as a two-dimensional Gaussian, and the

surround is modeled as another two-dimensional Gaussian with much larger extent and opposite (suppressive) polarity. The DoG model has remained extremely popular because it is concise – it only needs three parameters to define the size of each Gaussian and their relative strength – and it is easily fit from any of the RF measurements described above.

Along with the simplicity of the DoG model come several critical limitations. It is a model of space only without a temporal component, so on its own, it does not offer information about kinetics, e.g. to distinguish between transient and sustained RGC types, or to predict the response to a moving object. The DoG model also assumes a single polarity (ON or OFF) RF, so ON-OFF and SbC RGCs cannot be described.

The predictive power of DoG models is limited by several of its core assumptions. First, it assumes circular symmetry in both the RF center and surround (though it can be extended to elliptical shapes for RF center and surround with four additional parameters). While most RGC RFs are reasonably circularly symmetric, some, like orientation-selective (OS) RGCs are highly asymmetric (Bloomfield, 1994; Hammond, 1974; Joesch and Meister, 2016; Kim et al., 2008; Nath and Schwartz, 2016; Venkataramani and Taylor, 2016, 2010). Even non-OS RGCs deviate from elliptical shapes at high resolution (Gauthier et al., 2009). Second, the surround can only suppress the center response. While this is the most common first-order understanding of the surround for most RGCs, numerous "non-classical" surround effects have been described, including the shift-effect (McIlwain, 1966), a polarity switch from surround stimulation (Geffen et al., 2007), a complete absence of surround (Zhao et al., 2014), disinhibition past the classical RF (Chao-Yi et al., 1992), and size-dependent latency shifts beyond the RF center (Mani and Schwartz, 2017).

Finally, and perhaps most importantly, the DoG model is spatially linear. The responses of stimuli at different locations sum linearly, and positive and negative contrasts in the RF cancel. Spatial linearity is a key assumption in many RF models despite the fact that it was shown to be incorrect in most cases even in Kuffler's early work (Kuffler, 1953) and again by Enroth-Cugell and Robson for "Y" cells, which were the majority of cells encountered (Enroth-Cugell and Robson, 1966). The degree of success of spatially linear models, like the DoG model, in predicting RGC responses depends somewhat on the response regime of the RGC being modeled. Some studies have used low contrast and/or low spatial frequency stimuli, specifically to keep cells within their linear regime (Cooper et al., 2012; Enroth-Cugell and Robson, 1966), but measurements of natural scenes show a very large dynamic range of contrast and spatial frequency (Frazor and Geisler, 2006; Mante et al., 2005). We will explore spatially nonlinear RF models at the end of this section.

While the DoG model makes no explicit connection to circuit mechanisms in the retina, it is sometimes (over) interpreted as a circuit model in which the RF center corresponds to excitation from bipolar cells and the RF surround corresponds to inhibition from amacrine cells. Generalizability in the DoG model is limited mostly by its assumption of spatial linearity. For the subset of RGCs that are spatially linear (or probed in the linear regime), it can provide a reasonable prediction of the spatial pattern of RGC activation, but it fails for RGCs with nonlinear RFs when probed with naturalistic patterns (Frazor and Geisler, 2006; Heitman et al., 2016).

3.2. Linear-nonlinear (LN) models

Linear spatial RF models, like the DoG, were soon extended into the time domain. As described above, many RF estimation methods include a kinetic component. To make a RF model in time and space, the kinetics of the response are used to construct a temporal filter. The details of temporal filter construction depend on the RF measurement. Once constructed, the temporal filter is used along with the spatial filter to model the firing rate of a RGC responding to any spatiotemporal pattern of light.
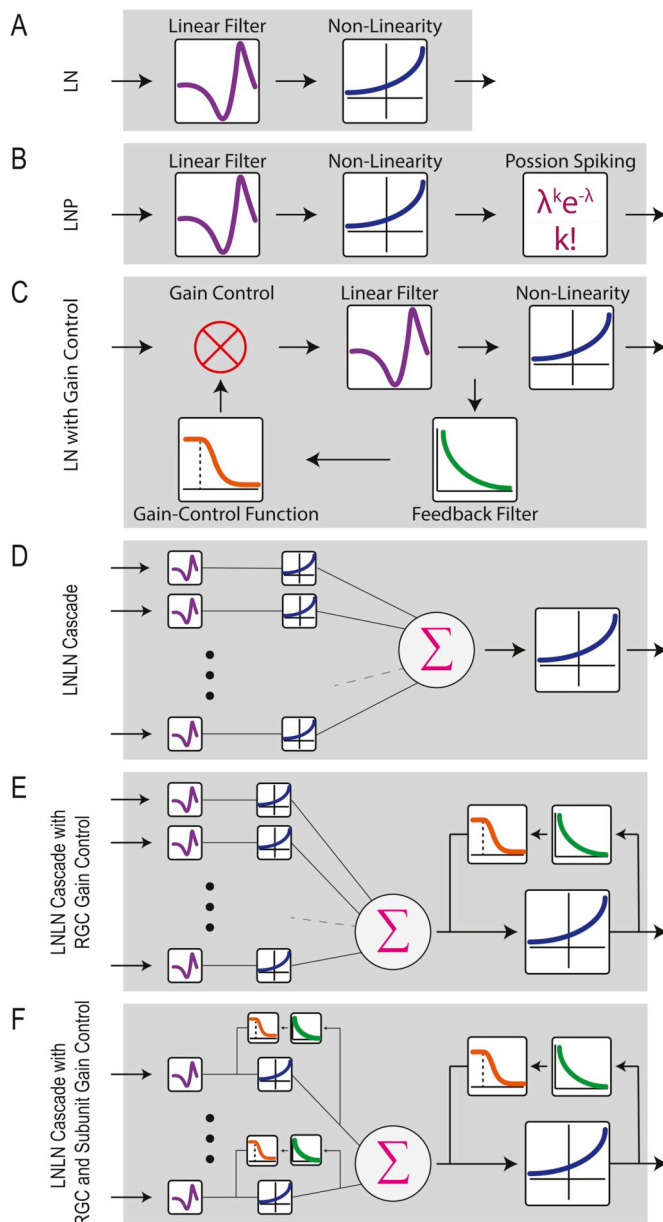
Fig. 4. Schematics of the classes of RGC RF models. (**A-C**) Spatially linear models. (**D-F**) Spatially nonlinear models.

The first spatiotemporal models using a linear temporal filter revealed a fundamental flaw: the models predicted unrealistic firing rates. For example, if an ON-center DoG model is probed with a dark spot (negative contrast), it will produce a negative value, which, when passed through a linear temporal filter, predicts that the RGC fires at a rate less than zero. On the opposite end of the contrast scale, purely linear models also predict increasing firing rates *ad infinitim*.

Both negative firing rates (a lack of rectification) and unrealistically high firing rates (a lack of saturation) can be fixed by introducing a static nonlinearity between the linear spatiotemporal RF model and the firing rate prediction (Chichilnisky, 2001; Victor and Shapley, 1979a). This solution gave rise to what is known as the linear-nonlinear (LN) class of RGC RF models (Fig. 4). Another important advantage of the static nonlinearity is that it allows predictions of both ON and OFF responses from a single spatiotemporal RF, because the U-shaped nonlinearity can predict positive firing rates for both positive and negative filter activation values. While the ON and OFF RFs must share the same spatial structure and the same temporal filter in such a model,

it at least allows ON-OFF RGCs to be included.

LN models of RGCs are very common because their parameters, including the static nonlinearity, are easily estimated from data (Chichilnisky, 2001), and they offer good predictive power for a restricted set of stimuli. Despite their strengths, LN models fail to generalize for many classes of stimuli, including naturalistic stimuli. Importantly, the static nonlinearity in LN models follows the spatiotemporal model, so LN models still assume spatial linearity. The spatial linearity assumption is responsible for many of the generalization failures of LN models (Heitman et al., 2016).

Like the DoG model, the LN model makes no explicit connection to circuit mechanisms; and also like the DoG model, it has, nonetheless, been interpreted as a circuit model. The static nonlinearity is often associated with spike generation in the RGC, since spike generation rectifies the minimum firing rate at zero and limits the maximum firing rate by the refractory period. While spike generation certainly contributes to the static nonlinearity measured in the LN model, additional nonlinear circuit elements (notably the synapses from bipolar cells) also contribute (Demb et al., 2001; Schwartz and Rieke, 2011)

3.3. Incorporating gain control

Most RGC RF modeling efforts over the last two decades have started with the LN model and introduced additional elements to improve the model's predictive power for particular stimuli. Some of the most successful additions have involved mechanisms for gain control (Fig. 4). In this context, gain control is any process that reduces the firing rate of a RGC temporarily following a period of high activity. The most typical stimulus parameters that cause changes in gain are intensity and contrast (reviewed by Rieke and Rudd, 2009). While neurons change state on a continuum of timescales, gain control is typically distinguished from adaptation on the basis of its fast timescale. For RGCs, gain control mechanisms act within the duration of the temporal filter – typically less than 250 ms – all the way down to the several millisecond timescale of spikes (Rieke and Rudd, 2009). Thus, modeling gain control is the first quantitative attempt to capture some of the dynamic nature of RGC RFs, but only in a limited context.

Early work recognized the importance of gain control in capturing the firing patterns of RGCs to spatial and temporal modulations of light (Shapley and Victor, 1981, 1978). More recently, gain control has been used in models of RGC responses to moving objects (Johnston and Lagnado, 2015). A LN model incorporating a gain control term was successful in capturing motion anticipation: the tendency of populations of RGCs to overcome upstream lag and fire with the leading edge of a moving object (Berry et al., 1999). On the finer timescale of the refractory period following individual spikes, models have incorporated a spike feedback term following a Poisson spike generator (Pillow et al., 2005) and have introduced post-spike "coupling terms" in a generalized linear model (GLM) framework to account for interactions among RGCs (Pillow et al., 2008). LN models with gain control have been quite successful at improving the predictive power in the temporal domain (van Hateren et al., 2002), but they remain largely unable to generalize to naturalistic scenes with large spatiotemporal correlations (Heitman et al., 2016; Maheswaranathan et al., 2018)

Gain control has several appealing correlate biological mechanisms in neurons. On the shortest timescale, well-known biophysical mechanisms, like Na^+ channel inactivation and the opening of delayed rectifier K^+ channels, contribute to the refractory period following each spike (Weick and Demb, 2011). Voltage-gated conductances in the RGC with slightly longer timescales, like Ca^{2+}-activated K^+ channels, can reduce gain on the timescale of tens of milliseconds (Hotson and Prince, 1980). Gain control mechanisms have been found at many levels in retinal circuits (Baccus and Meister, 2002; Kim and Rieke, 2003), so it is certainly an oversimplification to assume that all of the effect captured in such a model is the result of mechanisms in the RGC itself. A kinetic (Markov state) model was added to the standard LN model to account
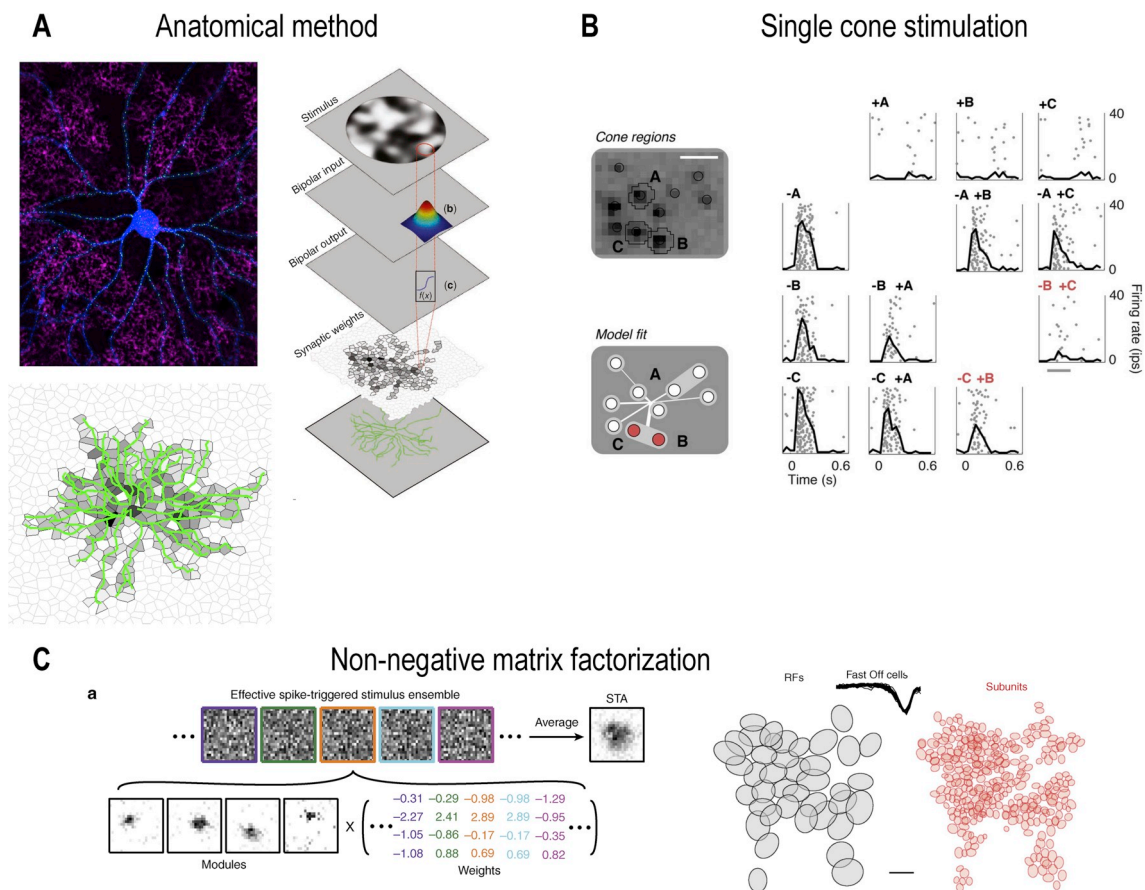
Fig. 5. Methods for estimating subunit locations. (**A**) In the anatomical method, a RGC cell fill (blue) is combined with a marker of synapses (green) and a stain for a particular bipolar cell type (magenta). A model estimates the number of synapses from each bipolar cell based on the dendritic morphology of the RGC. Adapted from (Schwartz et al., 2012). (**B**) The single cone stimulation method presents small spots of light aligned to the locations of cones. By presenting pairs of spots and measuring whether the responses combine linearly or nonlinearly in the RGCs, the experimenters were able to infer the locations of RF subunits. Adapted from (Freeman et al., 2015). (**C**) The non-negative matrix factorization technique is an analytical method that can be applied to data from spatiotemporal white noise experiments (left). The panel at the rights shows the linear RF (gray) and the corresponding subunit RFs (red) estimated from a multi-electrode-array recording in salamander retina. Adapted from (Liu et al., 2017).

for contrast adaptation with more explicit connections to biological mechanism than in previous models (Ozuysal and Baccus, 2012). A recent paper returned to the mechanistic basis for the gain control responsible for motion anticipation and found that it relies on post-synaptic inhibition to the dendrites of RGCs (Johnston and Lagnado, 2015).

3.4. Multi-pathway LN models

As mentioned above, ON-OFF RGCs are modeled in only a rudimentary way in standard LN models by introducing a non-monotonic nonlinearity following a single temporal filter. More recent models of ON-OFF RGCs have used separate spatiotemporal filters and separate nonlinearities for the ON and OFF channels (Gollisch and Meister, 2008a,b) Using the spatiotemporal white noise stimulus, one can use the spike-triggered covariance (STC) matrix rather than simply its mean (the STA) to extract separate ON and OFF filters (Cantrell et al., 2010; Fairhall et al., 2006). In addition to ON and OFF, the STC approach can reveal separate spatial filters, each with their own temporal components (Fairhall et al., 2006).

While it is very powerful in theory, STC requires much more data than STA, and in practice, it rarely produces more than two well-defined filters before reaching noise level (Fairhall et al., 2006; Liu and Gollisch, 2015). Nonetheless, multi-pathway LN models, whether fit from STC or constructed based on assumptions about the separate pathways and fit with another method, have been useful in capturing

some of the properties of RGCs that are missed with standard LN models (Baccus et al., 2008; Gollisch and Meister, 2008a,b; McFarland et al., 2013; Zhang et al., 2012).

In some cases, multi-pathway LN models are inspired by the structure of retinal circuits. ON-OFF RGCs receive ON and OFF input from different sets of bipolar cells, so a two-pathway LN model has a clear rationale. Other examples of multi-pathway LN models have been built to match known circuit elements, like separate excitatory and inhibitory pathways (Baccus et al., 2008; Kastner and Baccus, 2013). The multiple filters that emerge from STC are generally less well connected to particular circuit elements.

3.5. Spatially nonlinear RF models

All the RF models we have considered thus far share the assumption of linear spatial integration, even though early work on RGC RFs revealed strong spatial nonlinearities (Enroth-Cugell and Robson, 1966; Hochstein and Shapley, 1976; Kuffler, 1953). The biological basis for nonlinear spatial integration involves rectified synapses from bipolar cells (Demb et al., 2001, 1999; Schwartz and Rieke, 2011). Victor and Shapley led the way measuring and modeling nonlinear spatial integration in RGCs (Shapley and Victor, 1979; Victor and Shapley, 1979b, 1979a). Their work was later extended by Enroth-Cugell and Freeman to form the pooled subunits model (Enroth-Cugell and Freeman, 1987).

Variations on this influential model have evolved into the LNLN

cascade models that consistently outperform spatially linear RGC models for a variety of stimuli from white noise (Real et al., 2017) to object motion (Baccus et al., 2008; Ölveczky et al., 2003), to natural scenes (Gollisch, 2013; Heitman et al., 2016). Additional gain control elements at the level of individual subunits have been added in recent versions of these models to help predict responses to moving objects (Chen et al., 2014) and white noise (Real et al., 2017). The need for gain control at the level of the subunits matches experimental data showing that contrast gain control is sometimes localized on the scale of bipolar cells (Brown and Masland, 2001; Garvert and Gollisch, 2013), though it can also have components on the scale of the RGC RF (Garvert and Gollisch, 2013; Khani and Gollisch, 2017). Gap-junctional coupling between bipolar cells (via AII amacrine cells) is another addition to these models inspired by experimental data, and it has been important in capturing motion sensitivity in mouse and primate RGCs (Kuo et al., 2016; Manookin et al., 2018). Another recent model added a delay in the spatial pooling of subunits in the RF surround to account for the extra synapse between amacrine cells and RGCs (Real et al., 2017). Fig. 4 summarizes the structure of some of the variants of LN models that have been used to model RGC RFs.

While the sizes, temporal filters, and nonlinearities of the subunits in LNLN cascade models are estimated with reasonable reliability by fitting the models to RGC spike data, determining the spatial location of each subunit in two-dimensions has proved to be much more difficult (Fig. 5). Because the subunit weights to the RGC do not conform to the Gaussian ideal, determining their locations at high resolution is critical to achieve predictive power for complex spatiotemporal stimuli (Schwartz et al., 2012). An anatomical strategy was used in one study to predict the number of synapses received from each bipolar cell based on a traced image of the RGC dendrites. While this model predicted responses to arbitrary spatial images, it is not feasible to have a full morphological reconstruction of the RGC in most cases (Schwartz et al., 2012). Another recent approach used stimulation of individual cones to map the locations of bipolar cells synapsing onto primate midget RGCs. The method required only the RGC spikes as input data, but was a somewhat special case since midget RGCs receive less than 10 bipolar cell inputs (Freeman et al., 2015). Using only standard spatiotemporal white noise and an analysis method called non-negative matrix factorization, Liu et al., were able to map the bipolar subunit locations in salamander RGC RFs, also a case in which the number of subunits is ∼10 (Liu et al., 2017).

4. Feature selectivity: fluidity versus invariance

Kuffler realized years ahead of his time that RGC RFs are "flexible" and "fluid". Is the effort to build a generalizable RGC model then a Sisyphean task? Surely there are limits on the fluidity of RGC RFs, because the retina, despite its complexity, is still a primary sensory system with little feedback from the rest of the brain. This small amount of feedback comes from neuromodulatory retinopetal projections (Gastinger et al., 2006). The information conveyed by each RGC type must be stereotyped across individuals, because RGCs project selectively to many distinct targets in the brain, and these projection patterns appear to be genetically predetermined (Dhande and Huberman, 2014). Which aspects of a RGC's response are stable, and which are fluid?

We will argue that the answer to this question is connected to the concept of feature selectivity. The idea that RGCs act as detectors for specific, behaviorally relevant, features of the visual world was developed in parallel with the early history of RF modeling (Barlow, 1961; Lettvin et al., 1959; Levick, 1967). Invariance is central to the view of RGCs as feature detectors. If particular RGCs encode behaviorally relevant features, those representations should be robust to other changes in the visual scene, like luminance, contrast, and noise. Another conclusion that follows from this line of reasoning is that some of the RF properties that researchers typically measure and model, like response

polarity, size, and kinetics, may be fluid if they are not part of the core feature selectivity of the RGC. In this section, we will review a collection of recent reports on the fluidity of RGC RFs under different stimulus conditions, pointing out both the aspects of the RF that change and those that remain invariant.

4.1. Response polarity

Countless studies have used response polarity as a defining feature to classify RGCs, but recent evidence has shown that this aspect of RFs is not stable across illumination levels (Rivlin-Etzion et al., 2018). Tikidji-Hamburyan et al. showed that cells classified as ON at one luminance can become ON-OFF at another luminance (Tikidji-Hamburyan et al., 2015). Similarly, cells classified as OFF could develop an additional ON response in certain luminance regimes. These results were confirmed in both mouse and pig retina and in retino-recipient dorsal lateral geniculate nucleus (dLGN) *in vivo*.

Concurrent with this study, another group reported a similar luminance-dependent switch in ON:OFF ratio in three mouse RGC types (Pearson and Kerschensteiner, 2015). Interestingly, one of the RGC types that showed this ON:OFF switching behavior was a direction-selective (DS) type presumed to be equivalent to previously described ON-OFF DS RGCs. While its ON:OFF contrast ratio switched with luminance, its direction preference did not. Orientation-selectivity (OS) also remained stable across luminance (Pearson and Kerschensteiner, 2015). Perhaps the luminance invariance of DS and OS is an indication that these properties are the core feature selectivity of these particular RGC types. One of the RGC types shown in the Tikidji-Hamburyan et al. study to change from OFF to ON-OFF with luminance, called the OFF-transient alpha, has been implicated in selectivity for looming dark objects (Münch et al., 2009) and for image recurrence following saccades (Krishnamoorthy et al., 2017). It remains unknown whether these types of feature selectivity are invariant in OFF-transient alpha RGCs across luminance.

Properties other than luminance have also been shown to elicit ON:OFF switching behavior in RGCs. Several types of RGCs in mouse have been shown to switch polarity depending on stimulus size, including the JAM-B RGC (Kim et al., 2008) and the "high definition" (HD1 and HD2) (Jacoby and Schwartz, 2017) RGCs (Fig. 6). Transient stimulation of the surround with a phase shift of a grating can also change the RF center filter of some RGCs from OFF to ON (Geffen et al., 2007).

4.2. Spatial RF

Spatial properties of RGC RFs, like the size of the RF center and strength of the RF surround, have long been known to vary with luminance (Barlow, 1957; Barlow and Levick, 1969; Creutzfeldt et al., 1970; Enroth-Cugell and Lennie, 1975; Enroth-Cugell and Robson, 1966; Enroth-Cugell and Shapley, 1973; Farrow et al., 2013; Grimes et al., 2014a,b; Ogawa and Bishop, 1966; Reitner et al., 1991; Troy et al., 1999). Circuit mechanisms for these effects include luminance-dependent changes in gap-junction coupling in both the outer retina (DeVries and Schwartz, 1989; Lasater, 1987; Xin and Bloomfield, 1999) and the inner retina (Bloomfield et al., 1997; Hu et al., 2010), and luminance-dependent recruitment of spiking amacrine cells (Farrow et al., 2013). Since electrical coupling in the retina can be modulated by time of day independent of luminance, spatial components of RGC RFs are even subject to circadian regulation (Jin and Ribelayga, 2016; Ribelayga et al., 2008; Zhang et al., 2015).

4.3. Kinetics

In addition to its effects on polarity and space, luminance has long been known to alter the kinetics of RGC responses. Responses tend to become more transient and have shorter latency as luminance increases
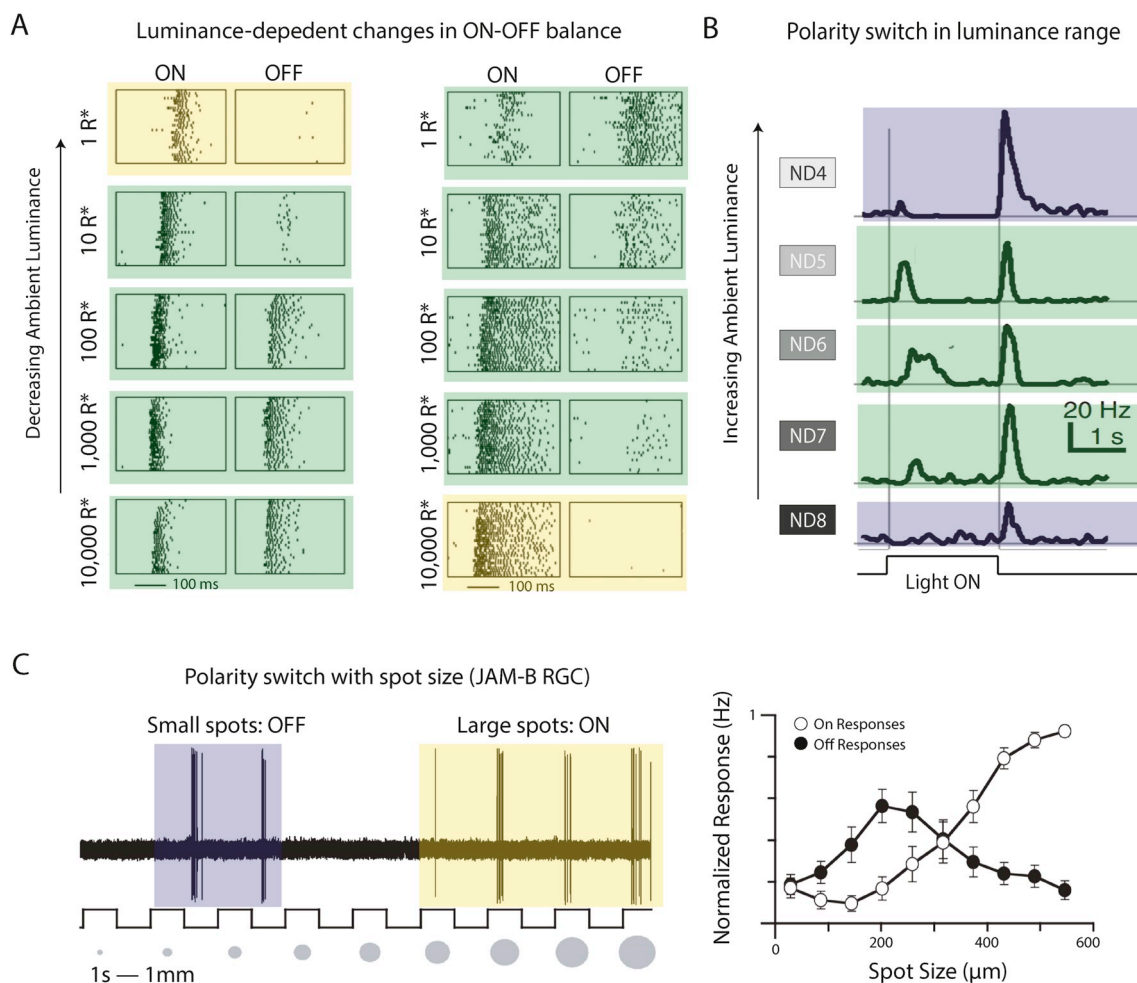
Fig. 6. Polarity switches in RGCs with stimulus conditions. (**A**) Spike rasters from 2 RGCs responding to ON and OFF contrast steps across 5 log units of luminance. Polarity switches are indicated by shading for ON (yellow), ON-OFF (green) and OFF (blue) polarity. Adapted from (Pearson and Kerschensteiner, 2015). (**B**) The firing rate of a RGC that becomes ON-OFF in a limited luminance range. Adapted from (Tikidji-Hamburyan et al., 2015). (**C**) The response polarity of JAM-B RGCs depends on stimulus size. Adapted from (Kim et al., 2008).

(Ogawa and Bishop, 1966; Tikidji-Hamburyan et al., 2015). Accelerations of light responses with increasing luminance are largely attributed to a switch from rod-dominated to cone-dominated transduction and subsequent kinetic changes within the cone phototransduction cascade (Attwell et al., 1984; Elias et al., 2004; Euler and Masland, 2000; Murphy and Rieke, 2011; Sharpe et al., 1993). Accelerations of circuit components downstream of photoreceptors also contribute to kinetic changes in RGC light responses with luminance (Dunn et al., 2007; Dunn and Rieke, 2006).

Luminance-dependent changes in kinetics are often ignored in RGC RF models designed to describe steady-state responses in a fixed luminance range, but what if another property of the light stimulus alters response kinetics? For some RGCs, response kinetics depends on the size of a visual stimulus (Fig. 7). These kinetic changes with increased spot size can manifest as the loss of a transient component, as in ON OS RGCs (Nath and Schwartz, 2016) or the response becoming more transient, as in F-mini[ON] RGCs. Response latency can also depend on stimulus size. ON DS RGCs increase in latency for larger spots while ON delayed RGCs show decreased response latency (Mani and Schwartz, 2017).

4.4. Spatial linearity

After response polarity, size, and kinetics, perhaps the most commonly used characteristic to distinguish RGC types is whether they integrate space linearly (called "X" cells) or nonlinearly ("Y" cells) (Enroth-Cugell and Robson, 1966). One cell type in mouse, called the ON-alpha RGC, has been show to integrate over space nearly linearly in low luminance and highly nonlinearly in high luminance (Fig. 8) (Grimes et al., 2014a,b). The site of this switch was localized to the output synapses from ON cone bipolar cells, which become more rectified (hence nonlinear) in bright conditions. Another result of this mechanistic change at the bipolar cell synapse is a change in the shape of the contrast sensitivity function of the RGC.

5. The next generation of measuring, modeling, and understanding RGC RFs

A decade ago, one of us had aspirations of writing a review about all that was wrong with the current state of RGC RF models until his graduate mentor asked a simple question, "What is the new framework you will propose?" This question promptly ended the review before it began; it's always easier to tear down old theories than to build new ones. Admittedly, our answer to his compelling question remains incomplete, but it is now at least informed by our answers to several related questions.
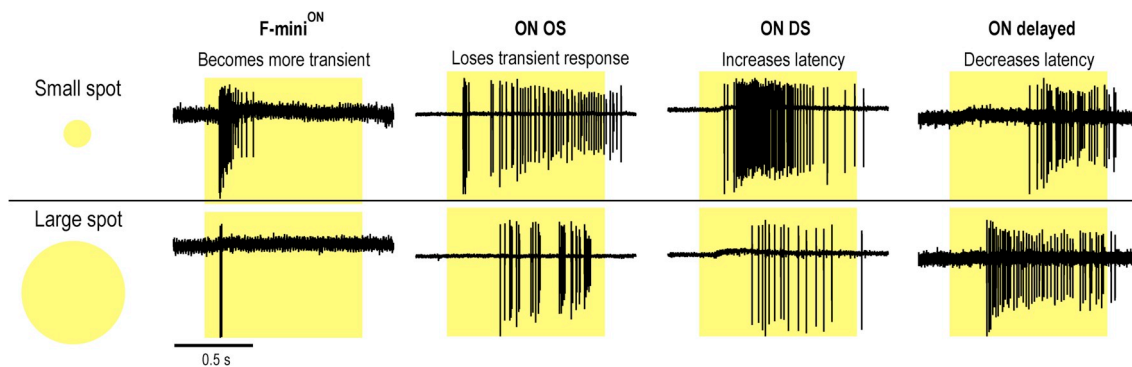
Fig. 7. RGCs respond with different kinetics to small and large spots of light. Four examples of RGC light responses to a spot of light (darkness to 200 isomerizations per rod per second) presented for 1 s. Top traces show responses to spots covering only the RF center (120 μm for the F-mini[ON] and 200 μm for the oher cells. Bottom traces show responses from the same four cells to a full-field spot (1200 μm) covering the RF center and surround.
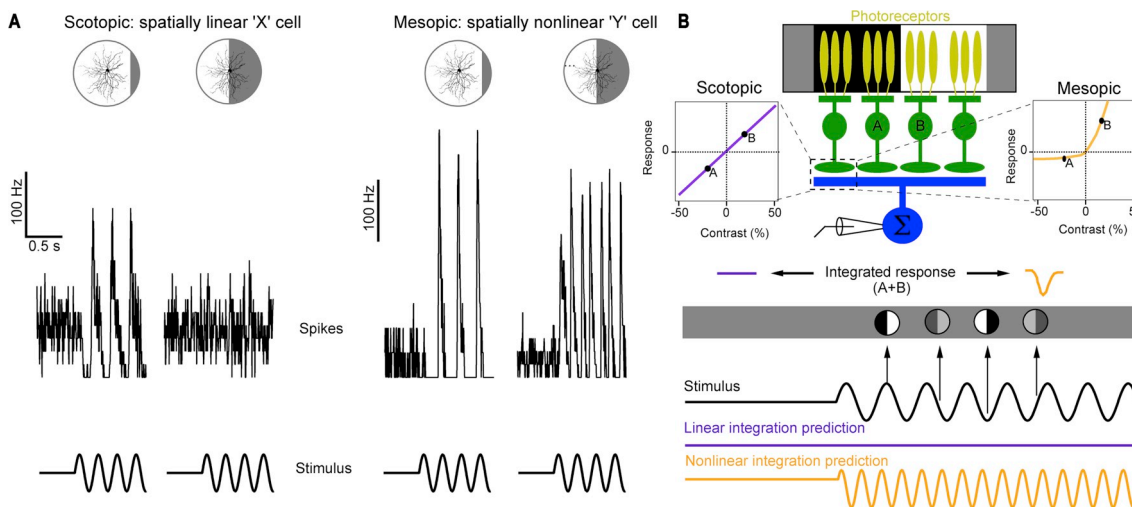

Fig. 8. Linear verses nonlinear spatial integration in RGCs can depend on luminance. (**A**) Example of the same ON-alpha responding to a contrast-reversing grating in scotopic and mesopic luminance. This is the same stimulus originally used to classify linear (X) vs. nonlinear (Y) RGCs (Enroth-Cugell and Robson, 1966). (**B**) A schematic of how a change in rectification at bipolar cell output synapses can account for a change in spatial integration in a RGC. Figure adapted from (Grimes et al., 2014a,b).

5.1. Can a unified computational framework capture the diversity of RGC RF properties?

Perhaps not. Researchers in the early days of work on RGCs described them in two very different ways. Lettvin and colleagues famously described a set of detectors for specific behaviorally relevant features of the visual world in "What the Frog's Eye Tells the Frog's Brain" (Lettvin et al., 1959). Much of the rest of the field moved instead in the direction of describing RGCs in the language of signal processing from engineering, as input-output layers of linear filters, nonlinear transformations, and feedback loops (see Fig. 4). The signal processing perspective and its possible implications for a framework of the population code of the retina were first considered in the visionary work of Horace Barlow (1961), inspired by Simon Laughlin's work on predictive coding (Laughlin, 1981, 1989; Srinivasan et al., 1982) and codified in the theoretical work of Atick (1990). This framework was based on the concept of efficient coding: imagining the population of RGCs as an efficient coder of certain properties of a visual scene, effectively reducing the redundancy that exists because of the high degree of spatio-temporal correlation in natural scenes. While the efficient coding hypothesis persists (Nirenberg et al., 2001), especially over the last decade there has been an accumulation of evidence that redundancy reduction might be the wrong framework for thinking about retinal computation. Consider that each location in visual space is sampled by 2–3 RGCs of ~40 different types (Bae et al., 2018). A system that evolved to

represent each pixel 80–120 times in its output does not seem to be optimized for redundancy reduction. Instead, the literature is full of examples of specialized computations in RGCs that were shaped by selective pressure to extract behaviorally relevant signals robustly. We have slowly returned to attempts to catalogue *what an animal's eye tells an animal's brain*. In a vague sense, this still represents an efficient code, but only through the lens of the full set of behavioral demands of an animal's visual system – a lens whose overwhelming majority remains obscured in our current understanding. In the absence of a framework for the visual repertoire of the brain, perhaps it is counterproductive to try to impose a unifying framework on the diversity of computations that exists among RGCs.

5.2. Do RGCs encode multiple features of the visual world depending on context?

Of course they must. Even with the ~40 different RGC channels, there must be substantial multiplexing to convey the entirety of the information necessary for higher order visual processing in the spikes of the optic nerve. The requirements of vision also vary dramatically with the context of both the stimulus and behavior. What is less clear is how we come to terms with multiplexed RGC codes in our descriptions and models of RFs. Some progress has been made in describing the response patterns of RGCs to moving stimuli. The same RGCs can report either the smooth motion of an object through their RF centers or the sudden
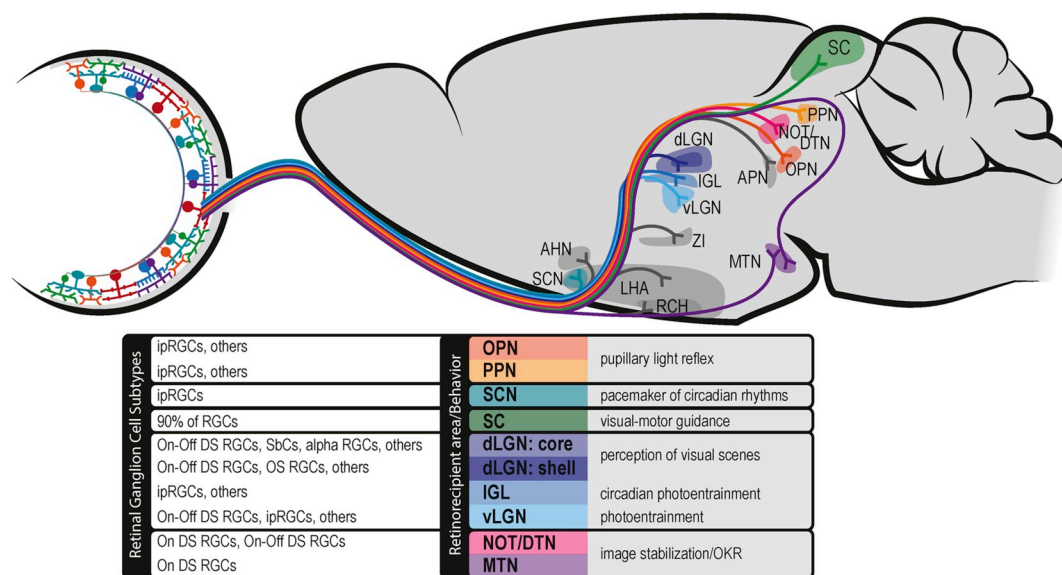
Fig. 9. A subset of retinorecipient areas of the brain. Well studied brain regions are in color and listed with their known RGC inputs and their behavioral function. Less well understood regions are shown shaded in gray. AbbreviationsAHN: Anterior Hypothalamic Nucleus, APN: Anterior Pretectal Nucleus, IGL: Intergeniculate Leaflet, LGN: Lateral Geniculate Nucleus, LHA: Lateral Hypothalamic Area, MTN: Medial Terminal Nucleus, NOT/DTN: Nucleus of the Optic Tract/Dorsal Tegmental Nucleus, OPN: Olivary Pretectal Nucleus, PPN: Pedunculopontine Nucleus, RCH: Retrochiasmatic Area, SC: Superior Colliculus, SCN: Suprachiasmatic Nucleus.

reversal of the object distant to the RF center (Schwartz et al., 2007). The multiplexed code for object motion was analyzed recently in more detail in a single type of RGCs in rat retina (Deny et al., 2017). In the broader sense, the field still grapples with the difference between selectivity and exclusivity. For example, ON-OFF DS RGCs are highly selective for a particular direction of motion, but they also respond robustly at the onset and offset of a flashed spot of light. Surely the brain does not misinterpret every spike from an ON-OFF DS RGC responding to a static object as evidence of motion in its preferred direction.

5.3. Can invariance inform our intuitions about the features that RGCs extract from the visual world?

It can and it should. The dynamic ranges of parameters in the visual world are enormous – 10 orders of magnitude of luminance (Rodieck, 1998), ~4 orders of magnitude of contrast (Frazor and Geisler, 2006; Mante et al., 2005), and multiple sizes and speeds of objects. It is extremely difficult to make a circuit out of biological elements that is robust over a large dynamic range. Finding such invariance in a RGC provides strong evidence that selective pressure played a role in establishing its feature selectivity. There are several examples of such invariance in RGCs. ON-OFF DS RGCs employ a variety of mechanisms to maintain their selectivity across a large range of luminance, speed, contrast, and in the presence of background noise (Chen et al., 2016; Nowak et al., 2011; Poleg-Polsky and Diamond, 2016; Sethuramanujam and McLaughlin., 2016). OFF OS RGCs maintain orientation selectivity across seven orders of magnitude of luminance and a wide range of spatiotemporal frequencies (Nath and Schwartz, 2017). Small bistratified RGCs in primates are blue-yellow color opponent in a variety of different stimulus contexts (Dacey and Lee, 1994; Field et al., 2007). Evolutionary conservation can also be a sign of behaviorally relevant feature selectivity in a RGC type. Object motion sensitive RGCs have similar dendritic morphology and circuit mechanisms in a variety of species (Jacoby and Schwartz, 2017; Kim and Kerschensteiner, 2017; Puller et al., 2015; Venkataramani et al., 2014; Zhang et al., 2012).

On the other hand, RGC computations that are not robust offer a hint that there may remain an undiscovered aspect of feature selectivity. JAM-B RGCs were characterized as DS (Kim et al., 2008) in a narrow luminance regime (Joesch and Meister, 2016) before it was

discovered that they encode OS invariant to luminance (Nath and Schwartz, 2017). F-mini^{ON} RGCs were reported to be weakly DS over a limited range of speeds (Rousso et al., 2016). Perhaps they are more robustly selective for a different visual feature. For the vast majority of RGCs, robust and invariant feature selectivity remains to be discovered.

5.4. Can we work backward from the brain and behavior to discover the salient features encoded by RGCs?

Yes, and we should use a comparative approach. The latest estimate is that RGCs project directly to 59 different brain regions in mouse (Martersteck et al., 2017)! Similarly extensive retinal projection patterns have been reported in other species, with many conserved targets (Campbell et al., 1967; Hannibal et al., 2014; Major et al., 2003; Matteau et al., 2003; Reiner et al., 1996; Robles et al., 2014; Shimizu et al., 1994). This extreme diversity in the targets of RGCs must mean that visual signals are used in a host of innate behaviors distinct from conscious perception, and the conservation of these pathways suggests that they drove RGC feature selectivity throughout evolution (Fig. 9). Two of the most compelling success stories linking RGCs to behavior come from studies that worked backward from specific retino-recipient brain areas to discover the specific RGC types influencing the known functional roles of these brain regions.

By the 1990s it had become clear that a signal from the retina was required to entrain the circadian system to the light-dark cycle, and that this signal remained in people with extensive rod and cone loss (Zaidi et al., 2007). David Berson and colleagues injected a retrograde tracer in the super chiasmatic nucleus (SCN), the master regulator of the circadian clock, and looked for labeled RGCs. They discovered a new type of RGCs that, surprisingly, contained their own phototransduction cascade, independent from rods and cones, using the photopigment melanopsin (Berson and Dunn., 2002). These ganglion cell photoreceptors are now called intrinsically photosensitive (ip)RGCs, and they are specialized to integrate light signals over time to measure total luminance (Milner and Do, 2017; Wong, 2012). Subsequent work has revealed that ipRGCs comprise multiple subtypes with specific roles in both image-forming vision and several non-image forming visual behaviors (Chen et al., 2011; Ecker et al., 2010; Güler et al., 2008; Schmidt et al., 2014).

Another example of intuition from neuroethology driving a

discovery about RGCs is the tracing of cells projecting to the accessory optic system (AOS). Image stabilization during eye, head, and body movements requires a set of nuclei, collectively called the AOS, which receive both vestibular and visual input (Dhande et al., 2013; Gauvain and Murphy, 2015; Oyster et al., 1980; Simpson, 1984; Yonehara et al., 2009, 2008). Retrograde tracing studies from the AOS to the retina revealed a set of RGCs, called ON DS RGCs, which are selective to the direction of motion across the retina (Oyster et al., 1980). Unlike the previously identified ON-OFF DS RGCs, ON DS RGCs have large RFs and are specialized to report the slow speeds that drive the visual input for image stabilization before the vestibular system takes over at higher speeds (Ackert et al., 2006; Yonehara et al., 2009).

5.5. Future directions and conclusions

The study of RGC RFs over the last six decades has been a fascinating journey. From the beginning, Kuffler realized that a static representation would not be sufficient, but it has proved difficult to capture the dynamics of RGCs in a succinct way. Along the way, we have come to appreciate the enormous diversity of RGC types and the equally impressive diversity of their targets in the brain. The next generation of our understanding of RGCs should embrace both the dynamic nature of RGC RFs and both aspects of their diversity. Drawing inspiration from how specific RGCs evolved to serve particular behavioral needs may reveal the core computations of the visual system.

Acknowledgements

References

Ackert, J.M., Wu, S.H., Lee, J.C., Abrams, J., Hu, E.H., Perlman, I., Bloomfield, S.A., 2006. Light-induced changes in spike synchronization between coupled ON direction selective ganglion cells in the mammalian retina. J. Neurosci. 26, 4206–4215. http://dx.doi.org/10.1523/JNEUROSCI.0496-06.2006.

Antinucci, P., Suleyman, O., Monfries, C., Hindges, R., 2016. Neural mechanisms generating orientation selectivity in the retina. Curr. Biol. http://dx.doi.org/10.1016/j.cub.2016.05.035.

Atick, Redlich, 1990. Towards a theory of early visual processing. Neural Comput. 2, 308–320.

Attwell, D., Wilson, M., Wu, S.M., 1984. A quantitative analysis of interactions between photoreceptors in the salamander (Ambystoma) retina. J Physiol 352, 703–737.

Baccus, S.A., Meister, M., 2002. Fast and slow contrast adaptation in retinal circuitry. Neuron 36, 909–919.

Baccus, S.A.A., Olveczky, B.P.P., Manu, M., Meister, M., 2008. A retinal circuit that computes object motion. J. Neurosci. 28, 6807–6817. http://dx.doi.org/10.1523/JNEUROSCI.4206-07.2008.

Baden, T., Berens, P., Franke, K., Román Rosón, M., Bethge, M., Euler, T., 2016. The functional diversity of retinal ganglion cells in the mouse. Nature 529, 345–350. http://dx.doi.org/10.1038/nature16468.

Bae, J.A., Mu, S., Kim, J.S., Turner, N.L., Tartavull, I., Kemnitz, N., Jordan, C.S., Norton, A.D., Silversmith, W.M., Prentki, R., Sorek, M., David, C., Jones, D.L., Bland, D., Sterling, A.L.R., Park, J., Briggman, K.L., Seung, H.S., 2018. Digital museum of retinal ganglion cells with dense anatomy and physiology. Cell 173, 1293–1306. http://dx.doi.org/10.1016/j.cell.2018.04.040. e19.

Bailey, M.J., Cassone, V.M., 2005. Melanopsin expression in the chick retina and pineal gland. Mol. Brain Res. 134, 345–348. http://dx.doi.org/10.1016/J.MOLBRAINRES.2004.11.003.

Barlow, H.B., 1961. Possible principles underlying the transformations of sensory messages BT - sensory communication. In: Sensory Communication. The MIT Press, pp. 216–234.

Barlow, H.B., 1957. Increment thresholds at low intensities considered as signal/noise discriminations. J. Physiol 469–488.

Barlow, H.B., Levick, W.R., 1969. Changes in the maintained discharge with adaptation level in the cat retina. J Physiol 202, 699–718.

Berry, M.J., Brivanlou, I.H., Jordan, T.A., Meister, M., 1999. Anticipation of moving stimuli by the retina. Nature 398, 334–338.

Berson, D.M., Dunn, F., Takao, M.A., 2002. Phototransduction by retinal ganglion cells that set the circadian clock. Science 295, 1070–1073. http://dx.doi.org/10.1126/science.1067262.

Bloomfield, S.A., 1994. Orientation-sensitive amacrine and ganglion cells in the rabbit retina. J. Neurophysiol. 71, 1672–1691.

Bloomfield, S.A., Xin, D., Osborne, T., 1997. Light-induced modulation of coupling between AII amacrine cells in the rabbit retina. Vis. Neurosci. 14, 565–576.

Bölinger, D., Gollisch, T., 2012. Closed-loop measurements of iso-response stimuli reveal dynamic nonlinear stimulus integration in the retina. Neuron 73, 333–346.

Borghuis, B.G., Tian, L., Xu, Y., Nikonov, S.S., Vardi, N., Zemelman, B.V., Looger, L.L., 2011. Imaging light responses of targeted neuron populations in the rodent retina. J. Neurosci. 31, 2855–2867.

Boycott, B.B., Wassle, H., 1974. No title. J Physiol 240, 397–419.

Brown, S.P., He, S., Masland, R.H., 2000. Receptive field microstructure and dendritic geometry of retinal ganglion cells. Neuron 27, 371–383.

Brown, S.P., Masland, R.H., 2001. Spatial scale and cellular substrate of contrast adaptation by retinal ganglion cells. Nat. Neurosci. 4, 44–51. http://dx.doi.org/10.1038/82888.

Caldwell, J.H., Daw, N.W., 1978. New properties of rabbit retinal ganglion cells. J. Physiol 276, 257–276.

Campbell, C.B.G., Jane, J.A., Yashon, D., 1967. The retinal projections of the tree shrew and hedgehog. Brain Res. 5, 406–418. http://dx.doi.org/10.1016/0006-8993(67)90047-9.

Cantrell, D.R., Cang, J., Troy, J.B., Liu, X., 2010. Non-centered spike-triggered covariance analysis reveals Neurotrophin-3 as a developmental regulator of receptive field properties of on-off retinal ganglion cells. PLoS Comput. Biol. 6, e1000967.

Chao-Yi, L., Yi-Xiong, Z., Xing, P., Fang-Tu, Q., Cheng-Quan, T., Xing-Zhen, X., 1992. Extensive disinhibitory region beyond the classical receptive field of cat retinal ganglion cells. Vis. Res. 32, 219–228. http://dx.doi.org/10.1016/0042-6989(92)90131-2.

Chen, E.Y., Chou, J., Park, J., Schwartz, G., Berry, M.J., 2014. The neural circuit mechanisms underlying the retinal response to motion reversal. J. Neurosci. 34, 15557–15575.

Chen, E.Y., Marre, O., Fisher, C., Schwartz, G., Levy, J., Silviera, R.A., Berry, M.J. da, 2013. Alert response to motion onset in the retina. J. Neurosci. 33, 120–132.

Chen, Q., Pei, Z., Koren, D., Wei, W., 2016. Stimulus-dependent recruitment of lateral inhibition underlies retinal direction selectivity. Elife 5, e21053. http://dx.doi.org/10.7554/eLife.21053.

Chen, S.-K., Badea, T.C., Hattar, S., 2011. Photoentrainment and pupillary light reflex are mediated by distinct populations of ipRGCs. Nature 476, 92–95. http://dx.doi.org/10.1038/nature10206.

Chichilnisky, E.J., 2001. A simple white noise analysis of neuronal light responses. Netw. Comput. Neural Syst. 12, 199–213.

Cooper, B., Lee, B.B., Cao, D., 2016. Macaque retinal ganglion cell responses to visual patterns: harmonic composition, noise, and psychophysical detectability. J. Neurophysiol. 115, 2976–2988. http://dx.doi.org/10.1152/jn.00411.2015.

Cooper, B., Sun, H., Lee, B.B., 2012. Psychophysical and physiological responses to gratings with luminance and chromatic components of different spatial frequencies. J. Opt. Soc. Am. A 29, A314–A323.

Creutzfeldt, O.D., Sakmann, B., Scheich, H., Korn, A., 1970. Sensitivity Distribution and Spatial Summation within Receptive-field center of Retinal on-center Ganglion Cells and Transfer Function of the Retina, vol 33.

Dacey, D.M., Lee, B.B., 1994. The "blue-on" opponent pathway in primate retina originates from a distinct bistratified ganglion cell type. Nature 367, 731–735.

Dacey, D.M., Liao, H.-W., Peterson, B.B., Robinson, F.R., Smith, V.C., Pokorny, J., Yau, K.-W., Gamlin, P.D., 2005. Melanopsin-expressing ganglion cells in primate retina signal colour and irradiance and project to the LGN. Nature 433, 749–754. http://dx.doi.org/10.1038/nature03387.

Dacey, D.M., Peterson Beth, B., Robinson, F.R., Gamlin, P.D., 2003. Fireworks in the primate retina: in vitro photodynamics reveals diverse LGN-projecting ganglion cell types. Neuron 37, 15–27.

Daw, N.W., 1968. Colour-coded ganglion cells in the goldfish retina: extension of their receptive fields by means of new stimuli. J. Physiol 197, 567–592.

De Valois, R.L., William Yund, E., Hepler, N., 1982. The orientation and direction selectivity of cells in macaque visual cortex. Vis. Res. 22, 531–544. http://dx.doi.org/10.1016/0042-6989(82)90112-2.

DeAngelis, G.C., Ohzawa, I., Freeman, R.D., 1995. Receptive-field dynamics in the central visual pathways. Trends Neurosci. 18, 451–458. http://dx.doi.org/10.1016/0166-2236(95)94496-R.

Demb, J.B., Haarsma, L., Freed, M.A., Sterling, P., 1999. No title. J. Neurosci. 19 9756.

Demb, J.B., Zaghloul, K.A., Haarsma, L., Sterling, P., 2001. Bipolar cells contribute to nonlinear spatial summation in the brisk-transient (Y) ganglion cell in mammalian retina. J. Neurosci. 21, 7447–7454.

Deny, S., Ferrari, U., Mace, E., Yger, P., Caplette, R., Picaud, S., Tkacik, G., Marre, O., 2017. Multiplexed computations in retinal ganglion cells of a single type. Nat. Commun. 8http://dx.doi.org/10.1038/s41467-017-02159-y. 1964.

DeVries, S.H., 1999. Correlated firing in rabbit retinal ganglion cells. J. Neurophysiol. 81 908.

Devries, S.H., Baylor, D.A., 1997. Mosaic arrangement of ganglion cell receptive fields in rabbit retina. J. Neurophysiol. 78, 2048–2060. http://dx.doi.org/10.1152/jn.1997.78.4.2048.

DeVries, S.H., Schwartz, E.A., 1989. Modulation of an electrical synapse between solitary pairs of catfish horizontal cells by dopamine and second messengers. J. Physiol 414, 351–375.

Dhande, O.S., Estevez, M.E., Quattrochi, L.E., El-Danaf, R.N., Nguyen, P.L., Berson, D.M., Huberman, A.D., 2013. Genetic dissection of retinal inputs to brainstem nuclei controlling image stabilization. J. Neurosci. 33, 17797–17813.

Dhande, O.S., Huberman, A.D., 2014. Retinal ganglion cell maps in the brain: implications for visual processing. Curr. Opin. Neurobiol. 24, 133–142.

Dowling, J.E., 1967. The site of visual adaptation. Science 80 (155), 273–279.

Dunn, F.A., Lankheet, M.J., Rieke, F., 2007. Light adaptation in cone vision involves switching between receptor and post-receptor sites. Nature 449, 603–606.

Dunn, F.A., Rieke, F., 2006. The impact of photoreceptor noise on retinal gain controls. Curr. Opin. Neurobiol. 16, 363–370.

Ecker, J.L., Dumitrescu, O.N., Wong, K.Y., Alam, N.M., Chen, S.-K., LeGates, T., Renna, J.M., Prusky, G.T., Berson, D.M., Hattar, S., 2010. Melanopsin-expressing retinal ganglion-cell photoreceptors: cellular diversity and role in pattern vision. Neuron 67, 49–60. http://dx.doi.org/10.1016/j.neuron.2010.05.023.

Eiber, C.D., Lovell, N.H., Suaning, G.J., 2013. Attaining higher resolution visual prosthetics: a review of the factors and limitations. J. Neural. Eng. 10, 011002. http://dx.doi.org/10.1088/1741-2560/10/1/011002.

Eickenberg, M., Rowekamp, R.J., Kouh, M., Sharpee, T.O., 2012. Characterizing responses of translation-invariant neurons to natural stimuli: maximally informative invariant dimensions. Neural Comput. 24, 2384–2421. http://dx.doi.org/10.1162/NECO_a_00330.

Elias, R.V., Sezate, S.S., Cao, W., McGinnis, J.F., 2004. Temporal kinetics of the light/dark translocation and compartmentation of arrestin and alpha-transducin in mouse photoreceptor cells. Mol. Vis. 10, 672–681.

Enroth-Cugell, C., Freeman, A.W., 1987. The receptive-field spatial structure of cat retinal Y cells. J. Physiol 384, 49–79. http://dx.doi.org/10.1113/jphysiol.1987.sp016443.

Enroth-Cugell, C., Lennie, P., 1975. The control of retinal ganglion cell discharge by receptive field surrounds. J Physiol 247, 551–578.

Enroth-Cugell, C., Robson, J.G., 1966. The contrast sensitivity of retinal ganglion cells of the cat. J. Physiol 187, 517–552.

Enroth-Cugell, C., Shapley, R.M., 1973. Flux, not retinal illumation, is what cat retinal ganglion cells really care about. J. Physiol 233, 311–326.

Euler, T., Masland, R.H., 2000. Light-evoked Responses of Bipolar Cells in a Mammalian Retina, vol 83. pp. 1817–1829.

Fairhall, A.L., Burlingame, C.A., Narasimhan, R., Harris, R.A., Puchalla, J.L., Berry, M.J., 2006. Selectivity for Multiple Stimulus Features in Retinal Ganglion Cells, vol 96. pp. 2724–2738.

Farrow, K., Teixeira, M., Szikra, T., Viney, T.J., Balint, K., Yonehara, K., Roska, B., 2013. Ambient illumination toggles a neuronal circuit switch in the retina and visual perception at cone threshold. Neuron 78, 325–338.

Field, G.D., Chichilnisky, E.J., 2007. Information processing in the primate retina: circuitry and coding. Annu. Rev. Neurosci. 30, 1–30.

Field, G.D., Gauthier, J.L., Sher, A., Greschner, M., Machado, T.A., Jepson, L.H., Shlens, J., Gunning, D.E., Mathieson, K., Dabrowski, W., Paninski, L., Litke, A.M., Chichilnisky, E.J., 2010. Functional connectivity in the retina at the resolution of photoreceptors. Nature 467, 673–677.

Field, G.D., Sher, A., Gauthier, J.L., Greschner, M., Shlens, J., Litke, A.M., Chichilnisky, E.J., 2007. Spatial properties and functional organization of small bistratified ganglion cells in primate retina. J. Neurosci. 27, 13261–13272.

Fransen, J.W., Borghuis, B.G., 2017. Temporally diverse excitation generates direction-selective responses in on- and off-type retinal starburst amacrine cells. Cell Rep. 18, 1356–1365. http://dx.doi.org/10.1016/j.celrep.2017.01.026.

Frazor, R.A., Geisler, W.S., 2006. Local luminance and contrast in natural images. Vis. Res. 46, 1585–1598.

Freeman, J., Field, G.D., Li, P.H., Greschner, M., Gunning, D.E., Mathieson, K., Sher, A., Litke, A.M., Paninski, L., Simoncelli, E.P., Chichilnisky, E.J., 2015. Mapping nonlinear receptive field structure in primate retina at single cone resolution. Elife 4, 1–21. http://dx.doi.org/10.7554/eLife.05241.

Fukada, Y., 1971. Receptive field organization of cat optic nerve fibers with special reference to conduction velocity. Vis. Res. 11, 209–226. http://dx.doi.org/10.1016/0042-6989(71)90186-6.

Garvert, M.M., Gollisch, T., 2013. Local and global contrast adaptation in retinal ganglion cells. Neuron 77, 915–928.

Gastinger, M.J., Tian, N., Horvath, T., Marshak, D.W., 2006. Retinopetal axons in mammals: emphasis on histamine and serotonin. Curr. Eye Res. 31, 655–667. http://dx.doi.org/10.1080/02713680600776119.

Gauthier, J.L., Field, G.D., Sher, A., Greschner, M., Shlens, J., Litke, A.M., Chichilnisky, E.J., 2009. Receptive fields in primate retina are coordinated to sample visual space more uniformly. PLoS Biol. 7 http://dx.doi.org/10.1371/journal.pbio.1000063. e63–e63.

Gauvain, G., Murphy, G.J., 2015. Projection-specific characteristics of retinal input to the brain. J. Neurosci. 35, 6575–6583.

Geffen, M.N., de Vries, S.E.J., Meister, M., 2007. Retinal ganglion cells can rapidly change polarity from off to on. PLoS Biol. 5 e65.

Gollisch, T., 2013. Features and functions of nonlinear spatial integration by retinal ganglion cells. J. Physiol. Paris 107, 338–348.

Gollisch, T., Meister, M., 2010. Eye smarter than scientists believed: neural computations in circuits of the retina. Neuron 65, 150–164.

Gollisch, T., Meister, M., 2008a. Rapid neural coding in the retina with relative spike latencies. Science (Washington, D.C.) 80 (319), 1108–1111.

Gollisch, T., Meister, M., 2008b. Modeling convergent ON and OFF pathways in the early visual system. Biol. Cybern. 99, 263–278.

Goodchild, A.K., Ghosh, K.K., Martin, P.R., 1996. Comparison of photoreceptor spatial density and ganglion cell morphology in the retina of human, macaque monkey, cat, and the marmoset Callithrix jacchus. J. Comp. Neurol. 366, 55.

Grimes, W.N., Hoon, M., Briggman, K.L., Wong, R.O., Rieke, F., 2014a. Cross-synaptic synchrony and transmission of signal and noise across the mouse retina. Elife 3, e03892.

Grimes, W.N., Schwartz, G.W., Rieke, F., 2014b. The synaptic and circuit mechanisms underlying a change in spatial encoding in the retina. Neuron 82, 460–473. http://dx.doi.org/10.1016/j.neuron.2014.02.037.

Güler, A.D., Ecker, J.L., Lall, G.S., Haq, S., Altimus, C.M., Liao, H.-W., Barnard, A.R.,

Cahill, H., Badea, T.C., Zhao, H., Hankins, M.W., Berson, D.M., Lucas, R.J., Yau, K.-W., Hattar, S., 2008. Melanopsin cells are the principal conduits for rod–cone input to non-image-forming vision. Nature 453, 102–105.

Haider, B., Krause, M.R., Duque, A., Yu, Y., Touryan, J., Mazer, J.A., McCormick, D.A., 2010. Synaptic and network mechanisms of sparse and reliable visual cortical activity during nonclassical receptive field stimulation. Neuron 65, 107–121. http://dx.doi.org/10.1016/j.neuron.2009.12.005.

Hammond, P., 1974. Cat retinal ganglion cells: size and shape of receptive field centres. J. Physiol 242, 99–118. http://dx.doi.org/10.1113/jphysiol.1974.sp010696.

Hannibal, J., Kankipati, L., Strang, C.E., Peterson, B.B., Dacey, D., Gamlin, P.D., 2014. Central projections of intrinsically photosensitive retinal ganglion cells in the macaque monkey. J. Comp. Neurol. 522, 2231–2248. http://dx.doi.org/10.1002/cne.23588.

Hattar, S., Liao, H.W., Takao, M., Berson, D.M., Yau, K.W., 2002. Melanopsin-containing retinal ganglion cells: architecture, projections, and intrinsic photosensitivity. Science 295, 1065–1070. http://dx.doi.org/10.1126/science.1069609.

Heitman, A., Brackbill, N., Greschner, M., Sher, A., Litke, A.M., Chichilnisky, E.J., 2016. Testing Pseudo-linear Models of Responses to Natural Scenes in Primate Retina. BioRxiv.

Hochstein, S., Shapley, R.M., 1976. No title. J Physiol 262, 237–264.

Hoshi, H., Mills, S.L., 2009. Components and properties of the G3 ganglion cell circuit in the rabbit retina. J. Comp. Neurol. 513, 69–82. http://dx.doi.org/10.1002/cne.21941.

Hotson, J.R., Prince, D.A., 1980. A calcium-activated hyperpolarization follows repetitive firing in hippocampal neurons. J. Neurophysiol. 43, 409–419. http://dx.doi.org/10.1152/jn.1980.43.2.409.

Hu, E.H., Pan, F., Völgyi, B., Bloomfield, S.A., 2010. Light increases the gap junctional coupling of retinal ganglion cells. J. Physiol 588, 4145–4163.

Huxlin, K.R., Goodchild, A.K., 1997. Retinal ganglion cells in the albino rat: revised morphological classification. J. Comp. Neurol. 385, 309–323. http://dx.doi.org/10.1002/(SICI)1096-9861(19970825)385:2<309::AID-CNE9>3.0.CO;2–5.

Isayama, T., Berson, D.M., Pu, M., 2000. Theta ganglion cell type of cat retina. J. Comp. Neurol. 417 32.

Jacoby, J., Schwartz, G.W., 2017. Three small-receptive-field ganglion cells in the mouse retina are distinctly tuned to size, speed, and object motion. J. Neurosci. 37, 610–625. http://dx.doi.org/10.1523/JNEUROSCI.2804-16.2017.

Jacoby, J., Zhu, Y., DeVries, S.H., Schwartz, G.W., 2015. An amacrine cell circuit for signaling steady illumination in the retina. Cell Rep. 13, 2663–2670.

Jin, N.G., Ribelayga, C.P., 2016. Direct evidence for daily plasticity of electrical coupling between rod photoreceptors in the mammalian retina. J. Neurosci. 36, 178–184.

Joesch, M., Meister, M., 2016. A neuronal circuit for colour vision based on rod-cone opponency. Nature 532, 236–239. http://dx.doi.org/10.1038/nature17158.

Johnston, J., Ding, H., Seibel, S.H., Esposti, F., Lagnado, L., 2014. Rapid mapping of visual receptive fields by filtered back projection: application to multi-neuronal electrophysiology and imaging. J. Physiol. 592 (22), 4839–4854.

Johnston, J., Lagnado, L., 2015. General features of the retinal connectome determine the computation of motion anticipation. Elife 4, e06250. http://dx.doi.org/10.7554/eLife.06250.

Jones, J.P., Palmer, L.A., Jones, J.P., Palmer, L.A., 1987. The two-dimensional spatial structure of simple receptive fields in cat striate cortex. J. Neurophysiol. 58, 1187–1211.

Kastner, D.B., Baccus, S.A., 2013. Spatial segregation of adaptation and predictive sensitization in retinal ganglion cells. Neuron 79, 541–554.

Kastner, D.B., Baccus, S.A., Sharpee, T.O., 2015. Critical and maximally informative encoding between neural populations in the retina. Proc. Natl. Acad. Sci 112, 2533–2538. http://dx.doi.org/10.1073/pnas.1418092112.

Katz, M.L., Viney, T.J., Nikolic, K., 2016. Receptive field vectors of genetically-identified retinal ganglion cells reveal cell-type-dependent visual functions. PLoS One 11. http://dx.doi.org/10.1371/journal.pone.0147738.

Khani, M.H., Gollisch, T., 2017. Diversity in spatial scope of contrast adaptation among mouse retinal ganglion cells. J. Neurophysiol. 118, 3024–3043. http://dx.doi.org/10.1152/jn.00529.2017.

Kim, I.-J., Zhang, Y., Yamagata, M., Meister, M., Sanes, J.R., 2008. Molecular identification of a retinal cell type that responds to upward motion. Nature 452, 478–482.

Kim, K.J., Rieke, F., 2003. Slow Na+ inactivation and variance adaptation in salamander retinal ganglion cells. J. Neurosci. 23, 1506–1516.

Kim, T., Kerschensteiner, D., 2017. Inhibitory control of feature selectivity in an object motion sensitive circuit of the retina. Cell Rep. 19, 1343–1350. http://dx.doi.org/10.1016/j.celrep.2017.04.060.

Kong, J.-H.H., Fish, D.R., Rockhill, R.L., Masland, R.H., 2005. Diversity of ganglion cells in the mouse retina: unsupervised morphological classification and its limits. J. Comp. Neurol. 489, 293–310.

Krishnamoorthy, V., Weick, M., Gollisch, T., 2017. Sensitivity to image recurrence across eye-movement-like image transitions through local serial inhibition in the retina. Elife 6, e22431. http://dx.doi.org/10.7554/eLife.22431.

Kuffler, S.W., 1953. Discharge patterns and functional organization of mammalian retina. J. Neurophysiol. 16, 37–68.

Kuo, S.P., Schwartz, G.W., Rieke, F., 2016. Nonlinear spatiotemporal integration by electrical and chemical synapses in the retina. Neuron 90, 320–332. http://dx.doi.org/10.1016/j.neuron.2016.03.012.

Lasater, E.M., 1987. Retinal horizontal cell gap junctional conductance is modulated by dopamine through a cyclic AMP-dependent protein kinase. Proc. Natl. Acad. Sci. Unit. States Am. 84, 7319–7323.

Laughlin, S., 1981. A simple coding procedure enhances a neuron's information capacity. Z. Naturforsch. C Biosci. 36, 910–912.

Laughlin, S.B., 1989. The role of sensory adaptation in the retina. J. Exp. Biol. 146, 39–62.

Lee, B.B., 1996. Receptive field structure in the primate retina. Vis. Res. 36, 631–644.

Leonardo, A., Meister, M., 2013. Nonlinear dynamics support a linear population code in a retinal target-tracking circuit. J. Neurosci. 33, 16971–16982. http://dx.doi.org/10.1523/JNEUROSCI.2257-13.2013.

Lesica, N.A., Ishii, T., Stanley, G.B., Hosoya, T., 2008. Estimating receptive fields from responses to natural stimuli with asymmetric intensity distributions. PLoS One 3http://dx.doi.org/10.1371/journal.pone.0003060. e3060.

Lettvin, J., Maturana, H., McCulloch, W., Pitts, W., 1959. What the Frog's eye tells the Frog's brain. Proc. IRE 47, 1940–1951.

Levick, W.R., 1967. Receptive fields and trigger features of ganglion cells in the visual streak of the rabbits retina. J. Physiol 188, 285–307.

Liu, J.K., Gollisch, T., 2015. Spike-triggered covariance analysis reveals phenomenological diversity of contrast adaptation in the retina. PLoS Comput. Biol. 11, e1004425.

Liu, J.K., Schreyer, H.M., Onken, A., Rozenblit, F., Khani, M.H., Krishnamoorthy, V., Panzeri, S., Gollisch, T., 2017. Inference of neuronal functional circuitry with spike-triggered non-negative matrix factorization. Nat. Commun. 8http://dx.doi.org/10.1038/s41467-017-00156-9. 149.

Maheswaranathan, N., McIntosh, L.T., Kastner, D.B., Melander, J., Brezovec, L., Nayebi, A., Wang, J., Ganguli, S., Baccus, S.A., 2018. Deep Learning Models Reveal Internal Structure and Diverse Computations in the Retina under Natural Scenes. BioRxiv.

Major, D.E., Rodman, H.R., Libedinsky, C., Karten, H.J., 2003. Pattern of retinal projections in the California ground squirrel (Spermophilus beecheyi): anterograde tracing study using cholera toxin. J. Comp. Neurol. 463, 317–340. http://dx.doi.org/10.1002/cne.10764.

Mani, A., Schwartz, G.W.W., 2017. Circuit mechanisms of a retinal ganglion cell with stimulus-dependent response latency and activation beyond its dendrites. Curr. Biol. 27, 1–12. http://dx.doi.org/10.1016/j.cub.2016.12.033.

Manookin, M.B., Patterson, S.S., Linehan, C.M., 2018. Neural mechanisms mediating motion sensitivity in parasol ganglion cells of the primate retina. Neuron 97, 1327–1340. http://dx.doi.org/10.1016/j.neuron.2018.02.006. e4.

Manookin, M.B., Puller, C., Rieke, F., Neitz, J., Neitz, M., 2015. Distinctive receptive field and physiological properties of a wide-field amacrine cell in the macaque monkey retina. J. Neurophysiol. 114, 1606–1616. http://dx.doi.org/10.1152/jn.00484.2015.

Mante, V., Frazor, R.A., Bonin, V., Geisler, W.S., Carandini, M., 2005. Independence of luminance and contrast in natural scenes and in the early visual system. Nat. Neurosci. 8, 1690–1697.

Martersteck, E.M., Hirokawa, K.E., Evarts, M., Bernard, A., Duan, X., Li, Y., Ng, L., Oh, S.W., Ouellette, B., Royall, J.J., Stoecklin, M., Wang, Q., Zeng, H., Sanes, J.R., Harris, J.A., 2017. Diverse central projection patterns of retinal ganglion cells. Cell Rep. 18, 2058–2072. http://dx.doi.org/10.1016/j.celrep.2017.01.075.

Masland, R.H., 2012. The neuronal organization of the retina. Neuron 76, 266–280.

Mastronarde, D.N., 1983. Interactions between ganglion cells in cat retina. J. Neurophysiol. 49, 350–365.

Matteau, I., Boire, D., Ptito, M., 2003. Retinal projections in the cat: a cholera toxin B subunit study. Vis. Neurosci. 20, 481–493. http://dx.doi.org/10.1017/S0952523803205022.

McFarland, J.M., Cui, Y., Butts, D.A., 2013. Inferring nonlinear neuronal computation based on physiologically plausible inputs. PLoS Comput. Biol. 9, e1003143. http://dx.doi.org/10.1371/journal.pcbi.1003143.

McIlwain, J.T., 1966. Some evidence concerning the physiological basis of the periphery effect in the cat's retina. Exp. Brain Res. 1, 265–271.

Meister, M., 1996. Multineuronal codes in retinal signaling. Proc. Natl. Acad. Sci 93, 609–614.

Milner, E.S., Do, M.T.H., 2017. A population representation of absolute light intensity in the mammalian retina. Cell 1–12. http://dx.doi.org/10.1016/j.cell.2017.09.005.

Münch, T.A., da Silveira, R.A., Siegert, S., Viney, T.J., Awatramani, G.B., Roska, B., 2009. Approach sensitivity in the retina processed by a multifunctional neural circuit. Nat. Neurosci. 12, 1308–1316.

Murphy, G.J., Rieke, F., 2011. Electrical synaptic input to ganglion cells underlies differences in the output and absolute sensitivity of parallel retinal circuits. J. Neurosci. 31, 12218–12228. http://dx.doi.org/10.1523/JNEUROSCI.3241-11.2011.

Nath, A., Schwartz, G.W., 2017. Electrical synapses convey orientation selectivity in the mouse retina. Nat. Commun. 8 (1), 2025. https://doi.org/10.1038/s41467-017-01980-9.

Nath, A., Schwartz, G.W., 2016. Cardinal orientation selectivity is represented by two distinct ganglion cell types in mouse retina. J. Neurosci. 36, 3208–3221. http://dx.doi.org/10.1523/JNEUROSCI.4554-15.2016.

Nirenberg, S., Carcieri, S.M., Jacobs, A.L., Latham, P.E., 2001. Retinal ganglion cells act largely as independent encoders. Nature 411, 698–701. http://dx.doi.org/10.1038/35079612.

Nobles, R.D., Zhang, C., Muller, U., Betz, H., McCall, M.A., 2012. Selective Glycine receptor 2 subunit control of crossover inhibition between the on and off retinal pathways. J. Neurosci. 32, 3321–3332.

Nowak, P., Dobbins, A.C., Gawne, T.J., Grzywacz, N.M., Amthor, F.R., 2011. Separability of stimulus parameter encoding by on-off directionally selective rabbit retinal ganglion cells. J. Neurophysiol. 105, 2083–2099.

Ogawa, T., Bishop, P.O., Levick, W.R., 1966. Temporal characteristics of responses to photic stimulation of single ganglion cells in the unopened eye of the cat. J. Neurophysiol. 29, 1–30.

Ölveczky, B.P., Baccus, S.A., Meister, M., 2003. Segregation of object and background motion in the retina. Nature 423, 401–408.

Ong, J.M., da Cruz, L., 2012. The bionic eye: a review. Clin. Exp. Ophthalmol. 40, 6–17. http://dx.doi.org/10.1111/j.1442-9071.2011.02590.x.

Oyster, C.W., Simpson, J.I., Takahashi, E.S., Soodak, R.E., 1980. Retinal ganglion cells projecting to the rabbit accessory optic system. J. Comp. Neurol. 190, 49–61. http://dx.doi.org/10.1002/cne.901900105.

Ozuysal, Y., Baccus, S.A., 2012. Linking the computational structure of variance adaptation to biophysical mechanisms. Neuron 73, 1002–1015. http://dx.doi.org/10.1016/j.neuron.2011.12.029.

Pang, J.-J.J., Gao, F., Wu, S.M., 2003. Light-evoked excitatory and inhibitory synaptic inputs to ON and OFF alpha ganglion cells in the mouse retina. J. Neurosci. 23, 6063–6073.

Partridge, L.D., Brown, J.E., 1970. Receptive fields of rat retinal ganglion cells. Vis. Res. 10, 455–460. http://dx.doi.org/10.1016/0042-6989(70)90002-7.

Pearson, J.T., Kerschensteiner, D., 2015. Ambient illumination switches contrast preference of specific retinal processing streams. J. Neurophysiol. 114, 540–550.

Peichl, L., Wassle, H., 1979. Size, scatter and coverage of ganglion cell receptive field centres in the cat retina. J. Physiol 291, 117–141.

Pillow, J.W., Paninski, L., Uzzell, V.J., Simoncelli, E.P., Chichilnisky, E.J., 2005. Prediction and decoding of retinal ganglion cell responses with a probabilistic spiking model. J. Neurosci. 25, 11003–11013.

Pillow, J.W., Shlens, J., Paninski, L., Sher, A., Litke, A.M., Chichilnisky, E.J., Simoncelli, E.P., 2008. Spatio-temporal correlations and visual signalling in a complete neuronal population. Nature 454, 995–999.

Piscopo, D.M., El-Danaf, R.N., Huberman, A.D., Niell, C.M., 2013. Diverse visual features encoded in mouse lateral geniculate nucleus. J. Neurosci. 33, 4642–4656.

Pitkow, X., Meister, M., 2012. Decorrelation and efficient coding by retinal ganglion cells. Nat. Neurosci. 15, 628–635.

Poleg-Polsky, A., Diamond, J.S., 2016. Retinal circuitry balances contrast tuning of excitation and inhibition to enable reliable computation of direction selectivity. J. Neurosci. 36, 5861–5876. http://dx.doi.org/10.1523/JNEUROSCI.4013-15.2016.

Provencio, I., Rodriguez, I.R., Jiang, G., Hayes, W.P., Moreira, E.F., Rollag, M.D., 2000. A novel human opsin in the inner retina. J. Neurosci. 20, 600–605. http://dx.doi.org/10.1523/JNEUROSCI.20-02-00600.2000.

Puller, C., Manookin, M.B., Neitz, J., Rieke, F., Neitz, M., 2015. Broad thorny ganglion cells: a candidate for visual pursuit error signaling in the primate retina. J. Neurosci. 35, 5397–5408.

Radon, J., 1986. On the determination of functions from their integral values along certain manifolds. IEEE Trans. Med. Imag. 5, 170–176. http://dx.doi.org/10.1109/TMI.1986.4307775.

Real, E., Asari, H., Gollisch, T., Meister, M., 2017. Neural circuit inference from function to structure. Curr. Biol. 1–10. http://dx.doi.org/10.1016/j.cub.2016.11.040.

Reid, R.C., Victor, J.D., Shapley, R.M., 1997. The use of m-sequences in the analysis of visual neurons: linear receptive field properties. Vis. Neurosci. 14http://dx.doi.org/10.1017/S0952523800011743. 1015.

Reiner, A., Zhang, D., Eldred, W.D., 1996. Use of the sensitive anterograde tracer cholera toxin fragment B reveals new details of the central retinal projections in turtles. Brain Behav. Evol. 48, 322–337. http://dx.doi.org/10.1159/000113211.

Reitner, A., Sharpe, L.T., Zrenner, E., 1991. Is colour vision possible with only rods and blue-sensitive cones? Nature 352, 798–800. http://dx.doi.org/10.1038/352798a0.

Ribelayga, C., Cao, Y., Mangel, S.C., 2008. The circadian clock in the retina controls rod-cone coupling. Neuron 59, 790–801.

Rieke, F., Rudd, M.E., 2009. The challenges natural images pose for visual adaptation. Neuron 64, 605–616.

Rivlin-Etzion, M., Grimes, W.N., Rieke, F., 2018. Flexible neural hardware supports dynamic computations in retina. Trends Neurosci. 41, 224–237. http://dx.doi.org/10.1016/j.tins.2018.01.009.

Robles, E., Laurell, E., Baier, H., 2014. The retinal projectome reveals brain-area-specific visual representations generated by ganglion cell diversity. Curr. Biol. 24, 2085–2096. http://dx.doi.org/10.1016/j.cub.2014.07.080.

Rockhill, R.L., Daly, F.J., MacNeil, M.A., Brown, S.P., Masland, R.H., 2002. The diversity of ganglion cells in a mammalian retina. J. Neurosci. 22, 3831–3843.

Rodieck, R.W., 1998. The First Steps in Seeing. Sinauer Associates.

Rodieck, R.W., Stone, J., 1965. Analysis of receptive fields of cat retinal ganglion cells. J. Neurophysiol. 28, 832–849.

Román Rosón, M., Bauer, Y., Berens, P., Euler, T., Busse, L., 2018. Mouse DLGN Receives Input from a Diverse Population of Retinal Ganglion Cells with Limited Convergence. BioRxiv.

Rousso, D.L.D.L., Qiao, M., Kagan, R.D.R.D., Yamagata, M., Palmiter, R.D.R.D., Sanes, J.R.J.R., 2016. Two pairs of on and off retinal ganglion cells are defined by intersectional patterns of transcription factor expression. Cell Rep. 15, 1930–1944. http://dx.doi.org/10.1016/j.celrep.2016.04.069.

Sakai, H.M., Naka, K., 1987. Signal transmission in the catfish retina 58, 1329–1350.

Sakmann, B., Creutzfeldt, O.D., 1969. Scotopic and mesopic light adaptation in the cat's retina. Pflügers Archiv 313, 168–185.

Sanes, J.R., Masland, R.H., 2015. The types of retinal ganglion cells: current status and implications for neuronal classification. Annu. Rev. Neurosci. 38, 221–246.

Schmidt, T.M., Alam, N.M., Chen, S., Kofuji, P., Li, W., Prusky, G.T., Hattar, S., 2014. A role for melanopsin in alpha retinal ganglion cells and contrast detection. Neuron 82, 781–788. http://dx.doi.org/10.1016/j.neuron.2014.03.022.

Schwartz, G., Rieke, F., 2011. Perspectives on: information and coding in mammalian sensory physiology: nonlinear spatial encoding by retinal ganglion cells: when 1 + 1 ! = 2. J. Gen. Physiol. 138, 283–290. http://dx.doi.org/10.1085/jgp.201110629.

Schwartz, G., Taylor, S., Fisher, C., Harris, R., Berry, M.J., 2007. Synchronized firing among retinal ganglion cells signals motion reversal. Neuron 55, 958–969.

Schwartz, G.W., Okawa, H., Dunn, F.A., Morgan, J.L., Kerschensteiner, D., Wong, R.O.L., Rieke, F., 2012. The spatial structure of a nonlinear receptive field. Nat. Neurosci. 15, 1572–1580. http://dx.doi.org/10.1038/nn.3225.

Sethuramanujam, S., McLaughlin, A.J., deRosenroll, G., Hoggarth, A., Schwab, D.J.J., Awatramani, G.B.B., 2016. A central role for mixed acetylcholine/GABA transmission in direction coding in the retina. Neuron 90, 1243–1256. http://dx.doi.org/10.1016/

j.neuron.2016.04.041.

Shapley, R.M., Victor, J.D., 1981. How the contrast gain control modifies the frequency responses of cat retinal ganglion cells. J. Physiol 318, 161–179.

Shapley, R.M., Victor, J.D., 1979. Nonlinear spatial summation and the contrast gain control of cat retinal ganglion cells. J. Physiol 290, 141–161.

Shapley, R.M., Victor, J.D., 1978. The effect of contrast on the transfer properties of cat retinal ganglion cells. J. Physiol 285, 275–298.

Sharpe, L.T., Stockman, A., Fach, C.C., Markstahler, U., 1993. Temporal and spatial summation in the human rod visual system. J Physiol 463 325.

Sharpee, T., Rust, N.C., Bialek, W., 2014. Analyzing neural responses to natural signals: maximally informative dimensions. Neural Comput. 16, 223–250.

Shimizu, T., Cox, K., Karten, H.J., Britto, L.R.G., 1994. Cholera toxin mapping of retinal projections in pigeons (Columba livia), with emphasis on retinohypothalamic connections. Vis. Neurosci. 11, 441–446. http://dx.doi.org/10.1017/S0952523800002376.

Shlens, J., Rieke, F., Chichilnisky, E.J., 2008. Synchronized firing in the retina. Curr. Opin. Neurobiol. 18, 396–402.

Silveira, L.C., Saito, C.A., Lee, B.B., Kremers, J., da Silva Filho, M., Kilavik, B.E., YAMADA, E.S., Perry, V.H., 2004. Morphology and physiology of primate M- and P-cells. Prog. Brain Res. 144, 21–46.

Simpson, J.I., 1984. The accessory optic system. Annu. Rev. Neurosci. 7, 13–41.

Sivyer, B., Van Wyk, M., Vaney, D.I., Taylor, W.R., 2010. Synaptic inputs and timing underlying the velocity tuning of direction-selective ganglion cells in rabbit retina. J. Physiol 588, 3243–3253.

Sivyer, B., Venkataramani, S., Taylor, W.R., Vaney, D.I., 2011. A novel type of complex ganglion cell in rabbit retina. J. Comp. Neurol. 519, 3128–3138.

Spillmann, L., 2014. Receptive fields of visual neurons: the early years. Perception 43, 1145–1176.

Srinivasan, M.V., Laughlin, S.B., Dubs, A., 1982. Predictive coding: a fresh view of inhibition in the retina. Proc. R. Soc. London - Biol. Sci. 216, 427–459. http://dx.doi.org/10.1098/rspb.1982.0085.

Sun, W., Li, N., He, S., 2002. Large-scale morphological survey of mouse retinal ganglion cells. J. Comp. Neurol. 451, 115–126.

Tien, N.-W., Pearson, J.T., Heller, C.R., Demas, J., Kerschensteiner, D., 2015. Genetically identified suppressed-by-contrast retinal ganglion cells reliably signal self-generated visual stimuli. J. Neurosci. 35, 10815–10820. http://dx.doi.org/10.1523/JNEUROSCI.1521-15.2015.

Tikidji-Hamburyan, A., Reinhard, K., Seitter, H., Hovhannisyan, A., Procyk, C.A., Allen, A.E., Schenk, M., Lucas, R.J., Münch, T.A., 2015. Retinal output changes qualitatively with every change in ambient illuminance. Nat. Neurosci. 18, 66–74.

Troy, J.B., Bohnsack, D.L., Diller, L.C., 1999. Spatial properties of the cat X-cell receptive field as a function of mean light level. Vis. Neurosci. 16, 1089–1104.

Troy, J.B., Einstein, G., Schuurmans, R.P., Robson, J.G., Enroth-Cugell, C., 1989. Responses to sinusoidal gratings of two types of very nonlinear retinal ganglion cells of cat. Vis. Neurosci. 3, 213–223.

Turner, M.H., Rieke, F., 2016. Synaptic rectification controls nonlinear spatial integration of natural visual inputs. Neuron 90, 1257–1271. http://dx.doi.org/10.1016/j.neuron.2016.05.006.

van Hateren, J.H., Ruttiger, L., Sun, H., Lee, B.B., 2002. Processing of natural temporal stimuli by macaque retinal ganglion cells. J. Neurosci. 22, 9945–9960.

Vaney, D.I., Sivyer, B., Taylor, W.R., 2012. Direction selectivity in the retina: symmetry and asymmetry in structure and function. Nat. Rev. Neurosci. 13, 194–208.

Venkataramani, S., Taylor, W.R., 2016. Synaptic mechanisms generating orientation selectivity in the on pathway of the rabbit retina. J. Neurosci. 36, 3336–3349. http://dx.doi.org/10.1523/JNEUROSCI.1432-15.2016.

Venkataramani, S., Taylor, W.R., 2010. Orientation selectivity in rabbit retinal ganglion cells is mediated by presynaptic inhibition. J. Neurosci. 30, 15664–15676.

Venkataramani, S., Van Wyk, M, Buldyrev, I., Sivyer, B., Vaney, D.I., Taylor, W.R., 2014. Distinct roles for inhibition in spatial and temporal tuning of local edge detectors in the rabbit retina. PLoS One 9, e88560.

Victor, J.D., Shapley, R.M., 1979a. The nonlinear pathway of Y ganglion cells in the cat retina. J. Gen. Physiol. 74, 671–689.

Victor, J.D., Shapley, R.M., 1979b. Receptive field mechanisms of cat X and Y retinal ganglion cells. J. Gen. Physiol. 74, 275–298.

Völgyi, B., Chheda, S., Bloomfield, S.A., 2009. Tracer coupling patterns of the ganglion cell subtypes in the mouse retina. J. Comp. Neurol. 512, 664–687.

Wagner, H.J., Wagner, E., 1988. Amacrine cells in the retina of a teleost fish, the roach (Rutilus rutilus): a Golgi study on differentiation and layering. Philos. Trans. R. Soc. Lond. B Biol. Sci. 321, 263–324.

Weick, M., Demb, J.B., 2011. Delayed rectifier K channels contribute to contrast adaptation in mammalian retinal ganglion cells. Neuron 71, 166–179. http://dx.doi.org/10.1016/j.neuron.2011.04.033.

Weiland, J.D., Fink, W., Humayun, M., Liu, Wentai, Rodger, D.C., Yu-Chong, Tai, Tarbell, M., 2005. Progress towards a high-resolution retinal prosthesis. In: 2005 IEEE Engineering in Medicine and Biology 27th Annual Conference. IEEE, pp. 7373–7375. http://dx.doi.org/10.1109/IEMBS.2005.1616215.

Wiesel, T.N., 1960. Receptive fields of ganglion cells in the cat's retina. J. Physiol 153, 583–594. http://dx.doi.org/10.1113/jphysiol.1960.sp006557.

Wong, K.Y., 2012. A retinal ganglion cell that can signal irradiance continuously for 10 hours. J. Neurosci. 32, 11478–11485.

Xin, D., Bloomfield, S.A., 1999. Dark- and light-induced changes in coupling between horizontal cells in mammalian retina. J. Comp. Neurol. 405, 75–87.

Yonehara, K., Ishikane, H., Sakuta, H., Shintani, T., Nakamura-Yonehara, K., Kamiji, N.L., Usui, S., Noda, M., 2009. Identification of retinal ganglion cells and their projections involved in central transmission of information about upward and downward image motion. PLoS One 4 e4320–e4320.

Yonehara, K., Shintani, T., Suzuki, R., Sakuta, H., Takeuchi, Y., Nakamura-Yonehara, K., Noda, M., 2008. Expression of SPIG1 reveals development of a retinal ganglion cell subtype projecting to the medial terminal nucleus in the mouse. PLoS One 3 e1533–e1533.

Yu, H.-H., De Sa, V.R., 2003. Nonlinear reverse-correlation with synthesized naturalistic noise. Cogn. Sci. Online 1, 1–7.

Zaidi, F.H., Hull, J.T., Peirson, S.N., Wulff, K., Aeschbach, D., Gooley, J.J., Brainard, G.C., Gregory-Evans, K., Rizzo, J.F., Czeisler, C.A., Foster, R.G., Moseley, M.J., Lockley, S.W., 2007. Short-wavelength light sensitivity of circadian, pupillary, and visual awareness in humans lacking an outer retina. Curr. Biol. 17, 2122–2128. http://dx.doi.org/10.1016/J.CUB.2007.11.034.

Zhang, Y., Kim, I.J., Sanes, J.R., Meister, M., 2012. The most numerous ganglion cell type of the mouse retina is a selective feature detector. Proc. Natl. Acad. Sci 109, E2391–E2398.

Zhang, Z., Li, H., Liu, X., O'Brien, J., Ribelayga, C.P., 2015. Circadian clock control of connexin36 phosphorylation in retinal photoreceptors of the CBA/CaJ mouse strain. Vis. Neurosci. 32 E009–E009.

Zhao, X., Stafford, B.K., Godin, A.L., King, W.M., Wong, K.Y., 2014. Photoresponse diversity among the five types of intrinsically photosensitive retinal ganglion cells. J. Physiol 592, 1619–1636.

List of abbreviations

AOS: Accessory Optic System
DoG: Difference of Gaussians
DS: Direction Selective
FBP: Filtered Back Projection
GLM: Generalized Linear Model
HD1/HD2: High Definition 1/High Definition 2
JAM-B: Junctional Adhesion Molecule B
LN: Linear Nonlinear
LNP: Linear Nonlinear Poisson
LNLN: Linear Nonlinear, Linear Nonlinear
MID: Maximally Informative Dimensions
OS: Orientation Selective
RF: Receptive Field
RGC: Retinal Ganglion Cell
ipRGC: intrinsically photosensitive RGC
SbC: Suppressed by Contrast
SCN: Suprachiasmatic Nucleus
STA: Spike Triggered Average
STC: Spike Triggered Covariance